US HL-LHC Accelerator Upgrade Project

Q1/Q3 Cryo-Assemblies Conceptual Design Report

Prepared by:
Giorgio Ambrosio, US HL-LHC AUP Magnets L2 Manager, FNAL
Daniel Chang, US HL-LHC AUP 302.2.07 Deputy Manager, LBNL
Guram Chlachidze US HL-LHC AUP 302.2.11 Manager, FNAL
Lance Cooley, US HL-LHC AUP 302.2.02 Manager, FNAL
Delio Duarte Ramos, HL-LHC WP3 Engineer, CERN
Sandor Feher, US HL-LHC AUP 302.2.09 and 302.2.10 Manager, FNAL
Paolo Ferracin, HL-LHC WP3 Scientist, CERN
Susana Izquierdo Bermudez, HL-LHC WP3 Scientist, CERN
Joseph Muratore, US HL-LHC AUP 302.2.08 Manager, BNL
Fred Nobrega, US HL-LHC AUP 302.2.05 Manager, FNAL
Heng Pan, US HL-LHC AUP 302.2.07 Engineer, LBNL
Ian Pong, US HL-LHC AUP 302.2.03 Manager, LBNL
Herve' Prin, HL-LHC WP3 Engineer, CERN
Emmanuele Ravaioli, US HL-LHC AUP 302.2.01 Scientist, LBNL
GianLuca Sabbi, US HL-LHC AUP 302.2.01 Scientist, LBNL
Jesse Schmalzle, US HL-LHC AUP 302.2.06 Manager, BNL
Ezio Todesco, HL-LHC WP3 Manager, CERN
Miao Yu, US HL-LHC AUP 302.2.04 Manager, FNAL

Reviewed by:
Giorgio Ambrosio, US HL-LHC AUP Magnets L2 Manager, FNAL
Ruben Carcagno, US HL-LHC AUP Deputy Project Manager, FNAL

Approved by:
Giorgio Ambrosio, US HL-LHC AUP Magnets L2 Manager, FNAL
Ruben Carcagno, US HL-LHC AUP Deputy Project Manager, FNAL
Giorgio Apollinari, US HL-LHC AUP Project Manager, FNAL

Revision History

Revision	Date	Section No.	Revision Description
V0	5/11/17	All	Initial Release
V1	7/17/17	All	All sections updated for check by L3s

Contents

1 Introduction

The Q1 and Q3 magnets for HL-LHC are based on a design developed by LARP (LHC Accelerator Research Program) and CERN through a series of short models (MQXFS). These quadrupoles have 150 mm aperture, nominal gradient of 132.6 T/m, and coil peak field of 11.4 T. They use Nb_3Sn conductor and a support structure made of segmented aluminum shells pre-loaded by using bladders and keys.

The MQXF design is based on the successful LARP HQ quadrupole series, which had 120 mm aperture. A 1st generation short models (MQXFS1) [1] was developed by LARP and CERN and tested in 2016. The final (2nd generation) MQXF design includes feedback from conductor development and magnet analysis that was not available at the time when the 1st generation design was frozen. The cable of the 2nd generation design has the same width and thickness of the 1st generation cable, whereas the keystone angle was decreased from 0.55° to 0.4° in order to minimize cabling degradation for all candidate conductors (BOST-RRP and BEST-PIT). Analysis of sections of 1st generation coils and measurements of cable expansion during heat treatment (HT) were used to reduce the room for conductor expansion during coil HT. Tighter control of turn position after HT should improve field quality. The coil cross-section was adjusted aiming at optimization of the integral field quality (FQ) and taking into account the cross-section deformation due to cool-down and energization. The insulation thickness on coil midplane and toward the pole was increased in order to allow for FQ fine tuning during coil production without having to change coil parts.

The 2nd generation MQXF design has been tested through a series of 1.5 m short models (MQXFS3/4/5) developed in close collaboration by LARP and CERN.

The MQXFA magnets for Q1 and Q3 have a magnetic length of 4.2 m, and two magnets are used in each Q1/Q3 cold mass. The first MQXFA prototype (MQXFA1) was fabricated and tested by LARP. Because of equipment limitation MQXFA1 has coils of 4 m magnetic length in a full-length structure. MQXFA2/3 and the first Q1/Q3 prototype are under development by HL-LHC-AUP.

References

[1] “MQXFS1 QUADRUPOLE DESIGN REPORT”, edited by G. Ambrosio and P. Ferracin, FERMILAB-TM-2613-TD, 2014.

2 Requirements

The Functional Requirements Specification for the MQXFA magnets can be found in [1]. These requirements are classified into two groups: "Threshold" requirements and "Objective" requirements. Threshold requirements are requirements that contain at least one parameter that the project must achieve, and Objective requirements are requirements that the project should achieve and will strive to achieve. Table 2.1 shows the summary of the MQXFA Threshold requirements. Table 2.2 shows the summary of the MQXFA Objective requirements. They are reported here for reference only, the updated and official version is available at [1].

Table 2.1: MQXFA Threshold Requirements Specification Summary Table.

ID	Description
R-T-01	The MQXFA coil aperture requirement is **150 mm**. This aperture is the nominal coil inner diameter at room temperature, excluding ground insulation, inner layer quench heaters, cold bore, and beam screens. The electrical insulation and heater thicknesses have to be compatible with an outer diameter of the cold bore of 145.75 mm at room temperature, ensuring a gap of 1.5 mm for the cooling between the coils and the cold bore. The cold bore has to be supported inside the magnet aperture by slides attached to the coil poles
R-T-02	The MQXFA physical outer diameter must not exceed **614 mm**.
R-T-03	The MQXFA magnet must be capable of operate at steady state providing a gradient of 143.2 T/m in superfluid helium at 1.9 K and for the magnetic length specified in R-T-04, when powered with current of 17.9 kA.
R-T-04	The MQXFA magnetic length requirement **is 4200 ± 5 mm** at **1.9 K**.
R-T-05	MQXFA magnets must be capable of operation in pressurized static superfluid helium (HeII) bath at **1.3 bar** and at a temperature of **1.9 K.**
R-T-06	The MQXFA cooling channels must be capable of accommodating **two (2)** heat exchanger tubes running along the length of the magnet in the yoke cooling channels. The minimum diameter of the MQXFA yoke cooling channels that will provide an adequate gap around the heat exchanger tubes is **77 mm.**
R-T-07	At least **40%** of the coil inner surface must be free of polyamide.
R-T-08	The MQXFA structure must have provisions for the following cooling passages: (1) Free passage through the coil pole and subsequent G-10 alignment key equivalent of **8 mm** diameter holes repeated every **50 mm**; (2) free helium paths interconnecting the yoke cooling channels holes; and (3) a free cross sectional area of at least **150 cm^2**
R-T-09	The MQXFA magnet structure must be capable of sustaining a sudden rise of pressure from atmospheric up to **26 bar** without damage and without degradation of subsequent performance.

R-T-10	The MQXFA magnet structure must be capable of surviving a maximum temperature gradient of 100 K, during a controlled warm-up or cool-down, and to experience the thermal dynamics following a quench without degradation in its performance.
R-T-11	The MQXFA magnets must be capable of operating at ±**30 A/s.**
R-T-12	The MQXFA magnet must withstand a maximum operating voltage of **670** V to ground during quench.
R-T-13	MQXFA magnets must be delivered with a (+) Nb-Ti superconducting lead and a (-) Nb-Ti superconducting lead, both rated for **18 kA** and adequately stabilized for connection to the Cold Mass LMQXFA or LMQXFAB electrical bus.
R-T-14	Splices are to be soldered with CERN approved materials.
R-T-15	Voltage Taps: the MQXFA magnet shall be delivered with **three redundant (3x2)** quench detection voltage taps located on each magnet lead and at the electrical midpoint of the magnet circuit; **two (2)** voltage taps for each quench strip heater; and **two (2)** voltage taps for each internal MQXFA Nb_3Sn-NbTi splice. Each voltage tap used for critical quench detection must have a redundant voltage tap.
R-T-16	The MQXFA magnet coils and quench protection heaters must pass a hi-pot test specified in **Table 3** of [1].
R-T-17	After a thermal cycle to room temperature, MQXFA magnets should attain the nominal operating current with no more than 3 quenches.
R-T-18	MQXFA magnets must not quench while ramping down at **300 A/s** from the nominal operating current
R-T-19	The MQXFA quench protection components must be compatible with the CERN-supplied quench protection system and comply with the corresponding interface document specified by CERN (US HiLumi DocDB # 216).
R-T-20	All MQXFA components must withstand a radiation dose of 35 MGy, or shall be approved by CERN for use in a specific location as shown in US HiLumi DocDB # 96.
R-T-21	MQXFA magnets will operate in the HL LHC era for an order of magnitude of 5000 cycles. The long term reliability of the design will be proven with a magnet submitted to 2,000 powering cycles in individual test
R-T-22	The MQXFA magnets must meet the detailed interface specifications with the following systems: (1) other LMQXFA (B) Cold Mass components; (2) the CERN supplied Cryogenic System; (3) the CERN supplied power system; (4) the CERN supplied quench protection system, and (5) the CERN supplied instrumentation system. These interfaces are specified in Interface Control Document (US HiLumi DocDB # 216).
R-T-23	The MQXFA magnets must comply with CERN's Launch Safety Agreement (LSA) for IR Magnets (WP3) (US HiLumi DocDB # 234).

Table 2.2: MQXFA Objective Requirements Specification Summary Table.

ID	Description
R-O-01	Variation of local position of magnetic center must be within **±0.5 mm**; variation of local position of magnetic axis within **±2 mrad**. Local positions are measured with a 500 mm long probe every 500 mm.
R-O-02	The MQXFA field harmonics must be optimized at high field. Table 2 of [1] provides specific target values for field harmonics at a reference radius of **50 mm.**
R-O-03	The fringe field target for the magnet installed in the cryostat is less than **50 mT** at 10 mm from the outer surface of the cryostat.
R-O-04	Splice resistance target is less than **1.0 nΩ** at 1.9K.
R-O-05	After a thermal cycle to room temperature, MQXFA magnets should attain the nominal operating current with a target of no more than **1** quench.
R-O-06	MQXFA magnets shall survive at least 50 quenches after the acceptance test.

The Functional Requirements Specification for the LMQXFA cold-masses can be found in [2]. Table 2.3 shows the summary of the LMQXFA Threshold requirements. Table 2.4 shows the summary of the LMQXFA Objective requirements. They are reported here for reference only, the updated and official version is available at [2].

Table 2.3: LMQXFA Threshold Requirements Specification Summary Table.

ID	Description
R-T-01	The LMQXFA assembly physical length (end cover to end cover, including tolerances) must be ≤ 10,100 mm. This dimension is at room temperature (296 K).
R-T-02	The LHe stainless steel vessel outer diameter, including tolerances, must not exceed 630 mm. This dimension is at room temperature (296 K).
R-T-03	The LMQXFA end cover must include pipings listed in Table 1 for cryogenic and electrical connectivity purposes.
R-T-04	The LMQXFA cold mass assembly must not have any obstructions or interferences that will prevent insertion along the entire LMQXFA length of the CERN-supplied 74 mm OD (plus 2 mm for tolerance value) heat exchanger tubes and their supports through the MQXFA cooling channels. The LMQXFA cold mass assembly must not have any obstructions or interferences that will prevent insertion along the entire LMQXFA length of the busbar cartridge used to connect in series the two magnets making the cold mass.
R-T-05	The LMQXFA magnetic elements are two identical MQXFA magnets connected in series. The MQXFA magnets must satisfy the MQXFA requirements specification (Ref 1 of [2]) and the LMQXFA interface specification (Ref 4 of [2]).
R-T-06	The distance between the two ends of the MQXFA magnetic lengths is 606 mm ± 5 mm at nominal operating temperature (1.9 K).

R-T-07	The LMQXFA is a pressure vessel that must be designed and documented in accordance with CERN and U.S. HL-LHC Accelerator Upgrade Project safety agreements (Ref 5 of [2]).
R-T-08	The LMQXFA pressure vessel material for the cylindrical shell and end covers must be Low cobalt content Austenitic Stainless Steel Grade 316L.
R-T-09	The LMQXFA provides a 1.9 K helium vessel that must be designed for a Maximum Allowable Working Pressure (MAWP) of 20 bar differential with an applied test pressure of 25 bar.
R-T-10	The LMQXFA cold mass assembly must be capable of sustaining loads resulting from up to 25 bar of pressure differential without physical damage or performance degradation.
R-T-11	The LMQXFA cold mass will have two main superconducting leads on each side going through the busbar line connection. An additional resistive lead (trim) is required to have current unbalance up to 35 A between the two magnets during operation. The additional lead exits the cold mass through the helium vessel connection. Four additional resistive leads (CLIQ, two per magnet) are required for protection system. These four additional leads exit the cold mass through the helium vessel connection.
R-T-12	The 18 kA busbars will be made with the same Nb-Ti cable used for the connections of the magnet.
R-T-13	The busbars must include expansion loops, to be contained within the end cover section and able to accommodate up to 30 mm of axial movement due to differential thermal expansion/contraction.
R-T-14	Splices are to be soldered with CERN approved materials (Ref 7 of [2]).
R-T-15	The 35 A lead and the CLIQ leads are copper resistive leads. The cross-section of the 35 A lead is to be specified. The CLIQ lead has a 10 mm^2 cross-section.
R-T-16	In each cold mass, two temperature sensors will be installed. These sensors are the short type thermometer assembly (36 mm x 12 mm x 10 mm) typically used by CERN and specified in Ref 8 of [2].
R-T-17	The LMQXFA cold mass assembly includes a minimum of 16 voltage taps.
R-T-18	Instrumentation wires type, preliminary quantity and function are given in Table 2 of [2].
R-T-19	The LMQXFA instrumentation wiring must exit the cold mass assembly through the helium vessel connection. Instrumentation of each magnet will exit the cold mass on opposite sides.
R-T-20	The LMQXFA cold mass assembly voltage limits must meet or exceed the MQXFA voltage limit requirements specified in Ref 1 of [2].
R-T-21	The LMQXFA cold mass assembly will have 12 mirrors positioned in groups of 4, in the mid-point and towards the cold mass ends, at 45°, 135°, 225° and 315°, to be used for the monitoring of the position of the cold mass inside the cryostat.

R-T-22	The LMQXFA quench performance requirements must meet or exceed the MQXFA magnet quench performance requirements specified in Ref 1 of [2].
R-T-23	After installation and routing of heat exchanger tubes, instrumentation wiring, and superconducting busbars there must be a free LMQXFA cross section area of 150 cm^2 in the helium volume.
R-T-24	All LMQXFA components should withstand a maximum radiation dose of 35 MGy, or shall be approved by CERN for use in a specific location
R-T-25	The LMQXFA cold mass assembly must meet the detailed interface specifications with the following systems: (1) MQXFA magnets; (2) The CERN supplied QQXFA/B Cryostats; (3) the CERN supplied piping; (4) CERN supplied Cryogenic System; (5) the CERN supplied power system; (6) the CERN supplied quench protection system, and (7) the CERN supplied instrumentation system. These interfaces are specified in Interface Control Document (Ref 4 of [2]).
R-T-26	The LMQXFA cold mass assembly must comply with CERN's Launch Safety Agreement (LSA) for IR Magnets (WP3) (Ref 5 of [2]).

Table 2.4: LMQXFA Objective Functional Requirements Specification Summary Table.

ID	Description
R-O-01	The maximum deviation of the MQXFA axis (of each magnet) along the common magnetic axis must be less than ±0.5 mm. The deviation of both MQXFA average field angles from the common magnetic field angle must be less than ±2 mrad.
R-O-02	The common magnetic axis of the two-magnet system should be determined with respect to cold mass fiducials with accuracy of ±0.2 mm to both nodal points. The common average MQXFA field angle with respect to cold mass fiducials should be measured with accuracy better than 0.5 mrad. The magnetic length and the *y*-center of the magnetic length need to be known within ±1 mm accuracy relative to external fiducials.
R-O-03	The busbars will include three internal splices. Splice resistance target value must be less than 1.0 nΩ at 1.9 K. A target value at room temperature will also be specified after the completion of the prototype program.
R-O-04	LMQXFA reliability requirements are the same as the MQXFA reliability requirements specified in Ref 1 of [2].

The Functional Requirements Specification for the LQXFA and LQXFB Cryostat Assembly can be found in [3]. The LMQXFA Cold Mass, when surrounded by the QQXFA or QQXFC cryostat shields, piping, and vacuum vessel, is then the LQXFA cryo-assembly for Q1 and the LQXFB cryo-assembly for Q3, as installed in the tunnel of LHC. CERN is responsible for the design and fabrication of the QQXFA and QQXFC cryostats.

References

[1] MQXFA Magnets Functional Requirements Specifications, US HiLumi DocDB # 36.

[2] LMQXFA Functional Requirements Specifications, US HiLumi DocDB # 64.

[3] LQXFA/LQXFB Cryostat Assembly Functional Requirements Specification, US HiLumi DocDB # 246.

3 Superconductor

The Rutherford cable for the MQXF magnets is fabricated using 40 Nb_3Sn strands of diameter 0.85 mm. The baseline strand is a Rod-Restack-Process RRP® strand manufactured by Oxford-Instrument Superconducting Technology (OST), a company of Bruker Energy & Supercon Technologies (BEST). Another option is the Powder-In-Tube PIT strand produced by Bruker Energy & Supercon Technologies (BEST). The prototype coils fabricated by US LARP (LHC Accelerator R&D Program) are using RRP conductor, whereas those made by CERN are using both RRP and PIT conductors.

3.1 Strand

Initial acceptance tests of several billets at OST and within LARP for a wire diameter of 0.778 mm (this diameter wire was used for the 120 mm aperture HQ magnets) showed that, although the wires meet the critical current requirement, the residual resistance ratio (RRR) was in many cases barely above the minimum requirements when reacted using the standard reaction schedule of 210°C/72 h + 400°C/48 h + 650°C/48 hr. The reaction used by OST to qualify the strand before delivery of strand to LARP is 210°C/48 h + 400°C/48 h + 650°C/50 h.

To increase the manufacturing margin and increase the likelihood of RRR exceeding 150 in the round wire, the tin content in the sub-element core was reduced by 5% from the standard amount. The wires from these "Reduced-Sn" billets showed a marked increase in RRR to values over 300, demonstrating that MQXF conductor requirements can be met by RRP conductor. The protection offered by the "Reduced-Sn" modification also allowed the final heat treatment temperature to be more aggressive for increasing critical current at 15 T, where the reaction used by OST changed the final stage to 665°C/75 h. The resulting statistical distribution of properties exhibited acceptable margins above both the RRR and critical current.

The number of superconducting filaments shall be equal to or larger than 108, and the mean copper/non-copper ratio shall be 1.2. These requirements imply that the sub-element diameter by design is ~ 55 μm. The US HL-LHC-AUP strand specification and requirements [1] are based on the LARP strand specification and requirements used to procure strands for the MQXF prototypes [2]. The main characteristics of the strand are summarized in Table 3.1.

Table 3.1 : Main Parameters of the HL-LHC AUP Strand.

Parameter or characteristic	Value	Unit
Superconductor composition	Ti-alloyed Nb_3Sn	
Strand Diameter	0.850 ± 0.003	mm
Critical current at 4.2 K and 12 T	> 632	A
Critical current at 4.2 K and 15 T	> 331	A
n-value at 15 T	> 30	
Count of sub-elements	≥ 108	

(Equivalent sub-element diameter)	(≤ 55)	(μm)
Cu : Non-Cu volume Ratio Variation around mean	≥ 1.2 ± 0.1	
Residual Resistance Ratio *RRR* for reacted final-size strand	≥ 150	
Magnetization at 3 T, 4.2 K (reported for information)	< 256 (< 320)	kA m^{-1} (mT)
Twist Pitch	19.0 ± 3.0	mm
Twist Direction	Right-hand screw	
Strand Spring Back	< 720	arc degrees
Minimum piece length	500	m
High temperature HT duration	≥ 40	Hours
Total heat treatment duration from start of ramp to power off and furnace cool	≤ 240	Hours
Heat treatment heating ramp rate	≤ 50	°C per hour
Rolled strand (0.7225 mm thick) critical current at 4.2 K and 12 T	> 600	A
Rolled strand critical current at 4.2 K and 15 T	> 314	A
Rolled strand *RRR* after reaction	> 100	

The QXF coil heat-treatment schedule for cables using this RRP strand is the following: 210°C/48h + 400°C/48h + 665°C/50h. This is based on supplier recommendation, and is consistent with past observations by LARP experts, showing that the reduction of the final stage duration, compared to the duration previously applied by the supplier, improved RRR for extracted strands at locations of the kinked edges from cabling, with negligible reduction in critical current.

3.2 Cable

The MQXFA cables have a reduced keystone angle of 0.40° (cf. first generation: 0.55°). They will have a minimum length of 455 m, respooled from 500 m of strands. The strand maps will be drawn up by LBNL to optimize wire usage with a reasonable billet blending. The strands will be respooled as-received (i.e. without pre-cable annealing). An online dual-axis optical micrometer will be used during respooling to verify diameter. The cables will be fabricated according to the latest "US-HiLumi Cable Specification" [3], which is based on the LARP specification used for the cables of the MQXF prototype coils fabricated by LARP. The salient cable parameters are listed below in Table 3.2.

Table 3.2 : MQXFA Cable Parameters.

Number of Wires in Cable	40
Cable Mid-Thickness	1.525 ± 0.010 mm
Cable Width	18.15 ± 0.05 mm
Cable Keystone Angle	0.40° ± 0.1°
Cable Lay Direction	Left
Cable Lay Pitch	109 ± 3 mm
Cable Core Material	316 L Stainless Steel
Cable Core Width	12 mm
Cable Core Thickness	0.025 mm
Cable Core Position	Biased towards the major edge
Maximum Cable Residual Twist	150°

The cables will be identified using the following scheme, which is compatible with the CERN system.

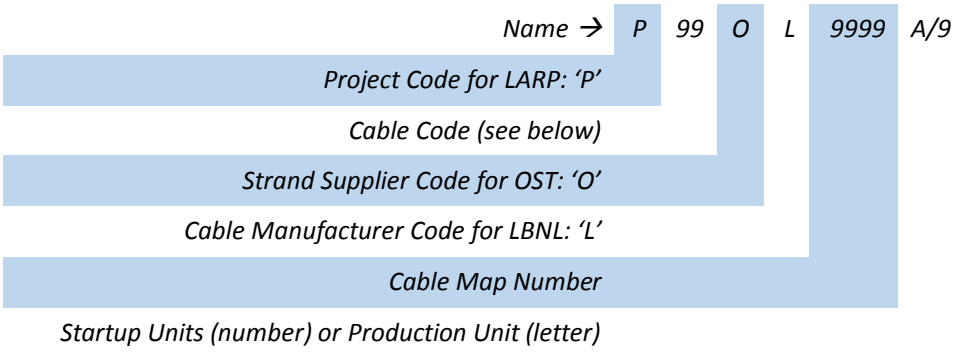

Figure 3.1: Cable ID Scheme based on US HiLumi DocDB # 41.

Table 3.3: Cable codes relevant to MQXF 2nd generation cable designs used during R&D and production.

Cable code	2nd Generation Cable Description
43	QXF R&D w/ Core, using un-annealed 108/127 wires
45	QXF R&D w/ Core, using un-annealed 132/169 wires
47	QXF R&D w/ Core, using un-annealed 144/169 wires

Each cable unit length will be accompanied by a Release Note (a.k.a. Cable Report), including a cable summary, the Respool Log (identifying the strand-spool-brake-fork relationship), charts of the cable dimension parameters (keystone angle, width, and mid-thickness) from the online measurements, optical micrograph (for assessing strand damage), and a report of any non-conformity. It will be formatted to allow exporting the required data to the Vector Database.

Strands representative of the billet blend will be extracted according to the Respool Log for I_C and RRR measurements. The heat treatment schedule used will be that specified for the coil heat treatment.

3.3 Cable Insulation

The MQXFA cables are insulated according to the HL-LHC AUP specification [5] based on LARP specification [6] using a high-strength glass yarn (S-2 Glass® direct sized yarn) made of 9 μm continuous glass strands twisted together and treated with an inorganic sizing ("933"), supplied by AGY (2558 Wagener Road, Aiken, South Carolina, USA 29801). The single-ply yarn is then made into a 2-ply yarn with a twist pitch of 3 inches (i.e. 0.34 twist per inch) by an undisclosed subcontractor of New England Wire Technologies (NEWT, 130 North Main Street, Lisbon, NH 03585), who braids the yarns of fiberglass onto our superconducting cables. The yarn is identified by HL-LHC-AUP and its vendors as "SCG75 1/0 0.7Z fiber with 933 sizing". For completeness, Table 3.4 translates the US- and EU-style nomenclature.

Table 3.4: US- and EU-style nomenclature.

US style	S	C	G	75	1/0	0.7Z
EU style	S	C	9	66	1x0	Z28
Meaning	High-strength glass	Continuous filament, aka strand	Filament diameter = 9 μm	Yield is 7500 yd/lb = 66 g/km (TEX)	1 strand twisted into continuous filament ends, no piling	Right hand twist at 0.7 turns per inch = 28 turns per meter

The braiding is done using a 48 bobbin-carrier braiding machine at NEWT, set to achieve 18 picks per inch in a vertical orientation. The bobbin payoff tension is between 1/4 to 3/8 lbs, and the cable payoff and take-up spool tensions are 2 and 12 lbs, respectively. The insulation specification thickness is 0.145 ± 0.005 mm, common between CERN and HL-LHC-AUP. The insulation thickness is checked at the start of the insulation run using a 5-foot sample according to a 10-stack measurement procedure agreed between CERN and HL-LHC-AUP. The insulated 10-stack cable is measured at 5 MPa during three loading cycles, repeated using the same stack with the insulation removed. The per-side insulation thickness (calculated by subtracting the bare-stack average from the insulated-stack average and then divided by two) measured by the vendor is communicated to HL-LHC-AUP and must be within the tolerance before commencing further work. A second 5-foot sample is sent to HL-LHC-AUP for verification measurements. At the end of the run, another 5-foot sample is taken and measured by the vendor using the same procedure.

References

[1] Specification for Quadrupole Magnet Conductor, US-HiLumi-doc-40.

[2] Specification for Quadrupole Magnet Conductor, US-HiLumi-doc-40; Original Release.

[3] US-HiLumi Cable Specification, US-HiLumi-doc-74.

[4] Nb_3Sn Superconductor Cable for LARP 150 mm Aperture Quadrupole Magnets, LARP-MAG-M-8005, and relevant amendments.

[5] Cable Insulation Specification, US-HiLumi-doc-75.

[6] QXF Magnet Cable Insulation Specification, LARP-MAG-R-8006-A (2014).

4 Magnet Design

4.1 2D Magnetic Design

4.1.1 Coil main parameters

The cross-section of the MQXFA coil is shown in Figure 4.1. It is based on the cos2θ-type design. With four blocks of conductor (two blocks per layer) the coil has enough free parameters to fine tune the multipoles (angular position) while keeping the complexity of the winding low. Besides providing a large gradient and a field quality within specifications, the selected coil also features:

- a total number of turn (50) close to the maximum one can get for this coil layout (a large number of turns is more favorable in terms of stability and load line margin).
- a balanced peak stress in both layers.
- a coil layout that is very similar to the 120 mm aperture HQ quadrupole. This is a valuable feature as the experience in Nb_3Sn coil fabrication gained with HQ, such as the layer jump configuration, was directly transferred to MQXF.

MQXFA coil main parameters are summarized in Table 4.1. Based on the measurements performed to characterize the conductor dimensional change during heat treatment [1], and in order to find the best compromise between performance and field quality, for the second generation design it was decided to: 1) reduce the radial space in the tooling to accommodate for a cable width expansion to 1.2% instead of 2%; 2) keep the same azimuthal space, corresponding to a thickness expansion of 4.5%. The reduction of the nominal insulation thickness from 150 µm to 145 µm without changing the actual insulation thickness will help to assure a better azimuthal position of the coil turns. Dimensions of the cable before and after reaction are both given in Table 4.1. Design calculations are based on the dimension of the reacted cable.

MQXFA features the second cross-section design (MQXF_v2) implementing various improvements with respect to the original design [2], which was used for the first short model (MQXFS1) and a few other coils. In order to minimize the impact on coil fabrication and tooling for the second generation design, the guidelines for coil re-optimization were: 1) to keep same number of conductors per block; 2) to keep the pole turns of the inner and outer layer aligned so as to have the same concept of layer jump (only hard way bending); 3) to keep the same coil inner and outer diameters. The free radial space due to the decreased cable width after reaction is partially absorbed by the inter-layer insulation (which increases from 0.500 mm to 0.660 mm) and the outer layer of S2-glass that is installed in the outer coil diameter before impregnation (which increases from 0.150 mm to 0.310 mm). For the second generation design, we also consider a thicker mid-plane and pole insulation to allow fine tuning of field quality. The insulation between the mid-plane and the first insulated conductor increases from 0.250 mm to 0.375 mm, and from 0.350 mm to 0.500 mm between the pole and the insulated conductor. More information about the modifications implemented in the second generation design can be found in [3].

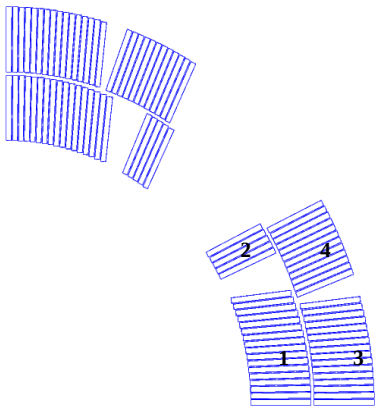

Figure 4.1: Cross-section of the MQXF coil.

Table 4.1: Nominal parameters of the MQXF coil.

	unit	
Coil aperture radius	mm	75.000
Layer 1 outer radius	mm	93.653
Inter-layer thickness	mm	0.660
Outer layer inner radius	mm	94.313
Outer layer outer radius	mm	112.966
Mid-plane shim thickness (per coil)	mm	0.375
Number of turns in block 1		17
Number of turns in block 2		5
Number of turns in block 3		16
Number of turns in block 4		12
Bare unreacted/**reacted** conductor width	mm	18.150/**18.363**
Bare unreacted/**reacted** conductor thickness	mm	1.525/**1.594**
Nominal keystone angle	deg	0.40
Nominal insulation thickness	mm	0.145

The relative position of the block number 2 and 4 (pole block of layer 1 and pole block of layer 2) is such that the broad face of the layer jump turn (orange conductor) is parallel to the broad face of the top conductor of the upper block outer layer (see Figure 4.2). This way a shim with a uniform thickness (~0.25 mm) can be used. Fabrication tolerances for cable and insulation are provided in the conductor section.

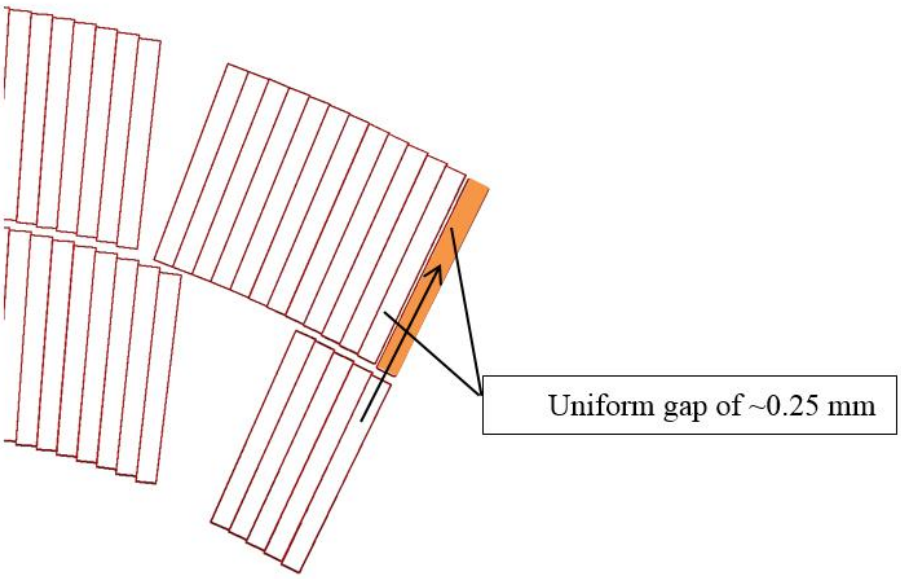

Figure 4.2: Coil layer jump.

Figure 4.3 compares the turn position for the first and second generation coil design.

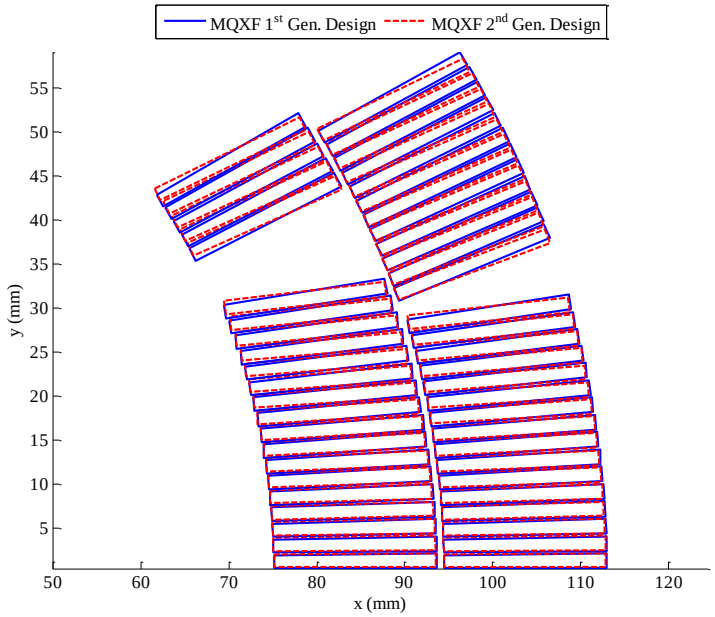

Figure 4.3: Cross-section of the MQXF second generation coil (red) superimposed to the cross-section of the first generation coil (blue).

4.1.2 Roxie model

The computation of the magnetic field was performed with the Roxie software [7]. In Figure 4.4 it is given the 2D data table as implemented in Roxie. The option "alignment of the conductor on the coil OD" was selected (ODFAC = 1) since it provides the best results based on the experience from previous magnets.

Block Data 2D

No	Type	NCab	X	Y	α	Current	Cable name	N1	N2	Imag	Turn
1	Cos	17	75	0.28648	0	16471	XF145HTH5	2	20	0	0
2	Cos	5	75	28.5	24	16471	XF145HTH5	2	20	0	0
3	Cos	16	94.313	0.22782	0	16471	XF145HTH5	2	20	0	0
4	Cos	12	94.313	19	20.8049	16471	XF145HTH5	2	20	0	0

Figure 4.4: Input-file of the MQXF coil used in ROXIE.

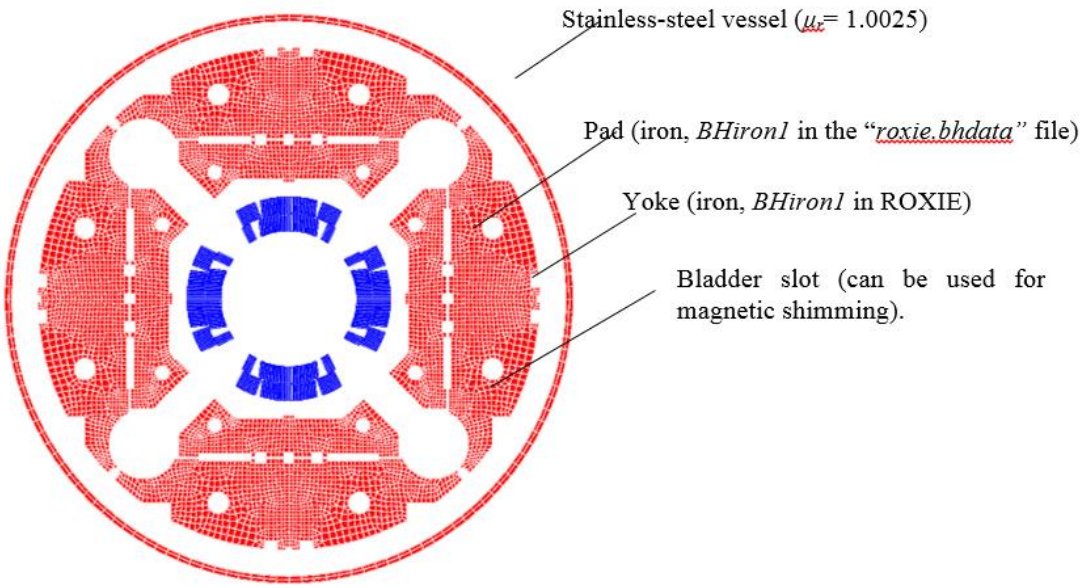

Figure 4.5: MQXF magnet model used in ROXIE.

In the MQXF assembly the superconducting coil is surrounded by iron pads and yokes which reinforce the field in the aperture and reduce the stray field outside the magnet. These elements are also integral components of the shell-based support structure. As a consequence the yoke and the pad implement slots for the insertion of the bladders and grooves for the keys. The 2D FEM model used for the computation of the magnetic field is shown in Figure 4.5. The *BH* characteristic used for the iron components is defined as "BHiron1" in the *roxie.bhdata* file. This *BH* curve assumes a filling factor of 1 (full body). Note that no thermal contraction factor was used for the computation of the harmonics, *i.e.*, the coil is assumed to be at room temperature. The impact of cool-down and mechanical deformation on field quality will be discussed later.

4.1.3 Magnet performance

Minimal requirements for wire manufacturing set by CERN and HL-LHC-AUP require a critical current larger than 632 A and 331 A in respectively 12 T and 15 T applied field and at a temperature of 4.2 K. For the computation of the magnet short sample current 5% degradation on the current due to cabling is assumed and a correction factor of 0.429 T/kA is used to take into account the strand self-field. It corresponds to the magnetic field produced at 89% of the radius of a straight wire. For the characterization of the critical surface the scaling law developed in [8] is used. In Table 4.2 the magnetic parameters of the MQXF magnet when powered at short sample (I_{ss}), nominal (I_{nom}) and ultimate-operation, or maximum (I_{max}) currents are given (Figure 4.6). The operational temperature of the MQXF magnet is 1.9 K.

In Figure 4.7 the magnetic field density in the coil (left) and in the yoke (right) at nominal current are plotted. At I = I_{nom} the peak field in the coil reaches 11.41 T. The peak field is located in the pole block of the inner layer (block 2). The proximity of the yoke to the coil results in a highly saturated iron yoke that translate in a ~9% reduction in the transfer function from injection to nominal current (Figure 4.8-left). For the same reason the differential inductance Ld is non-linear (Figure 4.8-right). In spite of being highly saturated the iron yoke still contribute to enhancing the magnet gradient by ~ 8% at I_{nom} (from 121.7 T/m to 132.6 T/m).

Table 4.2: Main magnetic parameters of the MQXF cross-section considering an operational temperature of 1.9 K.

Parameters	Units	I_{ss}	I_{max}	I_{nom}
Current	kA	21.24	17.89	16.47
I/I_{ss}	%	100	84	78
Gradient	T/m	168.1	143.2	132.6
Nominal peak field on the coil	T	14.5	12.3	11.4
Stored energy	MJ/m	1.89	1.38	1.18
Current sharing temperature	K	1.9	5.8	6.8
Differential inductance	mH/m	8.13	8.18	8.21
Superconductor current density (j_{sc})	A/mm^2	2059	1734	1596
Engineering current density (j_{eng})	A/mm^2	936	788	726
Forces x	MN/m	3.83	2.85	2.47
Forces y	MN/m	-5.68	-4.08	-3.48

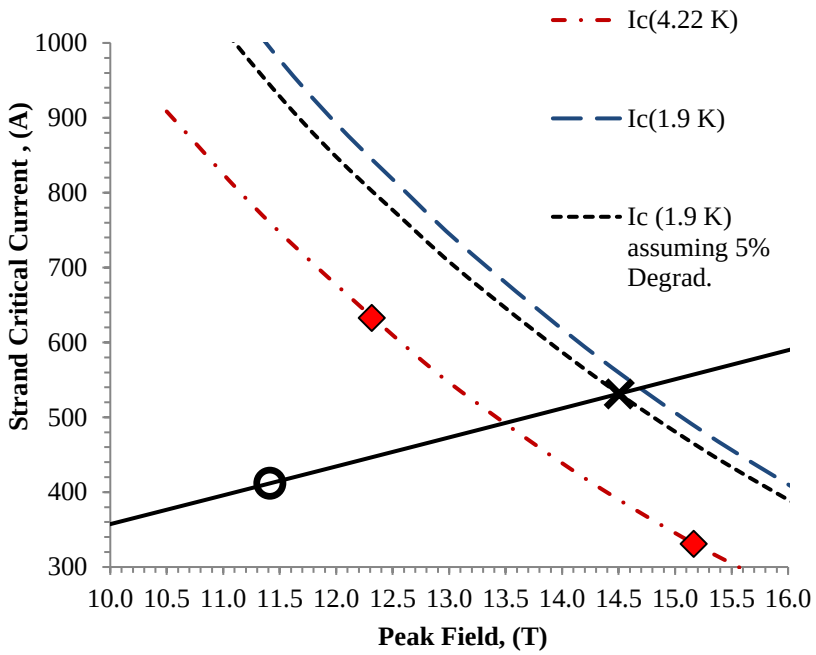

Figure 4.6: MQXF quadrupole load line (current in the cable versus peak field in the coil). The peak field is always located in block 2. The load line has been obtained by gradually increasing the current in the coil. This way the non-linearity of the load line is taken into account.

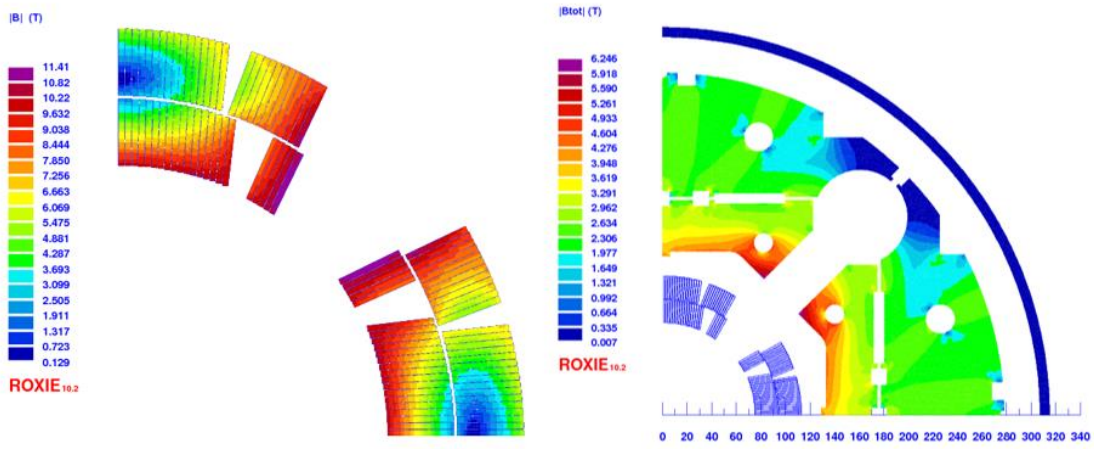

Figure 4.7: Magnetic flux density in the coil (left) and in the yoke (right) at nominal current (Inom).

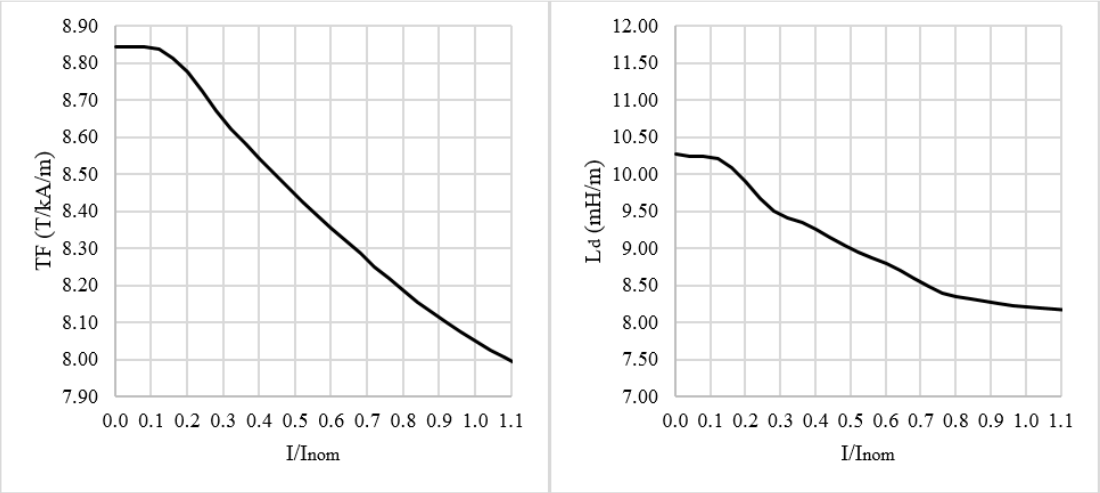

Figure 4.8: Left: Transfer function defined as the ratio between the gradient and the current and expressed in [T/m/kA] plotted versus I/Inom. Right: differential inductance Ld in mH/m. Roxie was used for the computations.

4.1.4 Field quality

Due to the large beam size and orbit displacement in the final focusing triplet, these magnets have challenging targets for field quality requirements at nominal operating current. The coil cross section is optimized such that all allowed harmonics are within one unit at 6.5 TeV. Field quality is optimized at 123 T/m (6.5 TeV) because the triplet will operate between 100% and 90% of the nominal gradient (132.6 T/m, 7 TeV) [3]. The following convention for the definition of the multipoles is used, taking as reference radius 2/3 of the coil aperture radius (R_{ref} = 50 mm).

$$B_y + iB_x = 10^{-4}B_2 \sum_{n=1}^{\infty} (b_n + ia_n) \frac{(x+iy)^{n-1}}{R_{ref}^{n-1}}$$

For the second generation design, coil cross section has been re-optimized to account for the effect of coil deformation on field quality [5] and the contribution of the splices and connection leads [6] to the integral field quality. The impact of coil deformation is an offset of +0.9 units on b_6, mostly caused by the azimuthal coil deformation during cool down as it can be observed in Figure 4.9. The evaluation of the impact of coil deformation on field quality was carried out by importing the coil displacement map extracted from the ANSYS solution into the 2D magnetic model implemented in Roxie. The displacement map corresponds to the state of the coil after the room temperature pre-load, the cool-down and the excitation to I_{nom}, and it is estimated with respect to the design coil geometry at room temperature without any pre-load. The computed displacements were applied to every strand of the magnetic model and a harmonic analysis was performed with the displaced strand distribution. The deformation of the iron yoke was not taken into account during this analysis. The results of the mechanical analysis indicate a radial displacement of the blocks of -0.3 to -0.4 mm and an azimuthal displacement of -0.04 to -0.05 mm. The output of the numerical

magnetic model showed a change in the normalized b_6 harmonic of about 0.9 units and a negligible change of other allowed harmonics such as b_{10} and b_{14}. The offset of the b_6 is mostly caused by the azimuthal coil deformation, which results from the pre-load applied to the structure during the assembly and the structure contraction during the cool-down phase. As expected for quadrupole magnets, the deformations resulting from the electro-magnetic forces have a negligible effect on the b_6.

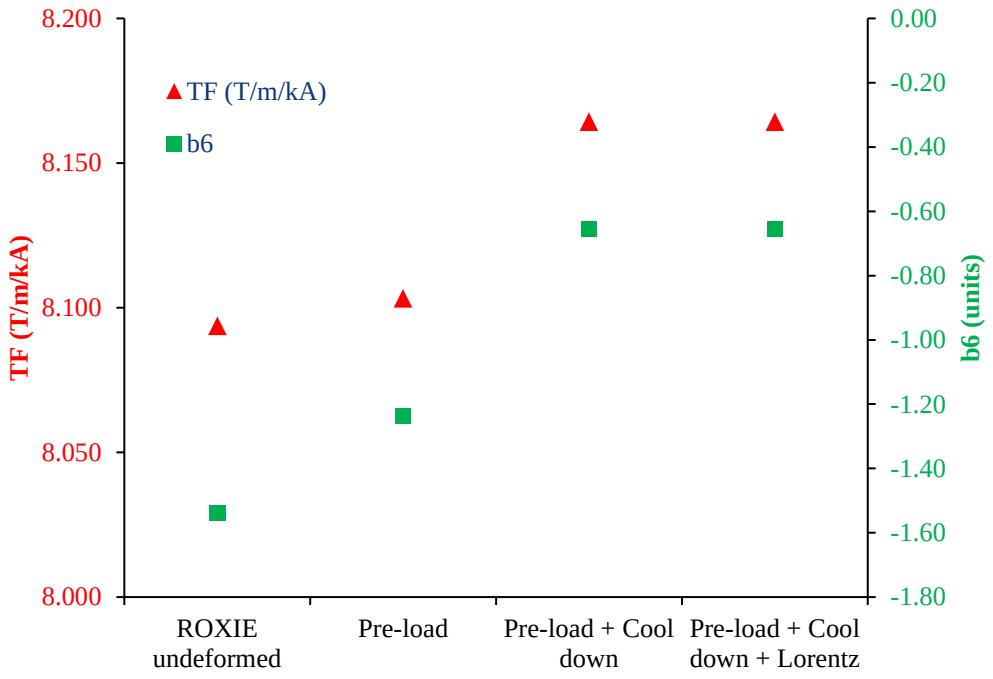

Figure 4.9: Impact of coil deformations due to cool-down, pre-loading, and energizing on the gradient and b6 at 6.5 TeV. In order to retain only the effect of the mechanical deformation, the magnet current is the same for the different steps to have the same contribution from the iron.

The contribution of the Nb_3Sn-NbTi splices and connection leads is an offset of +0.5 units on b_6 as it will be described in 3D section. The change on the rest of the harmonics is negligible. Figure 4.10 shows the evolution of b_6 as a function of the current including the mechanical deformations and 3D effects. As it can be seen from the plot, the main contribution to b_6 is coming from the iron saturation. Even if the difference between injection and nominal current is less than one unit, the maximum variation of b_6 for the full range of current is 4 units.

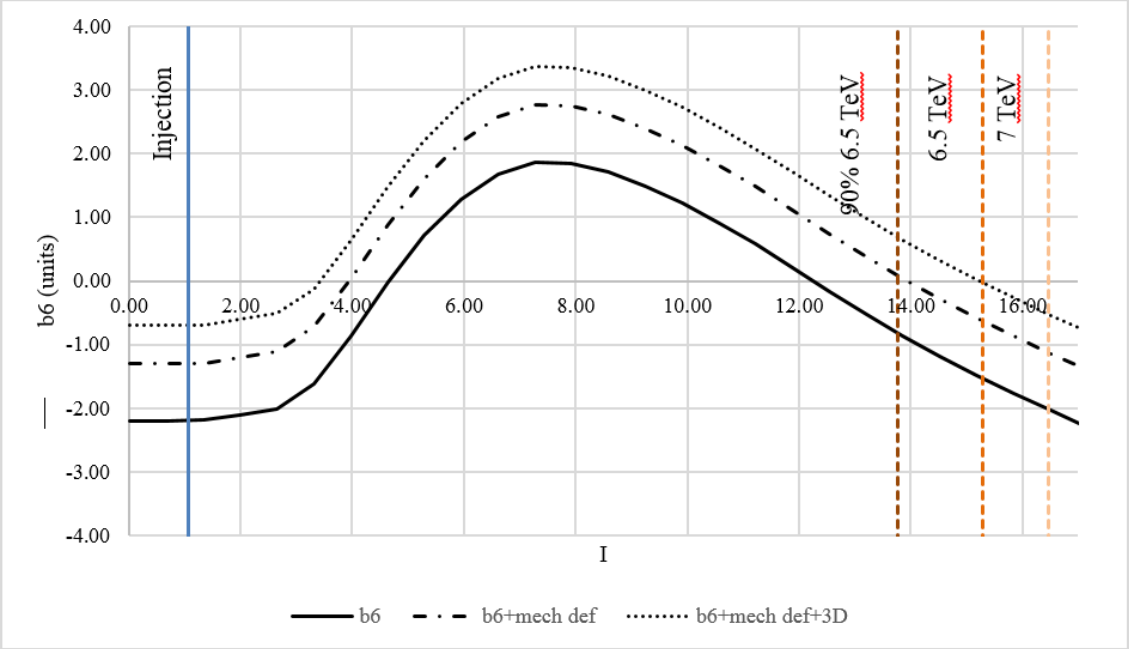

Figure 4.10: First allowed harmonic (b_6) plotted versus the current, including the contribution of the mechanical deformation and 3D effects. Harmonics are expressed in units.

The evolution of the first four allowed harmonics (b_6, b_{10}, b_{14} and b_{18}) with the current is plotted in Figure 4.11. Numerical values of the field components calculated for 7 TeV, 6.5 TeV and 5.85 TeV are given in Table 4.3.

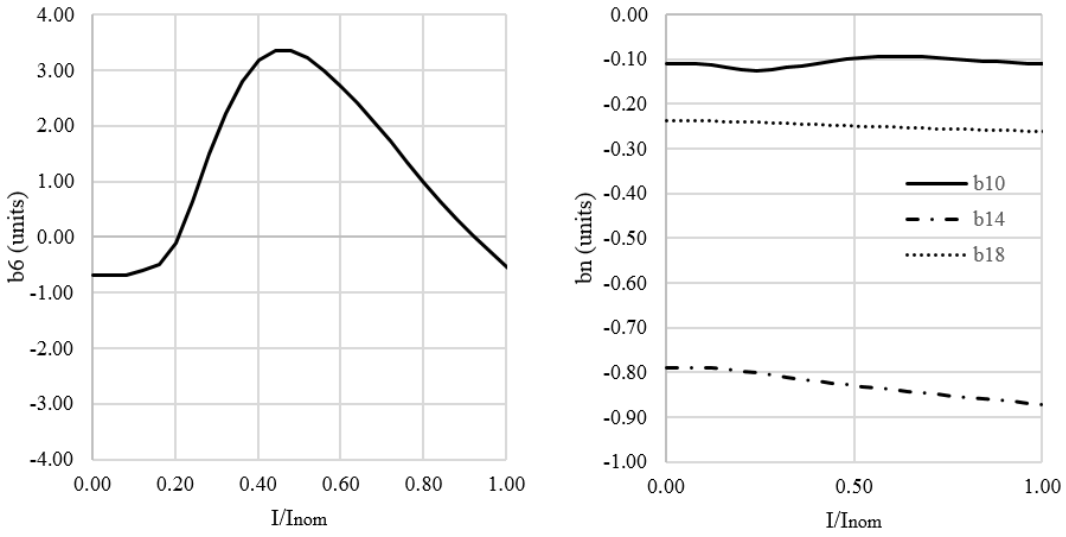

Figure 4.11: First four allowed harmonics (b_6, b_{10}, b_{14} and b_{18}) plotted versus the I/I_{nom} ratio. Harmonics are expressed in units.

Table 4.3: Field Harmonic components calculated for 7 TeV (Nominal), 6.5 TeV and 5.85 TeV.

	unit	*7 TeV*	*6.5 TeV*	*5.85 TeV*
Current	kA	16.47	15.29	13.76
Gradient	T/m	132.6	123.8	112.3
b_6	unit	-0.69	-0.03	0.63
b_{10}	unit	-0.11	-0.11	-0.11
b_{14}	unit	-0.26	-0.26	-0.26
b_{18}	unit	-0.86	-0.86	-0.86

4.1.5 Systematic field error

Field calculations are performed assuming that conductors are aligned on their OD based on the experience from previous (NbTi) magnet. However, it is clear that one does not totally control the position of the cable in the impregnation cavity due to the necessity to allow space for the cable to grow during heat treatment. Here we estimate the field errors due to various defects in tooling, coil size and asymmetry, and turn shifts.

Certain coil variances are observed from 1st generation coil cross section and CMM. At the winding and block level there are azimuthal and radial shifts and rotations. The position of turns near the pole and near the midplane have very little displacement as observed in coil cross sections. Therefore, shifts mostly affect the middle turns of each level near the wedge. The variability along the magnetic length alone is the subject of this analysis. A demonstration of each turn shift is shown in Figure 4.12 at greatly exaggerated magnitudes. Coil size and asymmetry is also included in this analysis based on 1st generation coil CMM data. Field errors due to tooling defects were calculated in the first generation MQXF design report and are included in this analysis.

A Monte-Carlo code was written in Java in conjunction with COMSOL Multiphysics to calculate the harmonics based on 40 line currents uniformly distributed within each cable. The code neglects effects from iron. Random turn/block/coil shifts have a normal distribution with a standard deviation of 50 μm. Errors larger than 1 standard deviation are not included.

The normal and skew harmonic standard deviations are presented in Table 4.4. All random harmonics assume a 50 μm independent RMS displacement. This level of RMS aberration is based on initial coil cross section analysis and coil CMM variance. Machining tolerance for coil parts is consistent with this choice of RMS aberration. Radial variation seems to have the largest effect on harmonics. This is partly an artifact that the entire block is shifted for radial variation as seen in coil cross sections while rotational and azimuthal variation principally is a shift of only the central turns between the midplane and pole. Regardless this analysis indicates that attention should be paid on the materials and thickness of radial insulation.

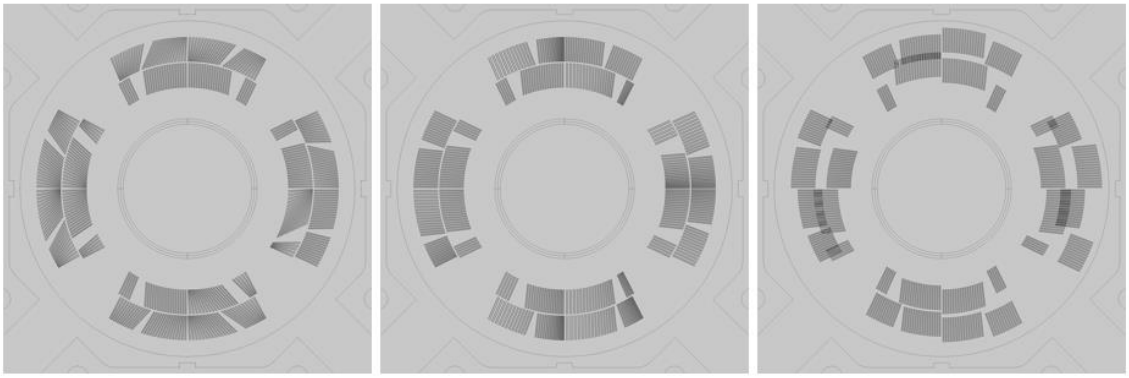

Figure 4.12: On the left a magnet cross section as displayed in COMSOL with random block rotations. The middle image has random azimuthal shifts. The right image has random radial shifts. Each type of shift has a standard deviation and peak greatly exaggerating displacements for demonstration purposes only.

Table 4.4: Random Harmonics based on 50 μm RMS variation in tooling defects, coil CMM, and turn shifts.

	b3	b4	b5	b6	b7	b8	b9	b10	b11	b12	b13	b14
Total Random Normal	**1.560**	**1.070**	**0.680**	**1.880**	**0.270**	**0.160**	**0.100**	**0.220**	**0.041**	**0.024**	**0.015**	**0.032**
Coil Size and Asymmetry	0.859	0.331	0.134	0.002	0.027	0.005	0.005	0.000	0.000	0.001	0.001	0.001
Tooling Defects	0.829	0.623	0.412	0.301	0.159	0.121	0.061	0.040	0.028	0.018	0.011	0.007
Radial Shifts	0.761	0.564	0.418	0.195	0.173	0.029	0.068	0.029	0.024	0.016	0.008	0.003
Azimuthal Shifts	0.650	0.566	0.317	0.287	0.128	0.096	0.047	0.022	0.015	0.004	0.005	0.000
Rotational Shifts	0.093	0.105	0.072	0.074	0.038	0.031	0.016	0.008	0.006	0.001	0.002	0.000

	a3	a4	a5	a6	a7	a8	a9	a10	a11	a12	a13	a14
Total Random Skew	**1.550**	**0.960**	**0.680**	**0.390**	**0.280**	**0.180**	**0.100**	**0.066**	**0.036**	**0.021**	**0.010**	**0.008**
Coil Size and Asymmetry	0.846	0.302	0.142	0.083	0.028	0.016	0.004	0.001	0.000	0.001	0.001	0.000
Tooling Defects	0.849	0.585	0.406	0.192	0.161	0.069	0.060	0.030	0.020	0.012	0.008	0.005
Radial Shifts	0.784	0.628	0.421	0.328	0.181	0.155	0.069	0.050	0.025	0.011	0.008	0.006
Azimuthal Shifts	0.594	0.311	0.305	0.007	0.124	0.052	0.043	0.030	0.015	0.012	0.005	0.004
Rotational Shifts	0.098	0.063	0.070	0.001	0.037	0.017	0.016	0.011	0.006	0.005	0.002	0.002

Coil size and asymmetry harmonics decay much quicker than other block or winding level aberrations as a function of harmonic order. This is expected because the aberration is applied over an entire coil rather than a single turn or block. Thus the coil size and asymmetry has seemingly negligible effect on high order harmonics. This partly explains the larger than expected a_3 and b_3 harmonic seen in MQXFS01 assembly test for example.

The 2nd generation MQXF design has increased radial and azimuthal insulation and has reduced the free space by roughly half the 1st generation design. It is expected therefore that 2nd generation MQXF should likewise have reduced longitudinal variability of turns.

4.2 3D Magnetic Design

4.2.1 Design objectives and process

From the magnetic point of view, the design objectives for coil ends optimization are:

- to limit the peak field enhancement in the ends;
- to keep the coil end as compact as possible in order to increase the magnetic length for a given coil length;
- to minimize the multipole content of the integrated field.

Magnetic and mechanical optimization of the coil ends for the first generation coil design is described in [6]. Following the positive feedback from winding and destructive inspection of the first generation practice coils, the overall shape of the coil ends was not modified. Only a fine tuning was needed to adapt to the new cable geometry and optimize field quality. In order to compensate the non-negligible positive contribution of the coil layer jump and Nb_3Sn/NbTi splice to b_6 [6], the following actions were taken: 1) The magnet longitudinal loading system has been moved from the connection side to the non-connection side of the magnet to minimize the length of the current leads; 2) Re-optimization of the longitudinal position of the coil blocks at the ends. Figure 4.13 compares the conductor longitudinal position for the first and second generation design; 3) Coil cross section has been optimized aiming to a b_6 close to -0.5 units in the straight section to minimize the b_6 integrated over the entire magnet length.

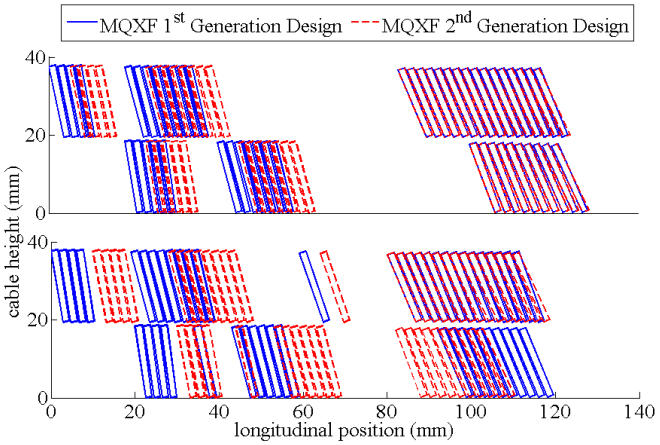

Figure 4.13: Comparison of the conductor position on coil ends for the first and second generation coil design.

Figure 4.14 to Figure 4.17 provide the 3D data table as implemented in ROXIE for each coil end.

Block Data 2D

No	Type	NCab	R	ϕ	α	Current	Cable name	N1	N2	Imag	Turn	Ne
1	Cos	10	75	0.28648	0	15310	XF145HTH5	2	20	0	0	1
2	Cos	7	75	14.2547	3.9938	15310	XF145HTH5	2	20	0	0	2
3	Cos	5	75	28.5	24	15310	XF145HTH5	2	20	0	0	3

More options :

No	String	N/a	N/a

Block Data 3D

Ne	Type	β	Bo	zo	Wi	Wo	Hwed	Horder
1	Diff. Geometry f	71	2	266	0.35	0.02	18.5	3.2
2	Diff. Geometry f	76	1.9	211	0.17	0.02	18.5	3
3	Diff. Geometry f	81	2.23	189	0.15	0.02	18.5	2.8

Figure 4.14: ROXIE input-file of the MQXF_V2 return end, inner layer.

Block Data 2D

No	Type	NCab	X	Y	α	Current	Cable name	N1	N2	Imag	Turn	Ne
1	Cos	10	75	1.6762	0.3994	-15310	XF145HTH5	1	1	0	0	1
2	Cos	6	75	15.6684	4.3932	-15310	XF145HTH5	1	1	0	0	2
3	Cos	1	75	28.5	24	-15310	XF145HTH5	1	1	0	0	3
4	Cos	4	75	29.8946	24.3994	-15310	XF145HTH5	1	1	0	0	4
5	Cos	10	75	0.28648	0	15310	XF145HTH5	1	1	1	90	1
6	Cos	6	75	14.255	3.9938	15310	XF145HTH5	1	1	1	90	2
7	Cos	1	75	22.8184	6.3901	15310	XF145HTH5	1	1	1	90	3
8	Cos	4	75	28.5	24	15310	XF145HTH5	1	1	1	90	5

More options :

No	String	N/a	N/a

Block Data 3D

Ne	Type	β	Bo	zo	Wi	Wo	Hwed	Horder
1	Diff. Geometry f	71	2	382	0.35	0.02	18.5	3.2
2	Diff. Geometry f	76	1.9	353	0.17	0.02	18.5	2.8
3	Diff. Geometry f	78	1.85	344	0.17	0.02	18.5	2.5
4	Diff. Geometry f	80	2.5528	330	0.15	0.02	18.5	2.8
5	Diff. Geometry f	80	2.2305	330	0.15	0.02	18.5	2.5

Figure 4.15: ROXIE input-file of the MQXF_V2 lead end, inner layer.

Block Data 2D

No	Type	NCab	R	ϕ	α	Current	Cable name	N1	N2	Imag	Turn	Ne
1	Cos	16	94.313	0.22782	0	15310	XF145HTH5	2	20	0	0	1
2	Cos	8	94.313	19	20.8049	15310	XF145HTH5	2	20	0	0	2
3	Cos	4	94.313	27.8448	23.9999	15310	XF145HTH5	2	20	0	0	3

More options :

No	String	N/a	N/a

Block Data 3D

Ne	Type	β	Bo	zo	Wi	Wo	Hwed	Horder
1	Diff. Geometry f	68.5	2	249	0.2	0.02	18.5	3
2	Diff. Geometry f	76	1.9	189	0.15	0.02	18.5	2.8
3	Diff. Geometry f	79	1.804	171	0.15	0.02	18.5	2.3

Figure 4.16: ROXIE input-file of the MQXF_V2 return end, outer layer.

Block Data 2D

No	Type	NCab	R	ϕ	α	Current	Cable name	N1	N2	Imag	Turn	Ne
1	Cos	15	94.313	0.22782	0	-15310	XF145HTH5	1	1	0	0	1
2	Cos	1	94.313	16.9004	5.9907	-15310	XF145HTH5	1	1	0	0	2
3	Cos	8	94.313	19	20.8049	-15310	XF145HTH5	1	1	0	0	3
4	Cos	4	94.313	27.8448	23.9999	-15310	XF145HTH5	1	1	0	0	4
5	Cos	15	94.313	1.3329	0.3994	15310	XF145HTH5	1	1	1	90	1
6	Cos	1	94.313	19	20.8049	15310	XF145HTH5	1	1	1	90	2
7	Cos	8	94.313	20.1054	21.2043	15310	XF145HTH5	1	1	1	90	3
8	Cos	3	94.313	28.9526	24.3993	15310	XF145HTH5	1	1	1	90	6
9	Cos	1	94.313	32.4347	25.5974	15310	XF145HTH5	1	1	1	90	5

More options :

No	String	N/a	N/a

Block Data 3D

Ne	Type	β	Bo	zo	Wi	Wo	Hwed	Horder
1	Diff. Geometry f	68.5	2	380	0.2	0.02	18.5	3
2	Diff. Geometry f	72	1.95	364	0.15	0.02	18.5	2.9
3	Diff. Geometry f	76	1.9	328	0.15	0.02	18.5	2.8
4	Diff. Geometry f	80	1.788	310	0.15	0.02	18.5	2.3
5	Diff. Geometry f	80	2.042	310	0.15	0.02	18.5	2.5
6	Diff. Geometry f	79.9968	2.042	311.996	0.15	0.02	18.5	2.5

Figure 4.17: ROXIE input-file of the MQXF_V2 lead end, outer layer.

4.2.2 Study of Integrated Field Harmonics

The objective is to have an integrated multipole content lower than the random components, defining the integrated multipole content as

$$\bar{b}_n = \frac{\int_{-\infty}^{+\infty} B_n(I,z)dz}{B_2^{ss} l_{mag}(I)}$$

where B_n follows the convention

$$B_y + iB_x = \sum (B_n + iA_n)(x+iy)^{n-1},$$

B_2^{ss} is the main field in the straight section and l_{mag} is the magnetic length defined as

$$l_{mag}(I) = \frac{1}{B_2^{ss}(I)} \int_{-\infty}^{+\infty} B_2(I,z)dz.$$

Integration limits are $\pm\infty$ when providing the total integral of the harmonic content. The contribution of each magnet end is also provided in a separate column in Table 4.5. As it can be observed, even if the integral of b_6 over the connection side of 400 mm length is close to 9 units, the total integral is 0.32 units for Q1/Q3 and -0.07 units for Q2a/b. The rest of the harmonics are also summarized in the table, providing the local contribution on the magnet connection side (RE), non-connection side (LE) and the total integral. Only the harmonics where the end contribution is larger than 0.1 units are included in the table.

Table 4.5: Field Harmonics (R_{ref} = 50mm).

		Ends		Integral	
	Straight part	RE	LE	Q1/Q3	Q2a/Q2b
Magnetic length	--	0.400	0.341	4.2	7.15
b_6	-0.640	8.943	-0.025	0.323	-0.075
b_{10}	-0.110	-0.189	-0.821	-0.175	-0.148
a_2	0.000	-31.342	0.000	-2.985	-1.753
a_6	0.000	2.209	0.000	0.210	0.124

4.2.3 Magnetic and Physical Lengths

In order to minimize the impact on beam dynamics of the reduction of the nominal gradient from 140 T/m to 132.6 T/m, the magnetic length has been increased by 200 mm for Q1/Q3 and by 350 mm for Q2a/b. Table 4.6 summarizes the magnetic and physical lengths of the coil, pad and yoke for MQXFS, for the 4.2-m length magnet (Q1/Q3) and for the 7.15-m length magnet (Q2a/Q2b).

Table 4.6: Magnetic length and physical lengths

Parameters	UNITS	MQXFS	Q1/Q3	Q2
Magnetic length at 1.9 K	mm	1196	4200	7150
Magnetic length at RT	mm	1200	4213	7172
Overall coil length at RT (including splice extension)	mm	1510	4523	7482
Magnetic yoke extension at RT	mm	1552	4565	7524
Magnetic pad extension at RT	mm	975	3988	6947
Cable length per coil	m	126	431	721
Cable unit length (including winding margin)	m	150	455	750

Changing the number of iron yoke laminations on the magnet's ends, the magnetic length will be affect.
The maximum increase of magnetic length we could achieve is around 18 mm (peak field enhancement on the coil ends of 0.4 T). The maximum decrease of magnetic length is around 23 mm (Figure 4.18).

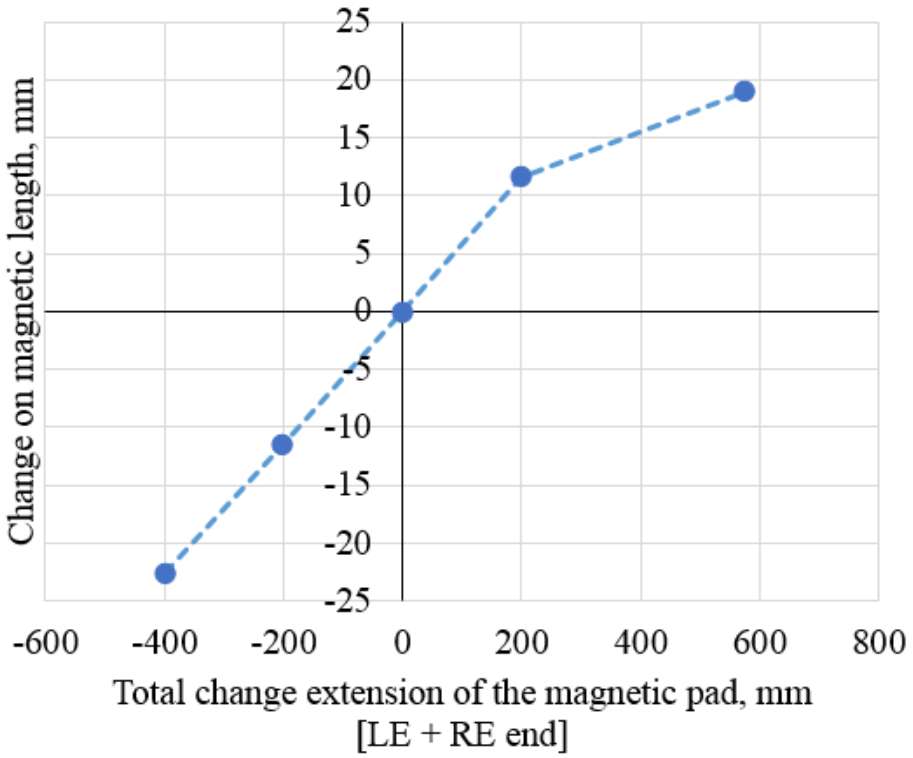

Figure 4.18: Magnetic length change respect to the extension of the magnetic pad change.

4.2.4 Fringe Field

The maximum field in a circular path 20 mm from the outer surface of the cryostat will be 0.0068T (Figure 4.19).

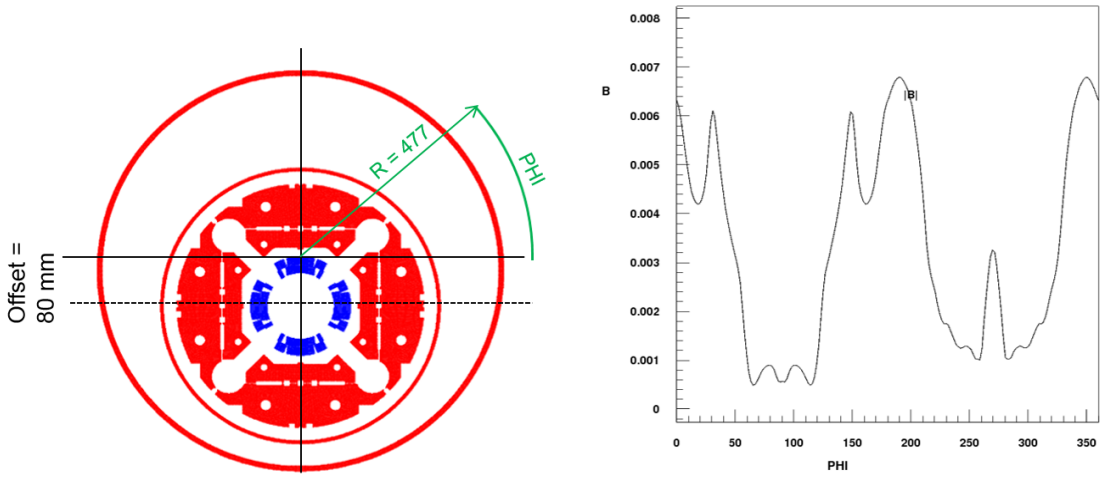

Figure 4.19: Magnetic field around the cryostat at 20 mm (function of the angle).

References

[1] E. Rochepault et al., "Dimensional Changes of Nb3Sn Rutherford cables during heat treatment", IEEE Trans. Appl. Supercond., vol. 26 no. 4, Jun. 2016.

[2] F. Borgnolutti et al., "Magnetic design optimization of a 150 mm aperture Nb3Sn low-beta quadrupole for the HiLumi LHC", IEEE Trans. Appl. Supercond., vol. 24, no. 3, Jun. 2013.

[3] S. Izquierdo Bermudez et al., "Second Generation Coil Design of the Nb3Sn low-beta Quadrupole for the High Luminosity LHC", IEEE Trans. Appl. Supercond., vol. 26 no. 4, Jun. 2016.

[4] E. Todesco, 4th Joint HiLumi LHC-LARP Annual Meeting, Tsukuba. November 2014. http://indico.cern.ch/event/326148

[5] P. Ferracin, et al., "Magnet design of the 150 mm aperture low-beta quadrupoles for the high luminosity LHC" , IEEE Trans. Appl. Supercond., vol. 24, no. 3, pp. 1051:8223, Jun. 2013.

[6] S. Izquierdo et al., "Coil End Optimization of the Nb3Sn Quadrupole for the High Luminosity LHC", IEEE Trans. Appl. Supercond., vol. 25, no. 3, pp. 4001504, Jun. 2015.

[7] http://cern.ch/roxie.

[8] A. Godeke et al., "A general scaling relation for the critical current density in Nb3Sn," *Supercond. Sci. Technol.*, vol. 19, pp. R100-R116, 2006.

[9] E. F. Holik et al., "Fabrication and Analysis of 150 mm Aperture Nb_3Sn MQXF Coils", IEEE Trans. Appl. Supercond., vol. 24, no. 3, Jun. 2013.

4.3 Structural Design

4.3.1 Design features and goals

The support structure of MQXF relies on an aluminum shell pre-stressed at room temperature with bladders and interference keys (i.e. bladder and key technology), which has been demonstrated in the previous successful series of LARP magnets such as HQ. The cross section of the structure of MQXF is a direct scale-up from the HQ models which featured a 120 mm aperture [1]. As shown in Figure 4.20, the MQXF quadrupoles feature an aperture of 150 mm and provides a nominal field gradient of 132.6 T/m by utilizing Nb3Sn superconductor over a magnetic length of 4.2 m (MQXFA) and 7.15 m (MQXFB) at cold [2].

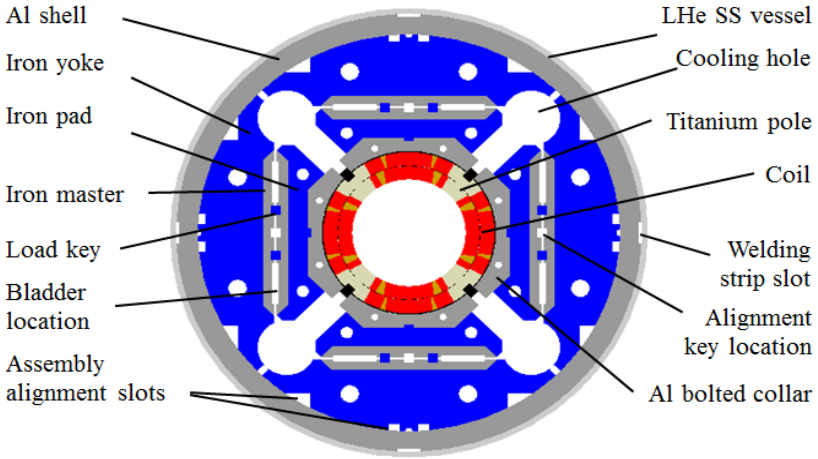

Figure 4.20: Cross section of the MQXF.

The design of the structure comprises an iron yoke assembly surrounded by a 29 mm thick aluminum shell, also includes four iron pads, and the coil-collar subassembly which includes four aluminum collars bolted around the coils engaged by the G11 pole alignment key. The yoke, pads and collars are made of thin laminations assembled with tie rods. Between each pad and yoke, there is master package per quadrant including two interference keys to balance the azimuthal tension in the outer shell with the azimuthal compression in the inner coils.

Maintaining contact between the coils and poles pieces at all stages is the major consideration in the structural design. This goal is achieved by azimuthal load applied on the shell: it relies on a system of water-pressurized bladders and keys to apply a partial pre-load to coil-pack and to pre-tension to aluminum shell at room temperature. During the preload operation, the pressurized bladders open up the master pack and allow inserting the load keys with shims of the designed interference. The final pre-load is achieved during the cool-down phase, when the tensioned aluminum shell compresses the structure components because of its high thermal contraction.

Upon the magnetic design (see Section *2D Magnetic* Design), the MQXFA magnet will experience a total Lorentz force in the axial (Z direction, parallel to the magnet's bore) direction on the order of 1.17 MN at nominal current. Axial pre-stress is therefore designed to withstand the total axial forces generated by the coil ends. Four tensioned steel rods within the yoke's cooling

holes are connected to endplates to provide the pre-stress. As same as the radial pre-stress, the initial designed axial pre-stress is tuned as to counteract 0.2 MN at room temperature and 0.55 MN after cool down (see Section *3D Analysis*).

In brief, the main features of the MQXF structural design are:

(1) Shell-based support structure replying on "bladder and key" technology to perform azimuthal pre-loads, which allows reversible assembly process and tunable preload;
(2) G11 alignment keys inserted into the pole pieces provide the coil alignment and intercept forces from the shell in pre-loading and cool-down;
(3) The aluminum shell is segmented into sections to minimize axial tension in the shell and to ensure a uniform azimuthal load on the coil;
(4) Axial pre-load is provided by four SS rods with a certain amount of pre-strain.

The design goals of the MQXF magnet are summarized below:

a) The coils should be solidly compressed at all times after pre-load to prevent any dimensional displacements or any changes of conductor movements.
b) The maximum coil stress no higher than 200 MPa at cold, although there are debates in the community.
c) The overall membrane and bending stress of ductile materials should be lower than the yield point at the corresponding temperature; the principal stress of the iron material should be lower than the yield point at all steps.
d) The interference applied between load key and pad-master is for the maximum gradient of 140 T/m.

4.3.2 2D Analysis

Both of fully parametric 2D and 3D structural models have been built in ANSYS® software by ANSYS APDL. Those models are both octant symmetric azimuthally. Each coil block, including cables, epoxy resin and fiberglass, is modeled as a homogenous object with an average properties determined in [2]. The 2D model, as shown in Figure 4.21, employs high order 8-node element (plane183) for the main structures; uses elements of CONTA172 and TARGE169 to model the contact areas with segmented Lagrange formulation. The shims for pre-loading are simulated by offset between load key / pad-master contact interface.

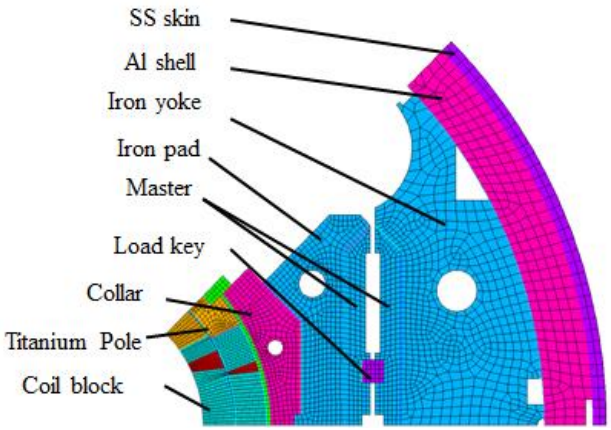

Figure 4.21: Mesh view of the 2D octant model (materials are displayed by colors).

Every part inside a coil will be bonded at all steps; frictional contact with frictional coefficient 0.2 was used at each interface of all the other components.

The 2D numerical model of the MQXF structure includes friction and simulates 5 steps:

- Bladder inflated at 300 bar (30 MPa)
- Keys inserted (bladder deflated)
- LHe vessel welding
- Cool-down
- Excitation: nominal 130 T/m & maximum gradient (140 T/m)

Material properties used for FEM analysis are shown in Table 4.7. The computations in both the 2D and 3D (discussed in next section) models were carried out in light of the following requirements [1]:

1) Keep the pole turns in contact with the winding poles with a pressure ≥ 2 MPa at the mid-radius at the maximum gradient of 140 T/m;
2) Limit the coil peak stress to 200 MPa at 1.9 K;
3) Maintain the stress in the support structure components within the material limits (Discussed in next section);
4) Contact interference of 850 μm was applied at the load key / pad-master interface for the shims.

Table 4.7: Material properties for the MQXF analysis.

Materials	E at 293K	E at 4.2K	Integrated thermal contraction (293K-4.2K)
	GPa	GPa	
Coil *	20	20	3.97E-03
Aluminum bronze	110	120	3.24E-03
Aluminum	70	79	4.20E-03
Iron	213	224	2.00E-03
G10 (normal direction)	7	7	7.30E-03
G10 (layer direction)	17	17	2.44E-03
Notronic 50	210	225	2.60E-03
Stainless Steel	193	210	2.90E-03
Titanium	115	125	1.70E-03

*the coil properties such as modulus has been updated upon the latest study conducted by Giorgio Vallone.

Stresses in the coils have been computed and displayed in a cylindrical coordinate system. Azimuthal stress distribution is checked in the coil as shown in Figure 4.22. The coils are compressed from the bladder operation to cool-down; as mentioned above, the inner and outer layers at the coil/pole interface show an average tension of about 24 MPa when energized to the normal gradient. The maximum σ_θ in coil is 124 MPa at RT with the stainless steel vessel welded outside the structure, and -177 MPa after cool-down. Coil stress from the 2D computation is within the limit; more detailed coil stress will be further discussed in next section (*3D Analysis*).

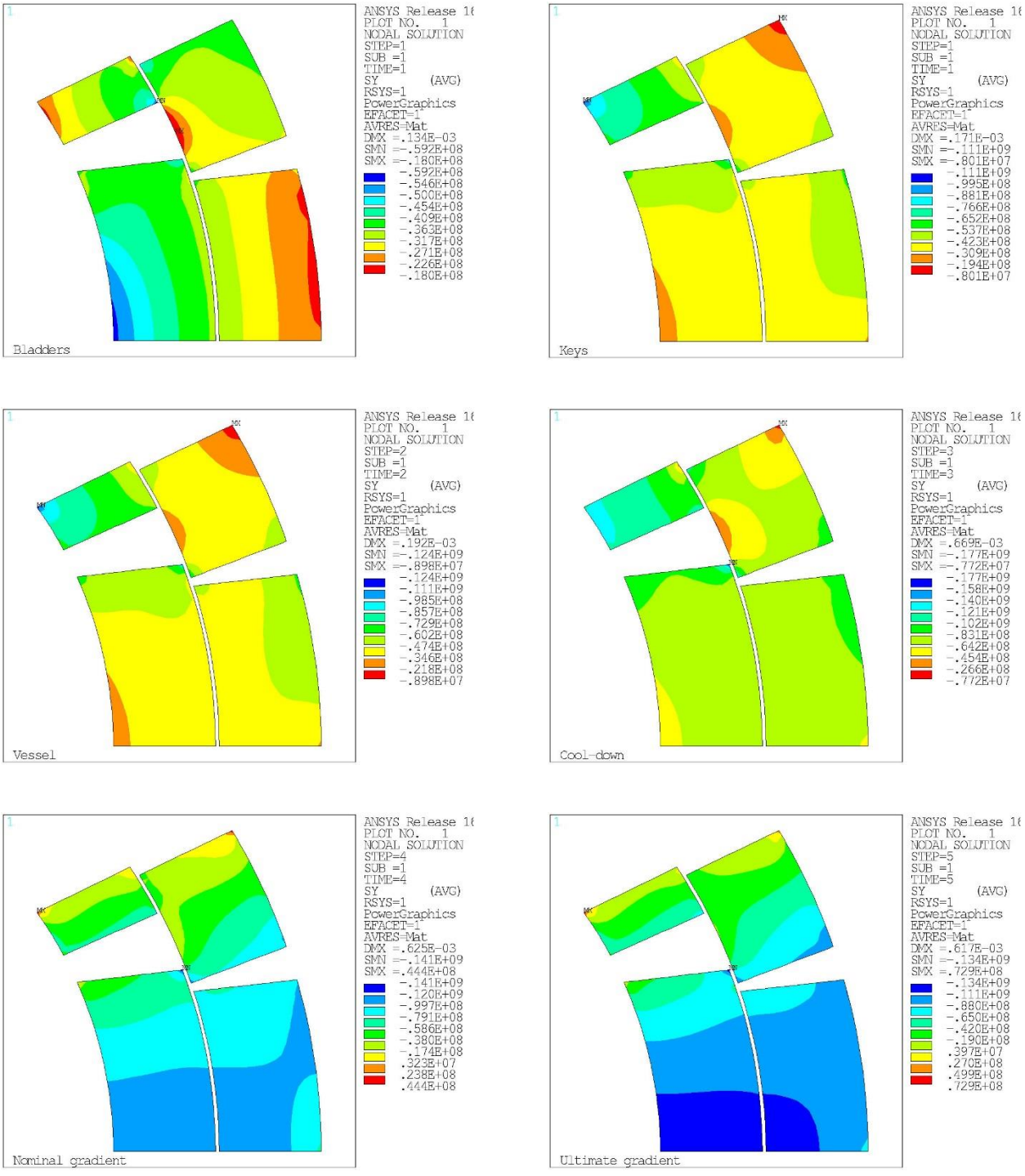

Figure 4.22: Azimuthal stress distribution with 300 bars of bladder pressure and 850 μm of loading key interference.

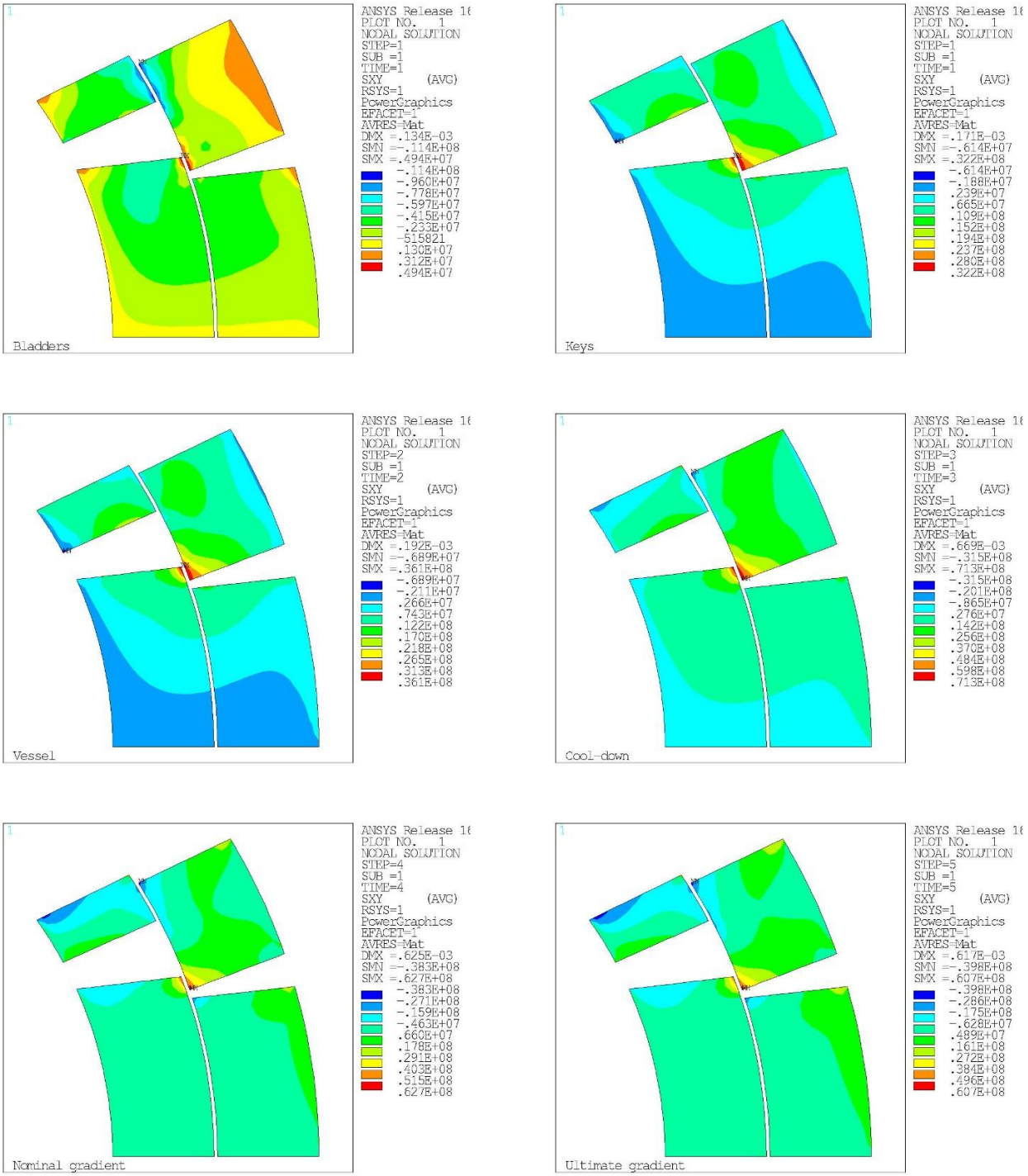

Figure 4.23: Shear stress distribution with 300 bars of bladder pressure and 850 μm of loading key interference.

Shear stress in the coils at 4.2 K varies in the ± 35 ~ 40 MPa range with the exception of a few corners (the outer corner of layer 1 pole turn and the inner corner of layer 2 pole turn, Figure 4.23). A peak shear stress of 71 MPa is observed after cool-down at the corners on the coil/wedge interface. According to measurements performed at 77K [3], the shear stress in side coil keeps in the acceptable range. Due to lack of longitudinal contribution, stresses in each part are studied in the 3D analysis section.

4.3.3 3D Analysis

In order to check the stress distribution throughout the assembly, 3D ANSYS mechanical analysis with the finalized shells and updated parameters and features was carried out. Higher order, 20-node elements (SOLID186) were used to create the mesh (Figure 4.24). Similarly, the 3D contact areas were modeled by CONTA174 and TARGE170 elements with similar contact parameters used in the 2D model. Only octant geometry was used to reduce the computational cost, and therefore 3 symmetry planes were defined (0° and 45° on azimuthal direction and Z=0 on the axial direction).

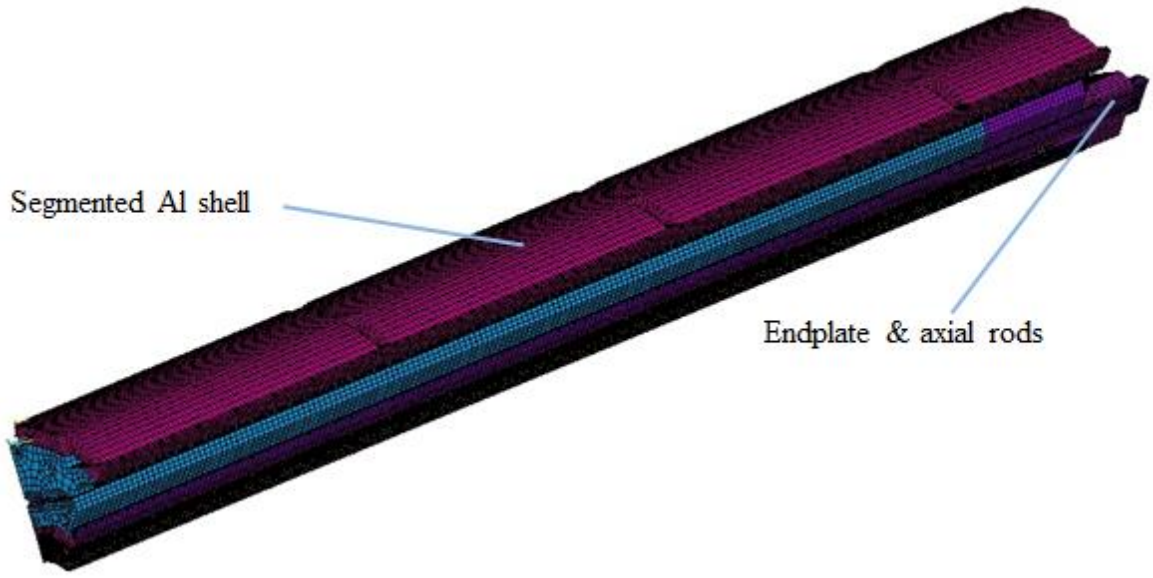

Figure 4.24: Mesh view of the 3D model (materials are displayed by colors).

In the 3D model, the pad is modelled as two parts: the iron pad covering the major straight section of the coil and the stainless steel covering the coil ends and end-shoe. The entire operation process was simulated by the following four steps [4]:

1) Key shimming: the interference shim was applied as the contact offset between load key and master pad.

2) Cool-down to 4.2 K: the temperature of all solids was changed from 300 K to 4.2 K.

3) Magnetic excitation to nominal gradient 130 T/m: Import the coil from ROXIE to opera, and then compute forces in opera and import from opera to ANSYS.

4) Magnetic excitation to maximum gradient 140 T/m: scale the imported Lorentz force to the level of the maximum gradient.

The 3D model also applied an interference of 850 μm as the baseline case to preserve the nominal coil shape allowing excessive stress at the maximum gradient of 140 T/m. Axial preload in the model is provided by pre-tensioning -600 με (126 MPa) on the axial steel rods.

The average azimuthal stress evolutions in the coil inner layers and shell are given in Figure 4.25. The round, triangle, and square markers indicate the azimuthal stresses, respectively at the mid-radius of the pole turn (center of the turn), at the mid-radius of the mid-plane turn and at 15° from the welding strip slot of the shells. During assembly, pre-stressing was stopped with 120 MPa of tension in the shell. It increased to 208 MPa during cool-down. The shell's tension is azimuthally uniform, except for some curvature changes near the iron gaps. The inner coil's azimuthal stress reaches -60 MPa (compression) during assembly, increasing to -125 MPa with cool-down. With Lorentz force, the stress in the shell is nearly constant, while the stress in the coil varies linearly with the square of the current.

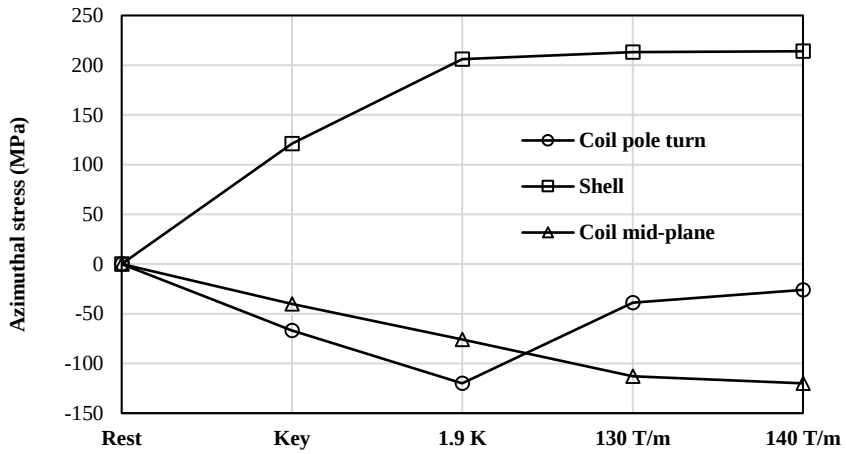

Figure 4.25: Azimuthal stress in the coil inner layer from assembly to excitation: mid-radius of the pole turn (round markers), mid-radius of the mid-plane turn (triangle markers), and the whole layer peak stress (square markers).

Figure 4.26 presents how the mechanical forces within the magnet evolve over the operation process. During the assembly, 55% of the force provided by the shell is transferred to the coil, the rest being intercepted by the pole key. After cool-down, the shell loads the coil to the target value based on the e.m. force. In this design, the pole key intercepts the similar fraction of the shell force at 1.9 K by orientating the key cloth fibers parallel to the azimuthal direction to prevent the pole key from losing due to higher thermal contraction in the normal direction. The coil pole turns are still under compression with the Lorentz forces; the compressive force on the pole key reduced a bit with Lorentz forces, but still indicates that coil alignment is maintained.

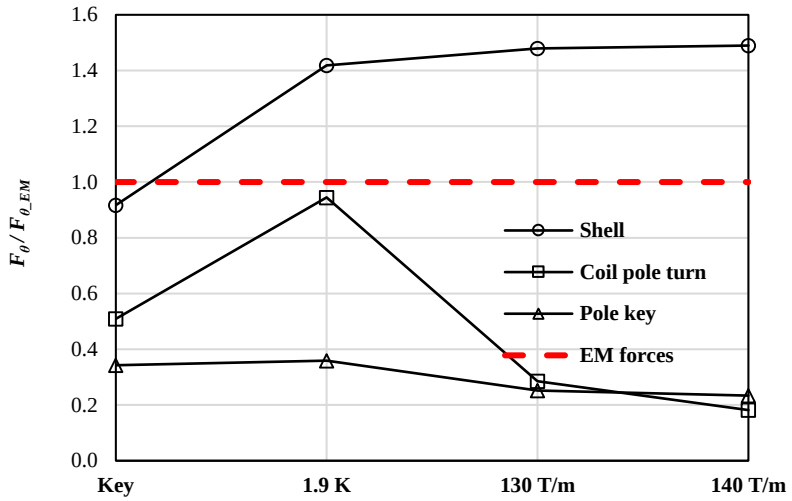

Figure 4.26: Azimuthal stress in the coil inner layer from assembly to excitation: mid-radius of the pole turn (round markers), mid-radius of the mid-plane turn (triangles), and the whole layer peak stress (squares).

Peak coil stress usually appears on the coil ends. Figure 4.27 presents the coil azimuthal stress at different steps. The coil reaches a maximum compression of −129 MPa during room temperature bladder operation, −192 MPa in the pole region at 1.9 K which remains safely below 200 MPa criteria, and −146 MPa on the mid-plane with Lorentz forces at 140 T/m.

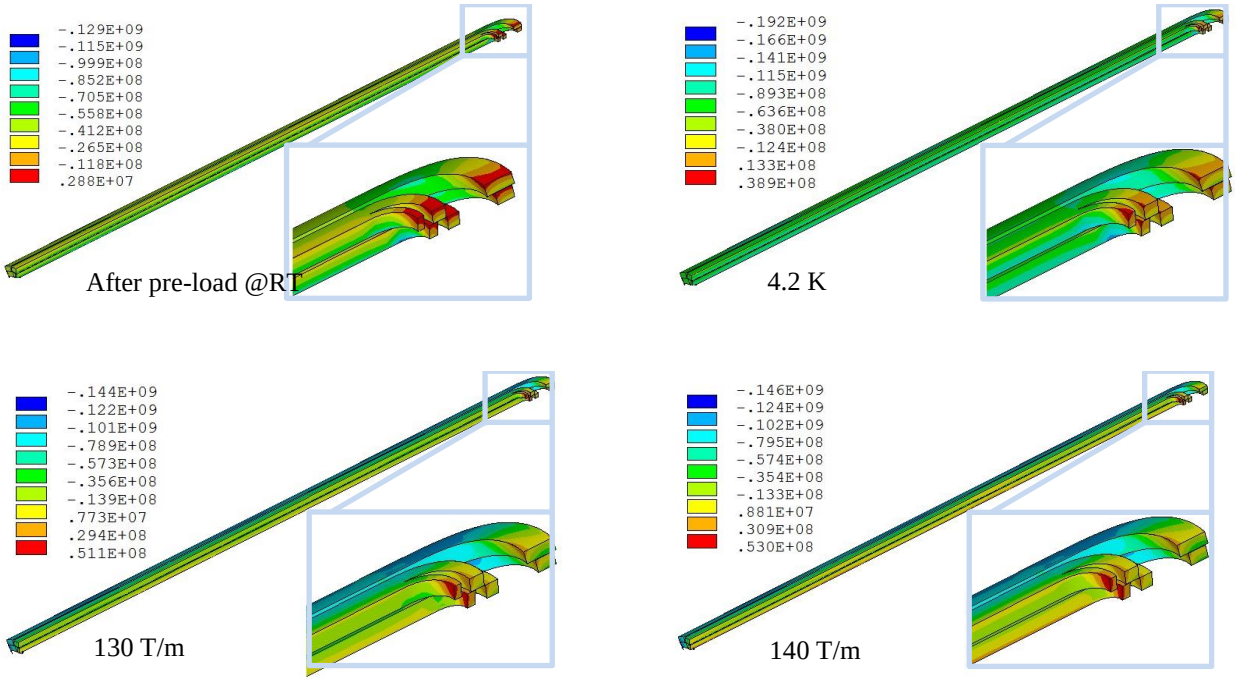

Figure 4.27: Coil azimuthal stress (Pa).

The contact pressure at the coil ends is shown in Figure 4.28. There are some areas around the pole tips show zero compression, but in general the coil is kept in contact with pole and spacers. The situation of zero compression around the pole tips is similar as seen in HQ models, and according to the experience from HQ magnets, the slight zero compression could be acceptable.

The axial load that counteracts the axial Lorentz force of 1.17 MN on the coils is provided by four pre-tensioned 32 mm diameter steel rods and two Nitronic 50 end plates, which prevent the coils from detaching from the pole or end-spacers. Although the rods and plates were sized to accommodate the full axial load (Fz), in the simulation the magnet was axially preloaded to only ~40% of this value due to friction forces between the coils and the support structures, which is based on previous experience on the HQ series. The four rods are pre-strained to ~600 με corresponding to 405 kN of total axial force at room temperature.

The stress in the structure parts should be maintained within the material limits listed in Table 4.8. For ductile material like aluminum, stainless steel, titanium and Nitronic 50, we use the Distortion Energy Theory as the criteria; for brittle materials like iron, we use the maximum normal stress criterion, which checks the principal stress instead of Von Mises stress. At 4.2 K, all the iron parts exhibit first principal stresses below 300 MPa with a safety factor of 2.41. The shell azimuthal stress remains below 350 MPa after cool-down. From the standpoint of coil stress, the baseline case reveals that the 850 μm interference could be the upper limit of the practical radial shim.

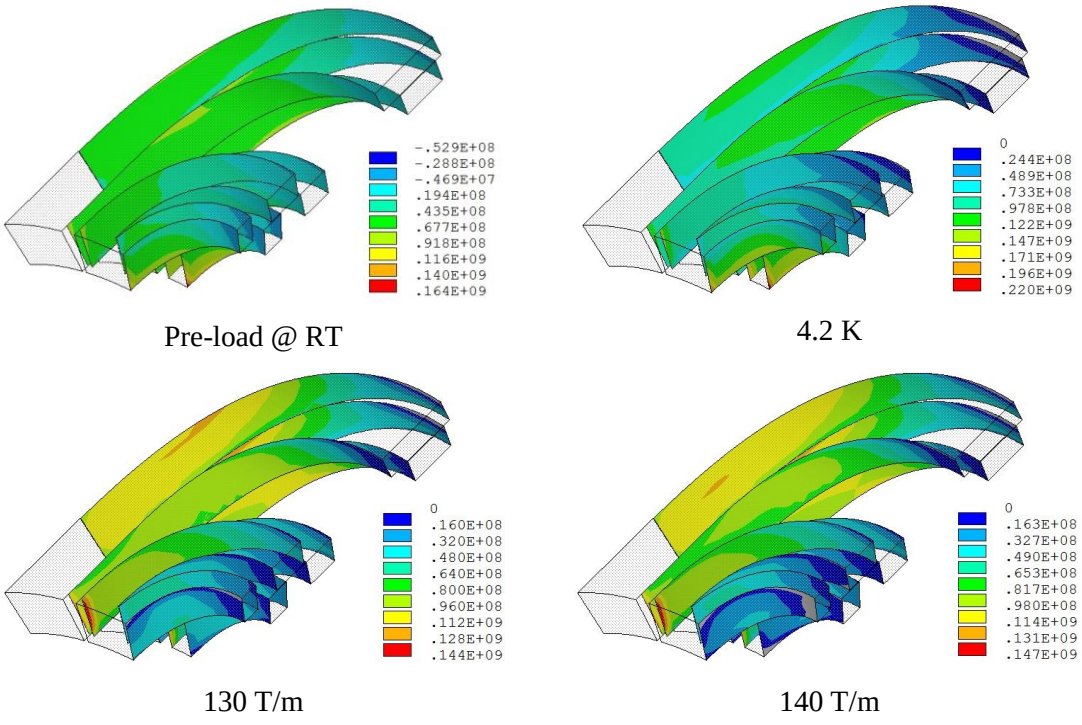

Figure 4.28: Contact pressures at the coil/spacers interfaces (Pa).

Table 4.8: Material strength limits.

Material	Yield strength (MPa)	
	293K	4.2 K
Al 7075	480	690
SS316 LN	350	1050
NITRONIC 50	350	1240
A36 Steel	180	720
Titanium	830	1650

References

[1] P. Ferracin, G. Ambrosio, M. Anerella, et. al, "Development of MQXFThe Nb3Sn Low- β Quadrupole for the HiLumi LHC", IEEE Transactions ON Applied Superconductivity, Vol, 26, No. 4, 2016

[2] G. Ambrosio , M. Anerella , F. Borgnolutti, et al. "MQXF Quadrupole Design Report"

[3] G. Ambrosio , R. Bossert , P. Ferracin, "Shear stress in LQ coils", FNAL Technical Division note: TD-08-001; LARP note 2008.

[4] H. Pan, E. Anderssen, G. Ambrosio, D. W. Cheng, M. Juchno, P. Ferracin, H. Felice, J. C. Perez, S. O. Prestemon, G. Vallone "Mechanical Design Studies of the MQXF Long Model Quadrupole for the HiLumi LHC", IEEE Transactions ON Applied Superconductivity, to be published.

4.4 Radiation Effects

Proton-proton collisions at 7 TeV generate about 120 secondary particles per interaction. Many of these particles, and their decay products, are intercepted by the detector components. However, those emitted at small angles with respect to the beam direction exit the detector region through the TAS, a 60 mm aperture, 1.8-m long absorber located at 20 m from the IP. While less than 10% of the secondary particles cross the TAS, they carry a large fraction of the total energy, resulting in 3.8 kW of power on each side of IP1 and IP5 at the nominal HL-LHC luminosity of $5\times10^{34}\text{cm}^{-2}\text{s}^{-1}$. This has a critical impact on both thermal loads and radiation dose to the IR quadrupoles.

The protection strategy of the IT magnets is centered on a tungsten absorber placed in the magnet bore between the beam pipe and the coil. The absorber is mounted on the beam screen, which is made of stainless steel and has an octagonal shape. This assembly allows both shielding the cold mass from a large fraction of the secondary particles, and collecting their energy at a higher temperature, reducing the heat load on the 1.9K system.

Detailed simulations of the radiation load for HL-LHC were carried out using FLUKA at CERN [1-2] and MARS at Fermilab [3-4]. Both codes have been extensively used and validated in past studies for LHC and many other applications. Both FLUKA and MARS simulations used identical models of the HL-LHC machine geometry and materials, and the results are in close agreement. A comprehensive analysis of the radiation effects for the High Luminosity LHC is reported in [5] and references therein. Details of the IR quadrupole model are shown in Figure 4.29.

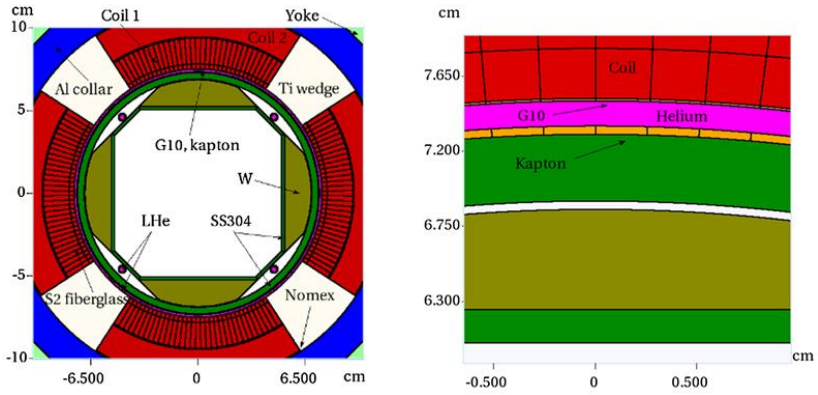

Figure 4.29: Details of the model used both in FLUKA and MARS for the inner region of the IR quadrupole Q1 (in Q2-Q3 a thinner tungsten absorber is used). [5]

The power density and dynamic heat load are normalized to a luminosity of $5\times10^{34}\text{cm}^{-2}\text{s}^{-1}$. The absorbed dose, neutron fluence and DPA are normalized to an integrated luminosity of 3000 fb^{-1}. Figure 4.30 shows the longitudinal profile of the peak power density on the inner coils of the IT magnets. The peak value in the Nb_3Sn quadrupoles is 2 mW/cm^3, considerably lower than the quench limit at the operating point. For the total length of the cold mass, the average dynamic heat load on it is ~14 W/m. This is within a design range of 10–15 W/m used for the LHC and assumed for the HL-LHC.

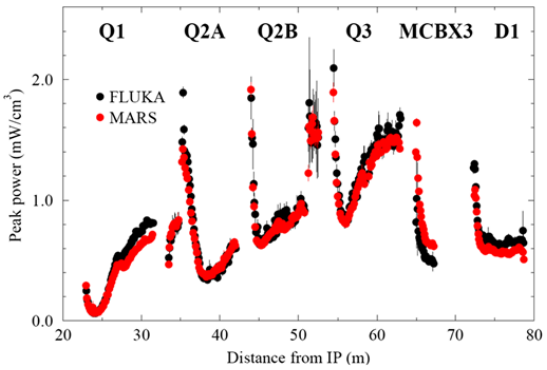

Figure 4.30: Longitudinal peak power density profile on the inner coils of the IT magnets [5].

Figure 4.31 shows the longitudinal profile of peak dose on the inner coils and insulating materials. Thanks to the increased aperture and tungsten absorbers, the dose in the HL-LHC inner triplet at 3000 fb^{-1} is comparable that of the present LHC at 300 fb^{-1}. The peak dose in the insulation reaches 28-30 MGy. The results of a detailed characterization of the radiation resistance of the ceramic epoxy used for MQXF are reported in [6]. The materials have been irradiated with 50 MGy, using 4 MeV electron beam at 77 K which well reproduces the expected radiation spectrum for the IR magnet case. The electrical strength of the irradiated samples was found to be between 45 kV/mm and 65 kV/mm, which is still significantly higher than the required 5 kV/mm. This provides adequate margin for the HL-LHC integrated luminosity target. Further studies of the beam screen and absorber configuration are underway to guide the engineering design incorporating all details required for fabrication and installation of these components.

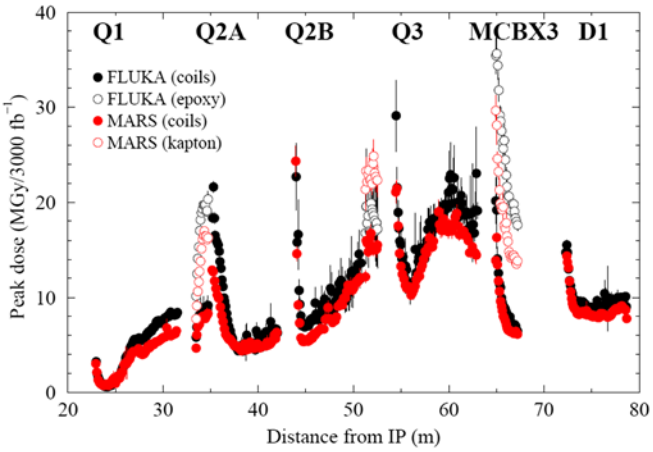

Figure 4.31: Longitudinal peak dose profile on inner coils and nearby insulators. [5]

The radiation effect on Nb_3Sn superconductor, copper stabilizer and structural components is best characterized by integrated neutron fluence and DPA over the expected magnet lifetime. Figure 4.32 shows the corresponding profiles on the quadrupole inner coils, where the peaks are located.

The highest DPA is about 2×10^{-4} DPA per 3000 fb−1 integrated luminosity, which is acceptable for the superconductor assuming periodic annealing during the collider shutdowns. A similar conclusion can be reached by comparing the neutron fluence in the coils with the known limits. In the quadrupole coils, the peak fluence is $\sim2\times10^{17}$cm^{-2} which is substantially lower than the 3×10^{18}cm^{-2} limit used for the Nb_3Sn superconductor. The integrated DPA in the magnet mechanical structures is 0.003 to 0.01 in the steel beam screen and tungsten absorber, $\sim10^{-4}$ in the collar and yoke, and noticeably less outside. These are to be compared to a ~10 DPA limit for mechanical properties of these materials. Neutron fluence in the IT mechanical structures range from 3×10^{16} cm^{-2} to 3×10^{17} cm^{-2} compared to the 10^{21} cm^{-2} to 7×10^{22} cm^{-2} limits.

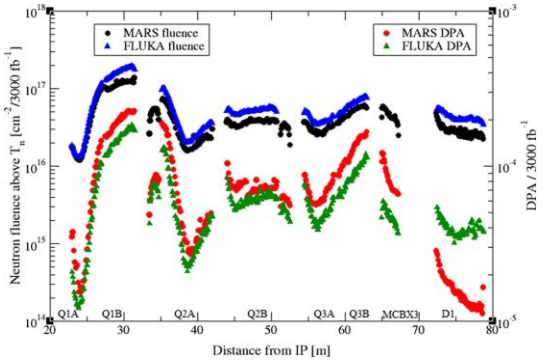

Figure 4.32: Longitudinal peak neutron fluence and peak DPA profiles along the hottest regions in the IT magnet coils [5].

References

[1] A. Ferrari et al., FLUKA, a multiparticle transport code, Report No. CERN-2005-010, 2005.

[2] T. Böhlen, F. Cerutti et al., The FLUKA code: Developments and challenges for high energy and medical applications, Nucl. Data Sheets 120, 211 (2014).

[3] N. Mokhov et al., MARS15 overview AIP Conf. Proc. 896, 50 (2007).

[4] N. Mokhov et al., MARS15 code developments driven by the intensity frontier needs, Prog. Nucl. Sci. Technol. 4, 496 (2014).

[5] N. V. Mokhov, F. Cerutti et al., Energy deposition studies for the high-luminosity Large Hadron Collider inner triplet magnets, Physical Review Special Topics - Accelerators and Beams 18, 051001 (2015)

[6] J. Polinski et al., Certification of the radiation resistance of coil insulation materials, EuCARD report July 31, 2013.

4.5 Thermal Design

The final focusing magnets will receive a heat load due to debris coming from the adjacent particle interaction points: the computed peak heat deposition in the coil is of the order of 7 mW/cm3 ([1], [2]).

The cooling method is based on the one used in the present LHC, and the overall cryogenic infrastructure needed is similar to the existing configuration. The cooling performance is evaluated in terms of temperature margin of the magnets under full steady state heat load conditions, and in terms of local maximum sustainable load.

An annular gap, filled with He, separates the cold bore from the superconducting coil, which is surrounded by the mechanical support structure to form the cold mass. The cold-mass is enclosed in a vessel, to be kept at the chosen operating temperature and supported in a vacuum insulated cryostat. This section is focused on the cooling configuration specific to the cold mass.

The heat loads due to debris from the adjacent interaction point are intercepted at two distinct magnet locations and temperature levels. A first heat intercept is on tungsten absorbers which are placed inside the beam pipe vacuum and which will be cooled in the 40 K to 60 K range. The remaining heat load will fall on the cold mass volume comprised of the yoke, collars and coils. For the purpose of the evaluation of the cooling, the heat load to the cold masses is taken at 1050 W for an ultimate luminosity of 7.5×1034 cm-1 s-1.

4.5.1 Cooling requirements for magnet cold masses

The cooling principle, depicted in Figure 4.33 is an evolution of the one proposed for the LHC-Phase-I Upgrade [3]. The cold masses will be cooled in a pressurized static superfluid helium bath at 1.3 bar and at a temperature of about 1.9 K. The heat generated in the magnets will be extracted by vaporization of superfluid helium which travels as a low pressure two-phase flow in two parallel bayonet heat exchangers (HX) protruding the magnet yokes (depicted as one bold line in Figure 4.33). The low vapor pressure inside the heat exchanger is maintained by a cold compressor system, with a suction pressure of 15 mbar, corresponding to the saturation temperature of 1.776 K.

The flow diagrams for the four site implementations (Left of IP1, Right of IP1, Left of IP5, and Right of IP5), are very similar. They differ in orientation left-right, so Q1 will always face the IP, and have slope dependence for the He II two-phase flow in the HX, so the flow is always down-stream. Figure 4.34 shows the flow diagram version applicable to the right side of IP5. On top are depicted the supply headers for cryogens, with two jumper connections between it and the magnet cryostats. All cryogenic valves are on the supply header-side.

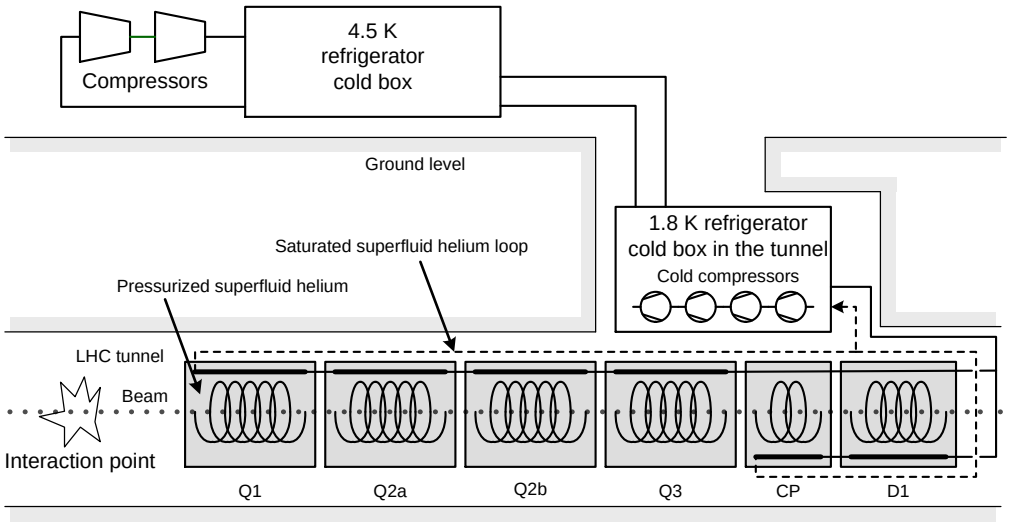

Figure 4.33: Architecture of the cooling by using superfluid helium.

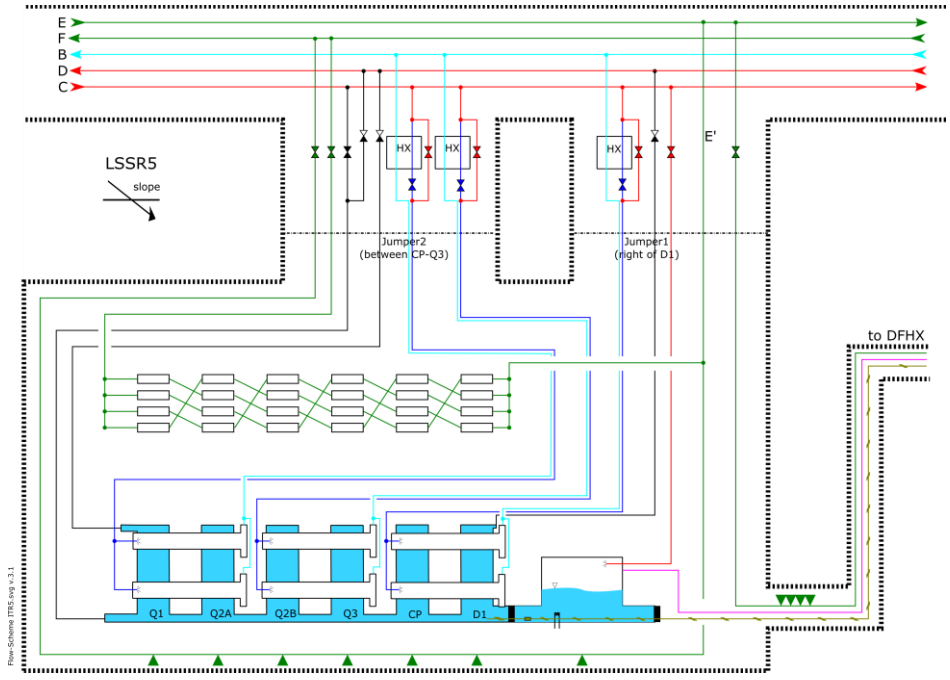

Figure 4.34: flow diagram for inner triplets, right of IP5

Due to constraints on magnet design, the bayonet heat exchangers cannot be continuous all the way from the quadrupole magnets through the corrector package and D1 dipole. The size and number of heat exchangers is determined by the maximum vapor velocity of 7 m/s above which the heat exchangers do not function anymore and the total available heat exchange area, when they are

wetted over their full length. For the quadrupole heat exchangers, the vapor velocity limit is the more stringent condition and is met if one uses two heat exchangers in parallel with inner diameters greater than 68 mm and lengths limited to two quadrupoles in series. As a consequence, the flow diagram exhibits three sets of bayonet heat exchanger cooling-units (D1+CP, Q3+Q2b, Q2a+Q1), each with their own supply and low vapor pressure return. These supply and return lines are forcibly proper to the cooling loops such as to keep the counter flow heat exchangers, situated on the cryogenic supply headers' side, balanced. Each of these cooling loops integrates a phase separator at its end. These have to absorb the liquid present in the bayonet heat exchangers in case magnet quenches would drive it out. The liquid volumes to accumulate, without obstructing the low-vapor pressure return inlet, are estimated to be 12.5 ℓ for each of the quadrupole cooling loops and 5.5 ℓ for the D1+CP cooling loop.

The heat exchangers themselves are to be made of copper to assure proper heat conduction across the walls. A wall thickness of about 3 mm is required to sustain the external design pressures of 20 bar. With, in addition, an annular space of 1.5 mm between the HX and the yoke to allow contact area of the pressurized superfluid helium on the coil-side, the yoke-hole size required is 77 mm minimum. With this configuration about 800 W can be safely extracted. The 77 mm yoke-hole size is compatible with the mechanical design of the magnet, but should not be increased otherwise one would need to increase as well the overall diameter of the cold mass. Coping with the remaining 250 W is to be done via active cooling of the D1 and CP. Two parallel bayonet heat exchangers of 51 mm ID through D1 and CP are foreseen, requiring yoke holes of 60 mm diameter.

For correct functioning of the two-phase heat exchanger configuration, heat must be given some freedom to redistribute along the length of the cold-masses. This is no hard criterion, and a free longitudinal area of $\geq 150\ cm^2$ through the Q1, Q2a, Q2b, Q3, and their interconnections and $\geq 100\ cm^2$ through D1, CP and their interconnections are deemed to be sufficient.

Two pressure relief devices are foreseen as safety in case of sudden energy release to the cold mass helium due to either magnet quenches or catastrophic loss of insulation vacuum. The quench energies released are substantial for the MQXF – quadrupoles and D1 – dipole only. The energy per local helium volume for the magnets in the corrector package are so low that they can be absorbed by the surrounding helium without consequences for the neighboring magnets

4.5.2 Radial heat extraction in IR quadrupoles

The Nb_3Sn quadrupole coils are fully impregnated, without any helium penetration. The heat loads from the coils and the beam-pipe area can only evacuate to the two heat exchangers by means of the pressurized He II. To this end, the cold mass design needs to incorporate the necessary radial helium passages.

Figure 4.35 shows the typical heat flow path: out from the coil areas, through the annular spacing between cold bore and inner coil-block, and subsequently via free passages through the titanium pole pieces and G10-alignment key, and around the axial rods towards the cooling channels where the two-phase flow bayonet heat exchangers will be inserted. They will occupy the two-upper yoke-holes marked "Cooling channel". Since only two of the four possible cooling channels will house bayonet heat exchangers, free helium paths interconnecting these four cooling channel holes shall be implemented in the cold mass design. Doing so allows for equilibrating the heat flows and increasing the heat extraction margins as a whole.

The annular space between cold bore and inner coil block is set at 1.5 mm and the free passage needed through the titanium insert and G10-alignment key should be of the order of 8 mm holes

repeated every 40 mm – 50 mm along the length of the magnet. Magnet design is presently integrating 8 mm diameter holes every 50 mm. This value and repetition rate will be used in the temperature margin evaluation in subsequent paragraphs. Around the axial rods a free passage of 1.5 mm has to be guaranteed.

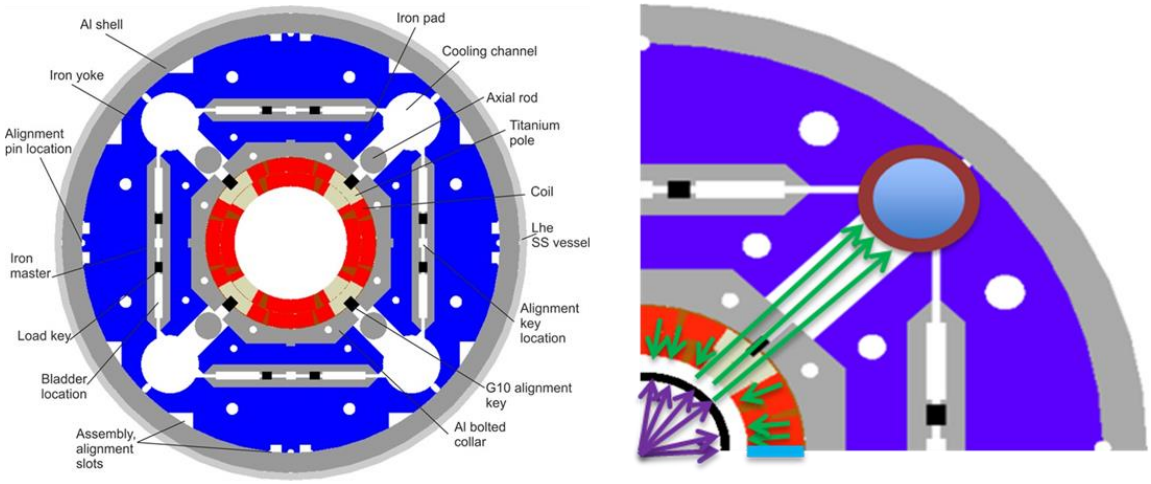

Figure 4.35: Heat flow paths from coil to one of the two-phase heat exchangers located in the upper right quadrant

4.5.3 Thermal performance evaluation

The heat load distribution at the most unfavorable location is used as reference (Figure 4.36) [3]. The peak power densities reached in the quadrupoles are close to 7 mW/cm^3.

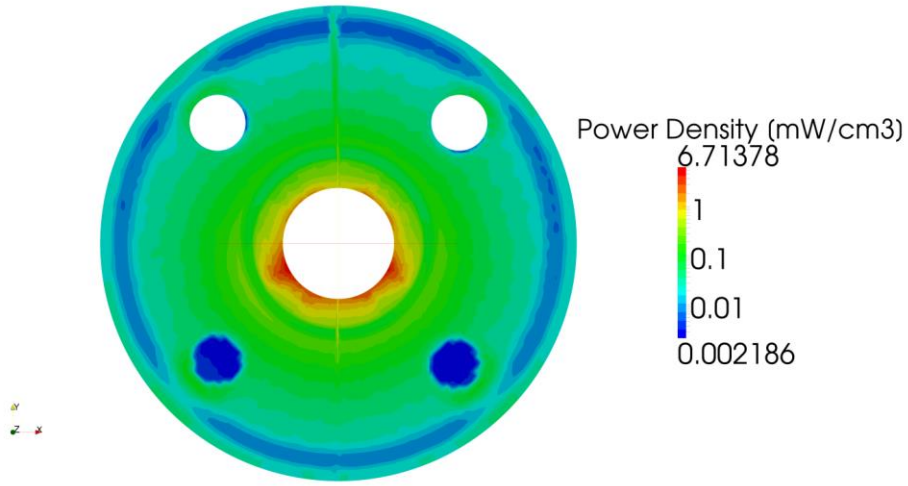

Figure 4.36: Power deposition map for Q3 at ultimate peak luminosity.

These power deposition maps are used as input to produce temperature distribution maps of the cold masses. The results are then converted into temperature margin maps by comparison with the

respective current sharing maps, calculated on an assumed homogeneous temperature distribution of 1.9 K (Figure 4.37).

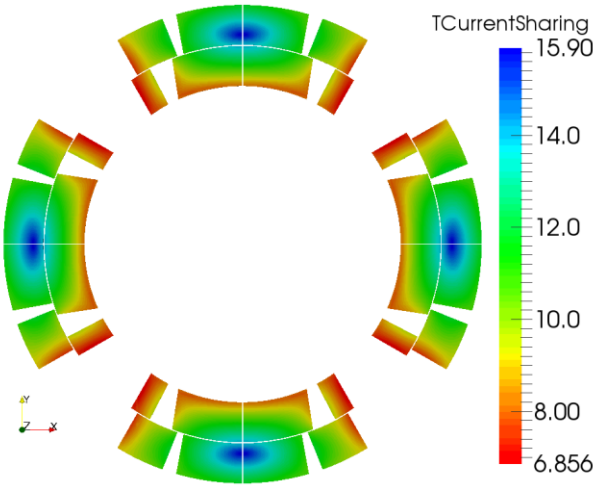

Figure 4.37: Current sharing map of MQXF quadrupole.

The MQXF-quadrupole coil materials were implemented with the coil pack details as shown in Figure 4.38. "Porous" quench heaters are assumed to be placed on the MQXF inner coil layer (Figure 4.39). This assumption will give conservative results (as these are right in the heat extraction path), should the inner layer quench heater later be retracted from the quench protection scheme.

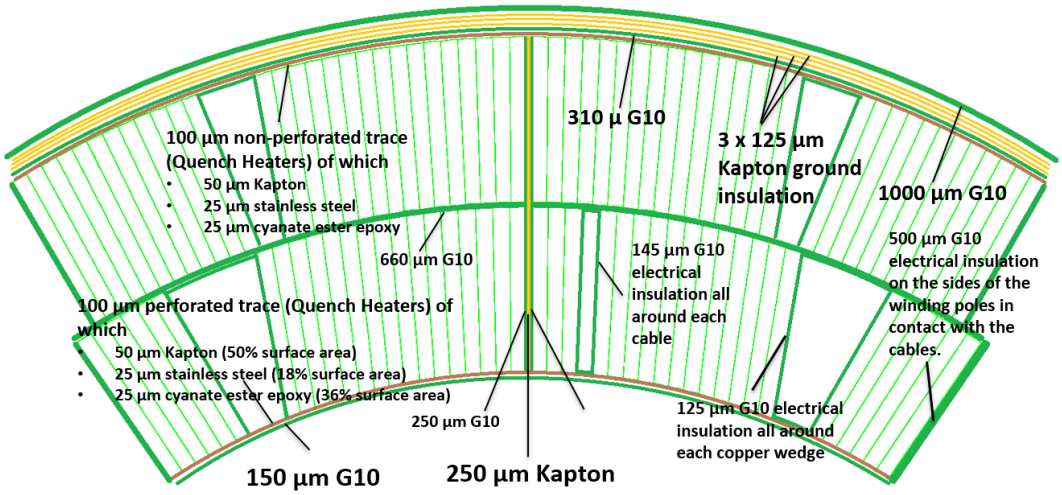

Figure 4.38: Quadrupole Nb_3Sn coil materials assumed for the calculations.

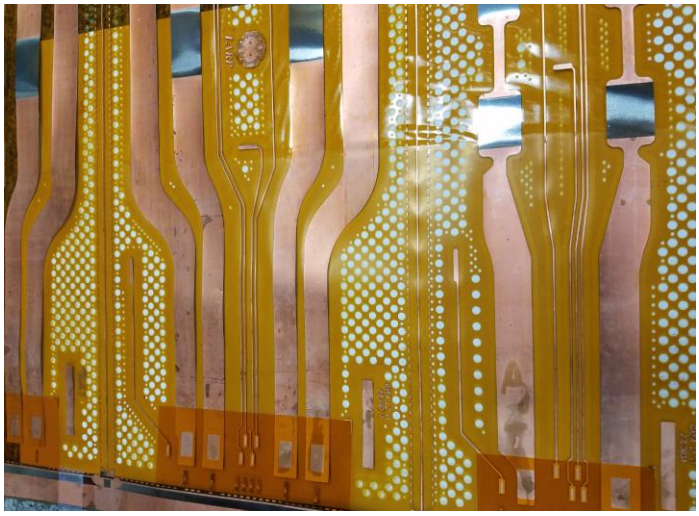

Figure 4.39: Perforated Kapton quench heaters.

4.5.4 Steady state temperature distribution, T margin and local maximum-sustainable load

Figure 4.40, Figure 4.41, Figure 4.42 and Figure 4.43 show the temperature and temperature-margin maps with their respective zooms. These were all calculated assuming a 1.9 K cold source (bayonet heat exchanger) temperature. Although the highest temperatures of about 3.15 K are reached in the outer coil layer, when combined with the current sharing maps, we find the most critical zones at the inner layer pole edges. There, the temperature margin goes down to about 4.1 K. Note that The value of 4.1 K is reached in a small fraction of the coil (Figure 4.43), and further optimization of the beam screen W absorber could remove this singularity and bring the temperature margin above 5 K all over the coil.

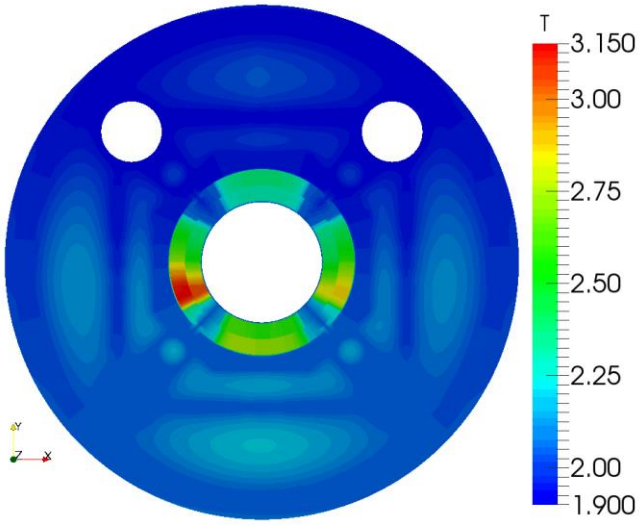

Figure 4.40: MQXF quadrupole temperature map; full section.

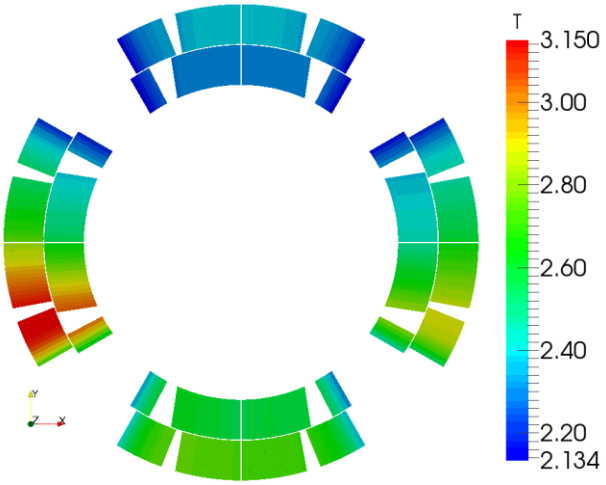

Figure 4.41: MQXF quadrupole temperature map; coil section.

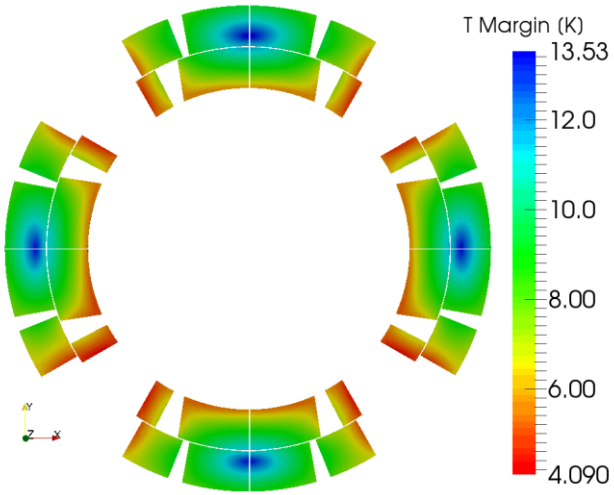

Figure 4.42: MQXF quadrupole temperature-margin map.

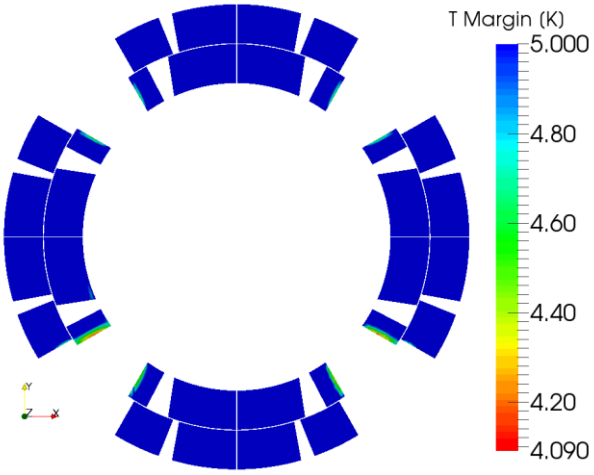

Figure 4.43: MQXF quadrupole temperature-margin map, capped off at 5 K to expose the critical zones.

The robustness of the MQXF thermal design is addressed by steady state local power deposit values that the coil can withstand without either the cooling breaking down or the cable reaching a temperature margin of 0 K. We found that in these steady state cases the local cooling break-down occurs first. Figure 4.44 shows that locally we can sustain powers from 56 mW/cm^3 at 1.9 K down to 19 mW/cm^3 at 2.1 K bayonet heat exchanger temperature. This constitutes a factor 8 at 1.9 K down to 3 at 2.1 K with respect to the expected peak load of 6.7 mW/cm^3 at ultimate luminosity.

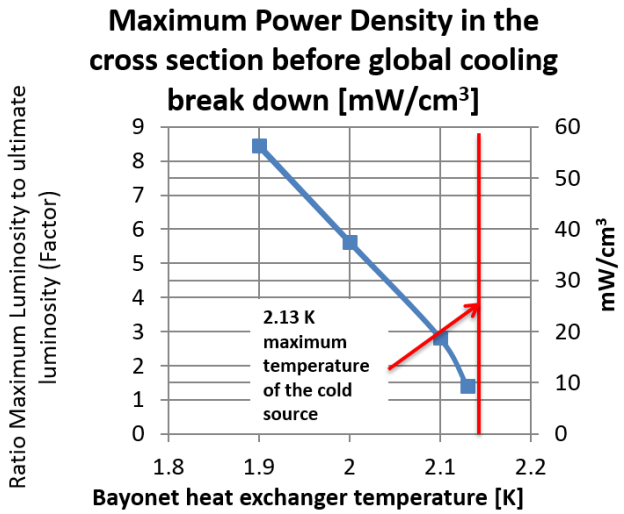

Figure 4.44: MQXF Quadrupole steady state power margin.

References

[1] *Energy deposition on triplet and D1*, L. Esposito, Joint HiLumi LHC-LARP Annual Meeting 2014, Tsukuba, Japan,

[2] *Recap of energy deposition*, F. Cerutti, WP3 Collaboration meeting, 21-08-2015

[3]*The Cryogenic Design of the Phase I Upgrade Inner Triplet Magnets for LHC*, van Weelderen, R.; Vullierme, B.; Peterson, T., 23rd International Cryogenic Engineering Conference, Wroclaw, Poland, 19 - 23 Jul 2010

4.6 Quench Protection

The requirements for MQXFA magnets protection in operating conditions are: hot-spot temperature < 350 K (based on analysis and recommendation presented in [1]; and coil-ground voltages < 1 kV (standard practice to keep the room temperature high-pot voltage < 5 kV).

The MQXFA is protected with a combination of quench heaters (QH) and Coupling-Loss Induced Quench (CLIQ) system [2-5]. Upon quench detection, both QH and CLIQ units are triggered simultaneously. The QH units introduce a current through the QH strips attached to the coil and heat up the conductor by heat diffusion through a thin insulation layer. The CLIQ units introduce oscillations in the magnet transport currents. The resulting local magnetic-field change introduces high inter-filament coupling loss, which heat the copper matrix of the strands. The two systems together constitute an effective synergy since they are based on different heating mechanisms and they deposit energy mainly in different parts of the winding pack.

Each magnet is equipped with 16 quench heater strips glued to the outer layers, 8 quench heater strips glued to the inner layers, and with two CLIQ terminals. Dedicated experimental studies are foreseen, aimed at demonstrating the quench protection of the MQXF magnets in the LHC tunnel and at assessing the performance of different types of quench heater strips, of alternative CLIQ configurations, and of combinations of these.

4.6.1 Quench heater strips

Six quench heater strips are glued to each pole:

- Two strips to the outer layer in the mid-plane low-field region (B01, B04)
- Two strips to the outer layer in the high-field region (B02, B03)
- Two strips to the inner layer (A01, A02)

The designs chosen for the outer and inner strips are “Copper-plated heater design 2 OL” and “Copper-plated heater design 2 IL”, with reference to the naming used in the MQXFS1 design report [6]. The design of the heater strips is schematized in Figure 4.45, and their position in the coil cross-section is shown in Figure 4.46. Note that the strips of each pole are numbered starting from the strip closest to the lead end.

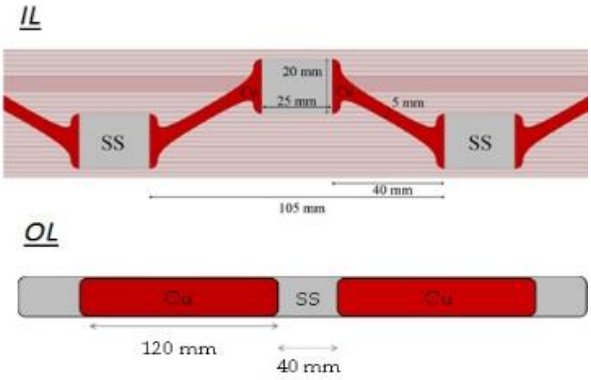

Figure 4.45: Design of the heater strips attached to the MQXFA magnets. Only three inner layer and two outer layer stations are shown.

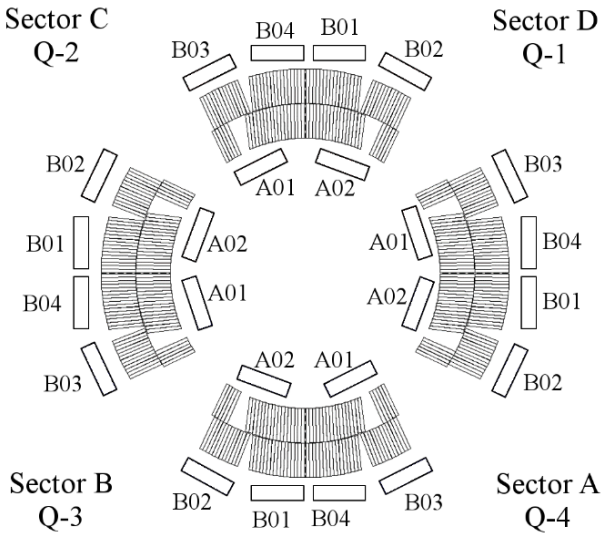

Figure 4.46: Position of the heater strips attached to the MQXFA magnets, viewed from the lead side.

The main parameters of the two types of heater strips and their estimated resistances at cryogenic and room temperature are summarized in Table 4.9. For the resistance calculations, the applied magnetic field is considered nihil, the resistivity of stainless steel is assumed to be 5.45E-7 and 7.31E-7 Ωm at 10 and 293 K, respectively (RRR=1.34), and that of copper 6.00E-10 and 1.76E-8 Ωm, respectively (RRR=29).

Table 4.9: Parameters of the quench heater strips attached to the MQXFA magnet

QH strip location	High-field outer layer	Low-field outer layer	Inner layer
QH design type [6]	Cu-plated 2 OL	Cu-plated 2 OL	Cu-plated 2 IL
Strip length [m]	4	4	4
Heater SS width [mm]	20	20	20
Heater Cu width [mm]	20	20	5
Heater SS thickness [mm]	0.025	0.025	0.025
Heater Cu thickness [mm]	0.01	0.01	0.01
Station length [mm]	40	40	25
Station period [mm]	160	160	65
Number of stations	25	26	62
Strip resistance @ 10 K [Ω]	1.10	1.14	1.73*
Strip resistance @ 293 K [Ω]	1.73	1.80	3.27*
Note: For the “Cu-plated 2 IL” design, the length of section between heating stations is approximated as (station period - station length)*1.15			

Each pair of QH strips is connected in series to an LHC standard QH power supply, featuring a capacitor bank of 7.05 mF charged to 600 V. In order to reduce the peak voltages to ground in the case of QH failures, the pairs are composed of strips glued to poles that are opposite to each other (P1-P3 and P2-P4), as shown in Figure 4.46. The resistance of the copper leads connected to the strips is assumed to be 0.6 Ω per circuit, the same as the present LHC QH circuits. The expected performances of the QH circuits are summarized in Table 4.10.

Table 4.10: Expected performances of the QH circuits protecting MQXFA

QH strip location	High-field outer layer	Low-field outer layer	Inner layer
Number of strips in series	2	2	2
Strip resistance @ 10 K [Ω]	1.10	1.14	1.73
Resistance of the warm leads [Ω]	0.60	0.60	0.60
QH circuit resistance @ 10 K [Ω]	2.80	2.89	4.05
QH supply charging voltage [V]	600	600	600
QH supply capacitance [mF]	7.05	7.05	7.05
Peak QH current [A]	214	208	148
QH discharge time constant [ms]	20	20	29
Peak QH power density [W/cm^2]	250	235	120
QH energy density [J/cm^2]	2.47	2.40	1.71

4.6.2 CLIQ terminals and leads

Each cold mass (Q1/Q3) is composed of two MQXFA magnets, powered in series. The MQXF electrical circuit is presented in [7]. The presence of parallel elements (thyristors, diodes) across each cold mass allows analyzing the discharge of each cold mass separately. In Figure 4.47, the part of the circuit corresponding to one cold mass is schematized. Each two MQXFA magnets are protected by two CLIQ units connected as shown in Figure 4.47. Two CLIQ leads are attached to each magnet, located at the joint between two electrically connected poles (see taps a and b shown in Figure 4.47). Their terminals are connected at the coil ends in the "pizza box" in Figure 8.10. The electrical order of the four poles is as follows: Q-1, Q-4, Q-2, Q-3 [8]. The resulting configuration, called "Crossed-Poles", allows introducing opposite current changes in poles which are physically adjacent (P1-P3 and P2-P4), which is the most effective option for this magnet [2,5].

Each CLIQ unit features a 40 mF capacitor bank charged to 600 V.

The parameters of the conductor used for the CLIQ leads are summarized in Table 4.11. The copper cross-section of the leads is dimensioned to avoid overheating during the CLIQ

discharge and to not limit the CLIQ performance due to an excessive electrical resistance. The temperature in the leads is expected to remain well below 300 K.

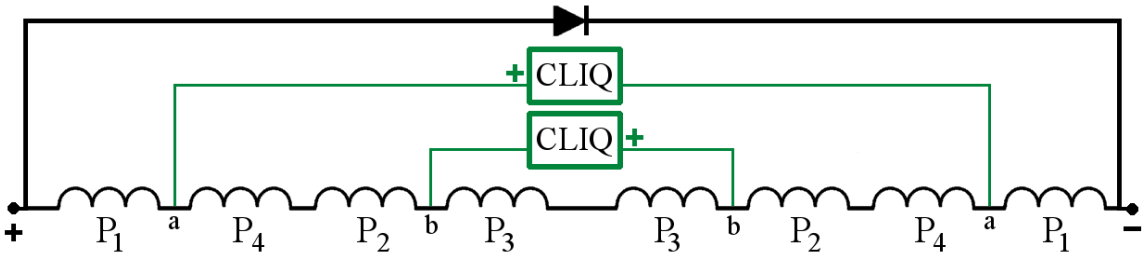

Figure 4.47: MQXFA electrical order of the poles and position of the CLIQ terminals.

Table 4.11: Parameters of the conductor used for the CLIQ leads of the MQXFA magnet

Parameter	Value
Material	Copper
Construction	133 filaments
Filament diameter	0.361 mm
Strand diameter	5.14 mm
Conductor area	13.61 mm^2
Conductor resistance per unit length	1.4 mΩ/m
Insulation material	Extruded polyimide
Strand diameter with insulation	6.0 mm
RRR	>100

4.6.3 Expected quench protection performance

The detailed study of the MQXF quench protection and redundancy is presented in [7]. This analysis actually shows the performance of the protection system in the case of the 7.15 m long Q2a/Q2b magnets, which have the same cross-section and conductor parameters but different length. However, the same limits and safety factors on the coil's hot-spot temperature and peak voltage to ground are assumed for the longer and shorter magnets. In particular, the electrical quality assurance of the 4.2 m long MQXFA magnet will be performed at the same voltages as the 7.15 m long magnet.

Three options for the quench protection system are analyzed in the above-mentioned report:

- QH attached to the coil's outer layers (O-QH)
- QH attached to the coil's outer and inner layers (O-QH + I-QH)
- QH attached to the coil's outer layers and CLIQ (O-QH + CLIQ).

The main quench protection simulation results, at nominal and ultimate current, are summarized in Table 4.12. Sensitivity to strand parameters and initial quench position are included

in the analysis. It is shown that a protection system including only quench heaters attached to the coil's outer layers does not offer the required level of redundancy and barely maintains the coil's hot-spot temperature below 350 K, which is considered a conservative limit against permanent degradation. On the contrary, the other two protection options effectively protect the magnet and limit the hot-spot temperature well below 350 K.

The consequences of QH circuit failures are studied, and the results reported in Table 4.13. The worst-case considered in the analysis is the failure of two independent QH circuits. Before the publication of the report [7], the worst-case $U_{g,peak}$ reference value was 520 V, calculated in the case of O-QH+CLIQ [8]. The increase with respect to this value comes from the improvement in the model accuracy and from the detailed analysis of the effect of the initial hot-spot position. However, it is recommended that no correction of the test values during electrical quality be asked, considering that prudent safety margins were applied.

Table 4.12: Simulated coil hot-spot temperature T_{hot}, peak voltage to ground $U_{g,peak}$ and peak turn to turn voltage $U_{t,peak}$ obtained after a quench at nominal and at ultimate current, for varying fraction of copper in the conductor, RRR and strand diameter. Uncertainty ranges also include the effect of different quench locations.

Configuration	T_{hot} [K]	$U_{g,peak}$ [V]	$U_{t,peak}$ [V]
Nominal current			
O-QH	293-364	304-619	62-123
O-QH + I-QH	230-263	438-592	46-90
O-QH + CLIQ	215-248	521-658	49-90
Ultimate current			
O-QH	312-389	362-860	72-145
O-QH + I-QH	253-290	552-766	57-109
O-QH + CLIQ	237-273	664-924	61-109

Table 4.13: Failure case analysis. Simulated hot-spot temperature, peak voltage to ground and peak turn to turn voltage obtained for one failure or two simultaneous failures of QH circuits, at nominal and at ultimate current. Uncertainty ranges are due to the different locations of the initial quench and of the failing QH circuits.

Configuration	T_{hot} [K]			$U_{g,peak}$ [V]			$U_{t,peak}$ [V]		
	No f	1	2	No f	1	2	No f	1	2
Nominal current									
O-QH	330-345	345-362	363-384	577	702	868	113	122	132
O-QH + I-QH	251-253	255-266	277-283	561	716	928	83	90	100
O-QH + CLIQ	236-237	238-240	239-242	641	668	666	83	84	86
Ultimate current									

O-QH	352-369	364-385	379-406	808	916	1068	133	141	152
O-QH + I-QH	276-279	279-292	301-310	725	898	1128	101	109	120
O-QH + CLIQ	260-262	261-264	262-267	874	910	909	101	103	105

4.6.4 Quench protection during single magnet tests

During the test of a single MQXFA magnet, one 40 mF, 600 V CLIQ unit is connected to the magnet. The resulting configuration, shown in Figure 4.48, allows introducing in the magnet poles the same oscillating currents as in the baseline LHC configuration.

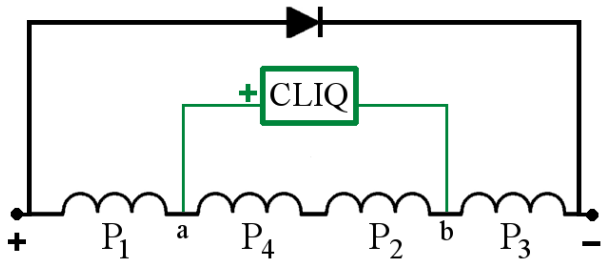

Figure 4.48: MQXFA electrical order of the poles and position of the CLIQ terminals.

4.6.5 Quench protection during cold mass tests

During the test of an entire cold mass, composed of two MQXFA magnets in series, the CLIQ configuration identical to the final LHC machine case. Accordingly, the CLIQ connection scheme follows that presented in Figure 4.47.

References

[1] G. Ambrosio, “Maximum allowable temperature during quench in Nb_3Sn accelerator magnets”, CERN Yellow Report CERN-2013-006, pp.43-46, doi: 10.5170/CERN-2013-006.43.

[2] E. Ravaioli, “CLIQ”, PhD thesis University of Twente, The Netherlands, 2015, doi: 10.3990/1.9789036539081.

[3] E. Ravaioli et al., “New, Coupling Loss Induced, Quench Protection System for Superconducting Accelerator Magnets”, IEEE Trans. Appl. Supercond., vol. 24, no. 3, June 2014, doi: 10.1109/TASC.2013.2281223.

[4] E. Ravaioli et al., “Protecting a Full-Scale Nb3Sn Magnet with CLIQ, the New Coupling-Loss Induced Quench System”, IEEE Trans. Appl. Supercond., vol. 25, no. 3, June 2015, doi: 10.1109/TASC.2014.2364892.

[5] E. Ravaioli et al., “Quench Protection System Optimization for the High Luminosity LHC Nb_3Sn Quadrupoles”, IEEE Trans. Appl. Supercond., 2017.

[6] G. Ambrosio, P. Ferracin, et al., “MQXFS1 quadrupole design report”, LARP note, 2015.

[7] E. Ravaioli, "Quench protection studies for the High Luminosity LHC inner triplet circuit", HL-LHC report, 2016.

[8] J. DiMarco, GL. Sabbi, and X. Wang, "Coordinate system for magnetic measurements of MQXF magnet", LARP note, 2015.7

5 MQXFA Coils

5.1 Coil Design and Parts

The QXFA coil is a two-layer cos-2θ coil with saddle-shaped ends. The two-layer coil is wound continuously, without a splice at transition between the inner and outer layers, using the double-pancake technique successfully used in all LARP coils and by several other Nb_3Sn magnets. The cross-section for magnetic design is shown in Figure 5.1. The coil inner radius is 75 mm, and the outer radius is 112.966 mm. In order to ensure reaching the target dimensions, the coil size is controlled at each fabrication step (described in the following paragraphs).

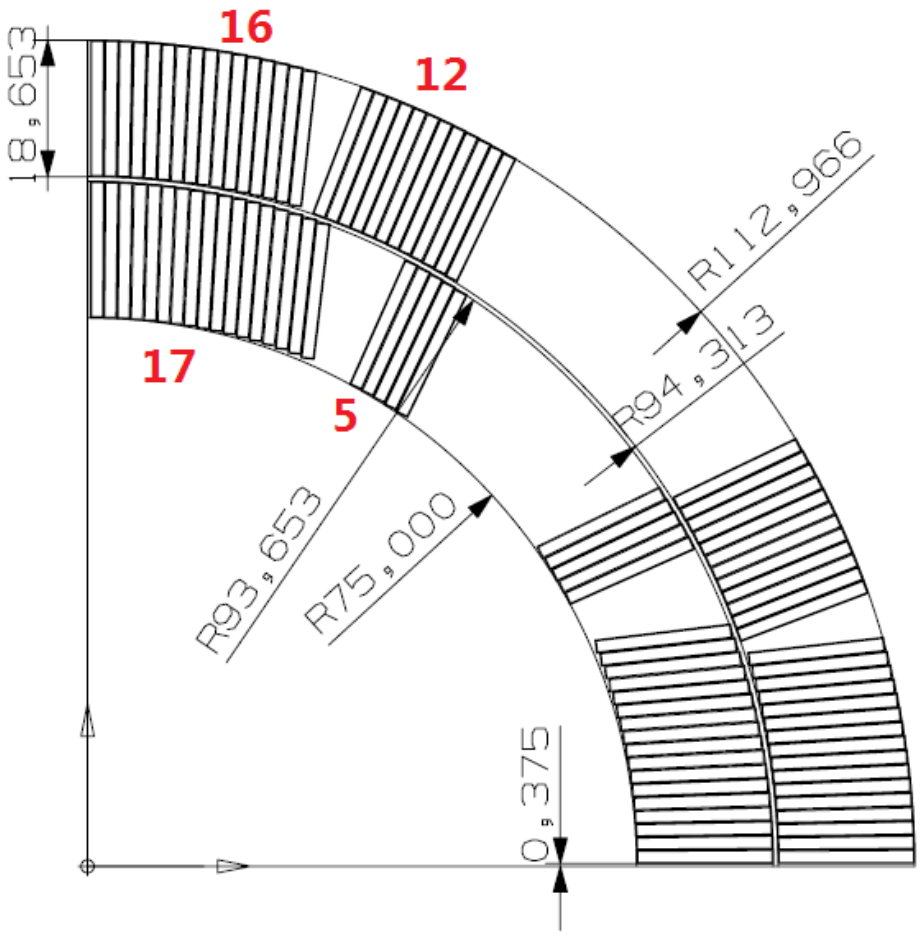

Figure 5.1: Coil Cross-section.

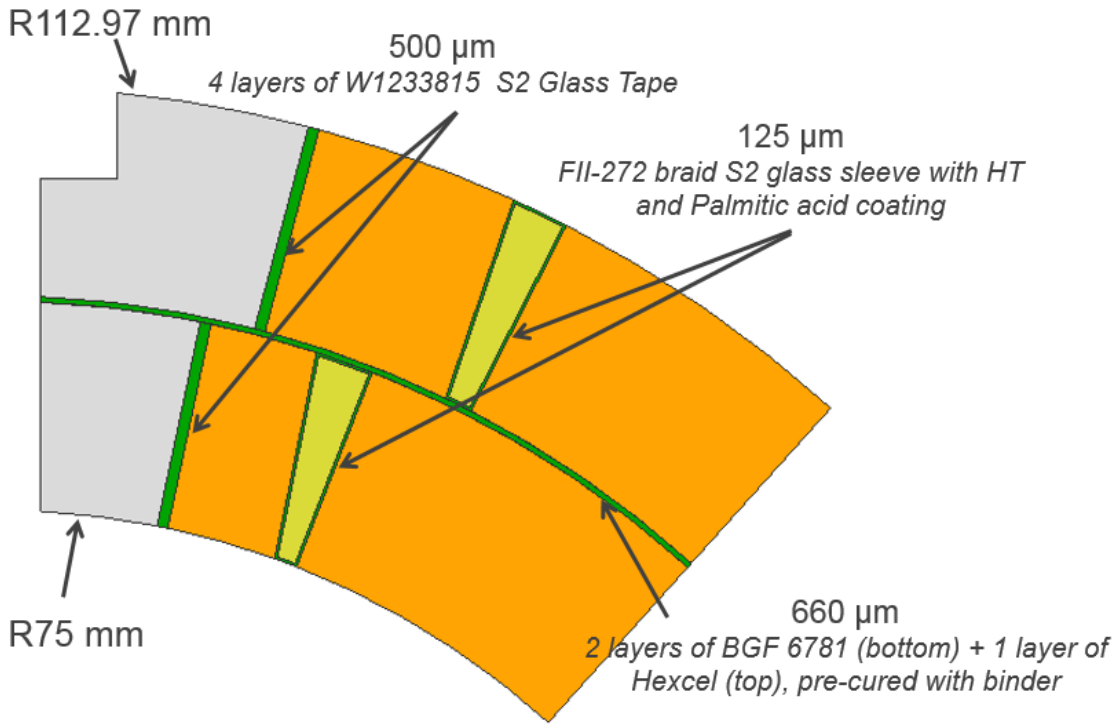

Figure 5.2: Coil Insulations.

The coil model is shown in Figure 5.3. To meet the requirement of a magnetic length of 4.2 m, the overall coil length will be 4.532 m. Due to the remaining pole gap after the fabrication, the coil length may vary from 4.532 m to 4.54 m.

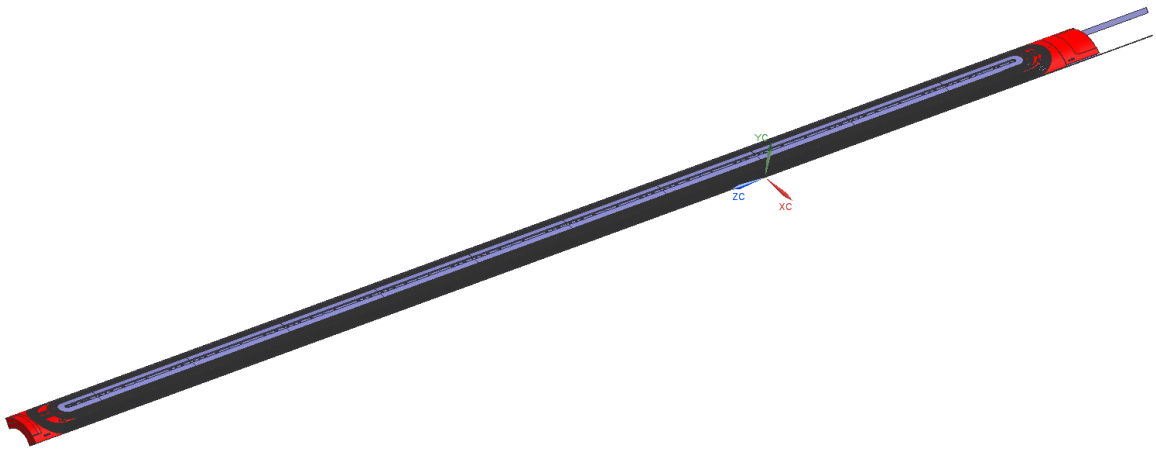

Figure 5.3: QXFA Coil Model

- **Pole Parts**

The QXFA coil is wound around the pole parts, and there are 1 piece of lead end pole, 9 pieces of center pole and 1 piece of return end pole for both the inner and the outer layer coil, as shown in Figure 5.4. Pole parts between inner and outer layers are aligned through the 8 mm dowel pins. The poles are bolted to the winding anchor bars through clearances holes. The fabricated coil is lifted through lifting holes. Both clearance holes and lifting holes are designed with minimum 8 mm diameter and 50 mm spacing. These holes are used as cooling channels to extract the heat from the coil aperture to the heat exchangers in the yoke. The pole parts are made of Ti-6Al4V STA (solution treated aging process) to have better straightness and strength.

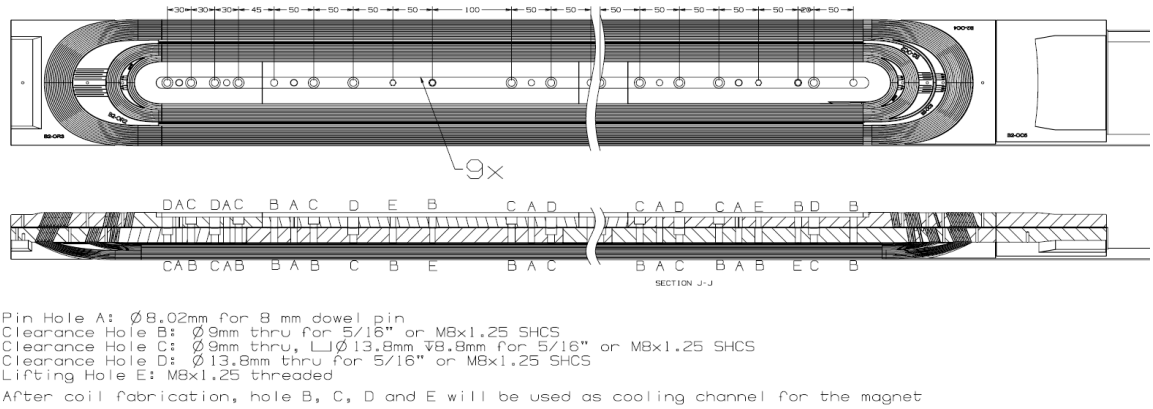

Figure 5.4: Pole Parts Layout

- **Wedges**

The wedge is fabricated through the extrusion process to have the best uniform shape for each coil. Witness notches are added to each wedge for identification and orientation. Figure 5.5 shows the wedges cross-section for both the inner layer and the outer layer coil. The wedges are made of phosphor bronze to have the similar thermal properties as Nb_3Sn cable.

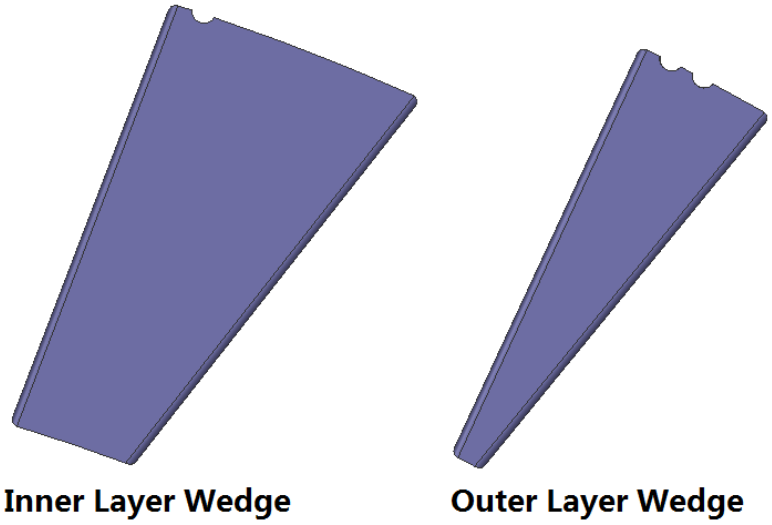

Figure 5.5: Wedges.

- **End Parts**

End parts, saddles and splice block are designed based on the nominal coil size after reaction. End parts have been designed and optimized using BEND and ROXIE, and both designs work well. LARP uses BEND parts, while CERN uses ROXIE parts.

During winding, the coil is not fully constrained inside the envelope. This effect is most pronounced at the ends. Prior to curing, the cable tries to separates from radial surface of the mandrel in some areas (springback), causing the shape of the turn not to match the shape of the end parts. The springback is larger with larger coil aperture and cable size. Therefore, flexible features (slits) have been introduced in QXFA coil design (Figure 5.6). This is an incremental change with respect to single slit design previously used in LARP coils. The end parts are made of SS 316L.

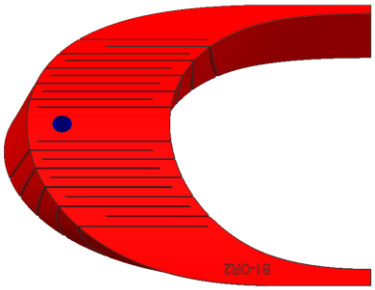

Figure 5.6: Slits Design for End Parts

End parts are plasma coated at 250 µm thickness to increase the dielectric strength. For identification number, instead of using the drawing number, Bx-xxx is adopted, where B represents BEND, the first "x" after B represents the design generation (the latest design generation is 2), the second "x" shall be either I (inner layer) or O (outer layers), the third "x" shall be either R (return end) or C (lead end), and the fourth "x" represents end part's number. For example, 2nd generation design, inner layer LE spacer 2, the identification number is B2-IC2. The identification number for each part is shown in Figure 5.7, which is laser cut on the surface of the part, and after coating it is still visible.

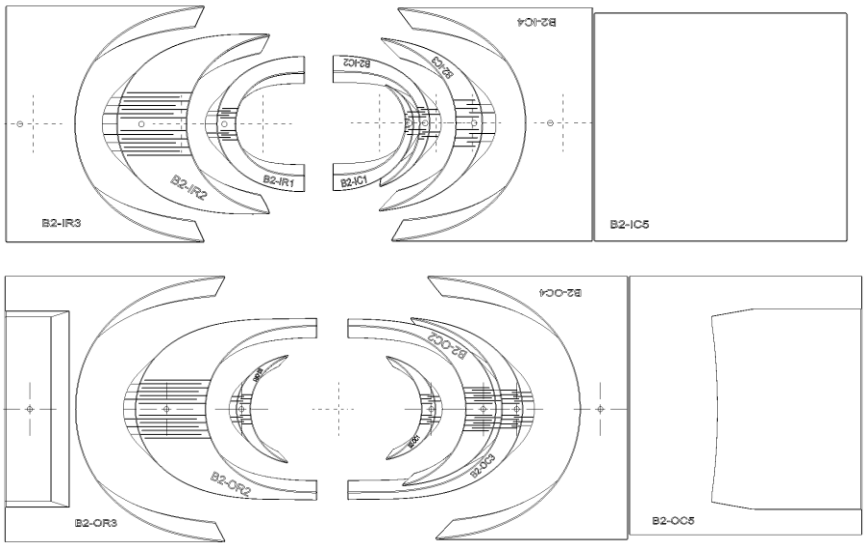

Figure 5.7: End Parts Identification.

- **NbTi Cable**

After the coil reaction, the Nb_3Sn lead is soldered to two pieces of 2.5 meter long NbTi cable. Subsequently 3 mil thick Kapton insulation is wrapped around the splice ground insulation (Figure 5.8).

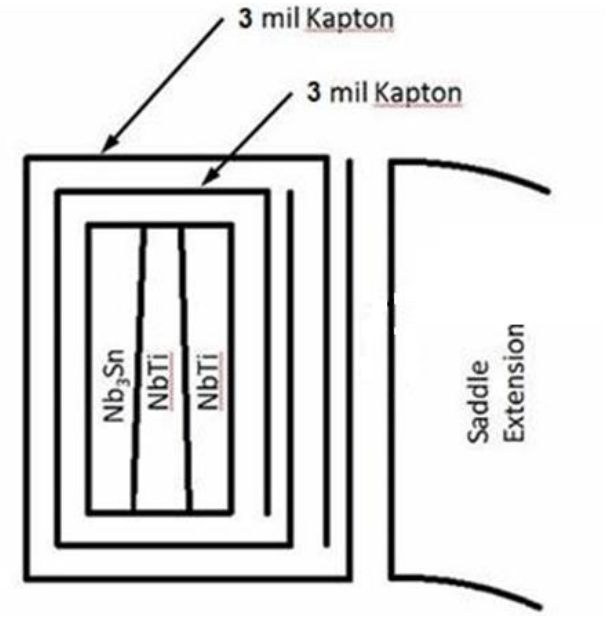

Figure 5.8: Lead Soldering for QXFA Coil.

The NbTi cable is provided by CERN, with the strand specification shown in Table 5.1. The cable dimension is shown in Figure 5.9, and its specification is listed in Table 5.2.

Table 5.1: NbTi Cable Strand Specification.

NbTi Cable Strand	
Coating type	Sn5wt%Ag
Diameter after coating (mm)	1.065 ± 0.0025
Copper to superconductor ratio	1.65 ± 0.05
Filament diameter (μm)	7
Number of filaments	~ 8900
RRR	≥ 150
Twist pitch after cabling (mm)	18 ± 1.5
Critical current (A) 10T, 1.9 K 9 T, 1.9 K	≥ 515
ΔM at 0.5 T and 1.9 K (mT)	≤ 30

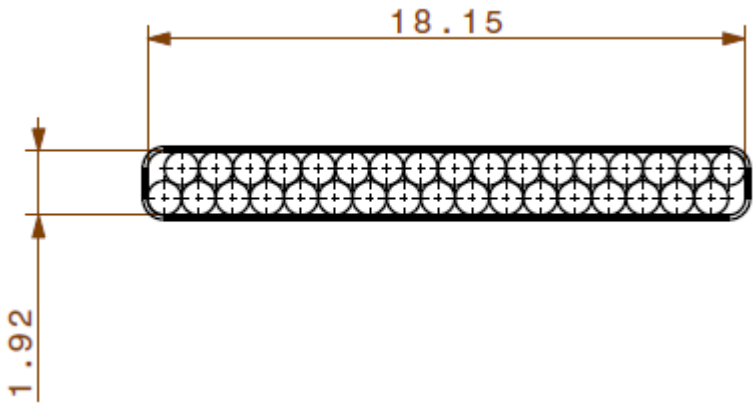

Figure 5.9: NbTi Cable.

Table 5.2: NbTi Cable Specification.

Strand Type	NbTi
Strand Diameter	1.065 mm
Number of Strands	34
Width	18.15 mm
Height	1.92 mm

- **Splice Materials**

Splice materials and procedure are in accordance to LHC requirements: namely non-activated flux (flux MOB 39), and lead-free solder (96/4 Tin/Silver).

Splice resistance must be <1 nΩ.

5.2 Coil Fabrication at FNAL

5.2.1 Winding and Curing

Fermilab will perform 46 QXFA coils winding and curing with equipment, tooling and processes successfully used for the prototype coils by LARP. SELVA winder, as shown in Figure 5.10, which was used during LHC low beta quadrupole coils fabrication, is used to wind the QXFA coils for LHC upgrade.

Figure 5.10: SELVA Winder.

The 2-layer QXFA coil is wound without a cable splice between the layers. The insulated cable, with minimum length 441 m, is measured to verify the overall length and then split into two spools for the inner layer and the outer layer.

Before winding, the inner pole parts are prepared and setup on the winding mandrel with 4 layers of 0.125 mm thick S2 glass insulation wrapped around. To accommodate the coil length shrink due to the tension release after curing and thermal effects during reaction, pole gaps totaling 12.7 mm are introduced to the 2nd generation coil fabrication, based on prototype coil experience. The total gap along the wedge is required to be no less than 2 mm/m longer than the pole gap, taking into account of the thermal shrinkage difference between the wedge and the coil.

The coil winding and curing process is shown in Figure 5.11. The inner layer is wound first. The wound inner coil is uniformly painted with binder (CTD-1202) at a rate of 1.7 g/m per cable, packaged with the curing tooling and shims, as shown in Figure 5.12. It is transferred to the curing mold through the rollover fixture. The inner layer coil is cured in the curing mold at 150°C for 1 hr and 45 mins, and after curing it is transferred back to SELVA through the rollover fixture. The 0.66 mm pre-cured interlayer insulation is placed on top of the inner layer coil, and the outer layer pole parts are set up on top of it with 4 layers of 0.125 mm thick S2 glass insulation wrapped around continuously from the inner layer. When the outer layer winding is completed, the outer layer is uniformly painted with binder at a rate of 1.7 g/m per cable, packaged as shown in Figure 5.13. It is transferred through the rollover fixture to the curing mold for 1 hr and 45 mins curing at 150°C. Each layer is cured under pressure in a precise closed cavity mold at 150 ˚C in air. While the coil is inverted relative to winding orientation, the pole is radially compressed with mandrel cylinders. Subsequently the coil is azimuthally compressed with the platen cylinders until closure which typically occurs at 13 MPa coil pressure. Curing is performed on the coil to set the coil size for reaction, as well as allow the coils to be easily handled, facilitating insertion into the reaction fixture without damage. Spacers simulating the outer layer are used during the curing of the inner layer.

The outer layer is cured on the top of the inner layer. Therefore, the same mandrel and mold are used to cure both the inner and the outer layer.

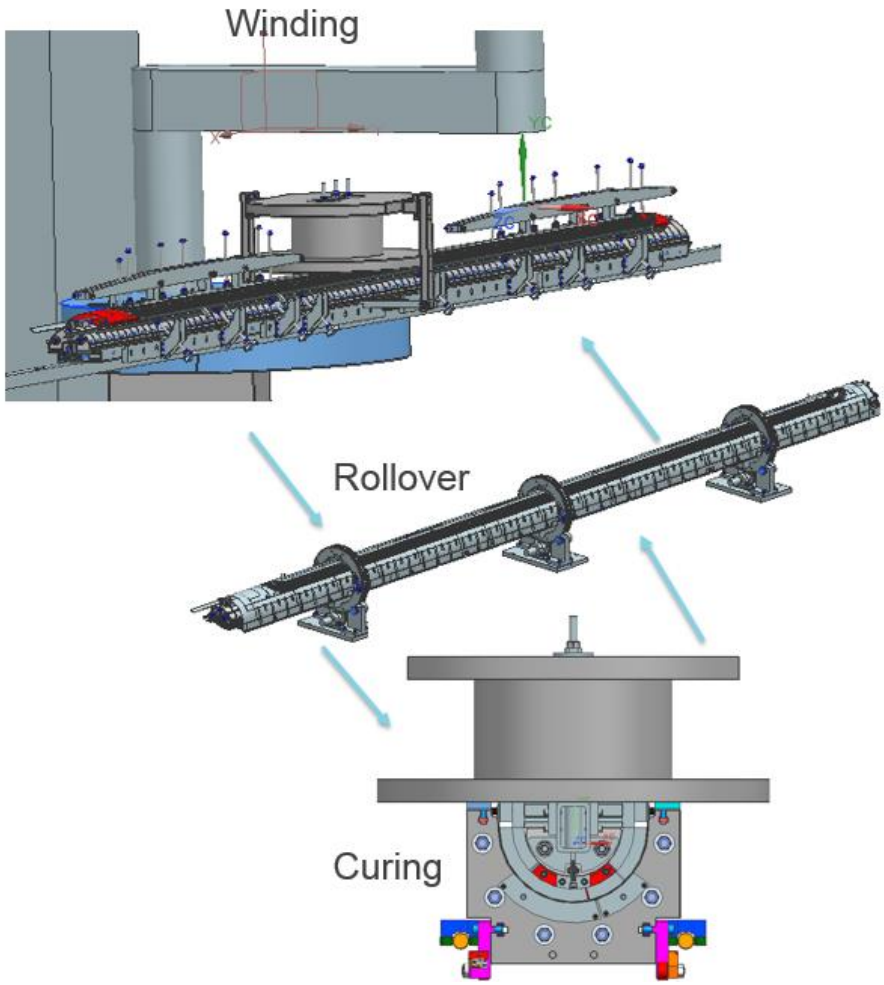

Figure 5.11: Winding and Curing Process.

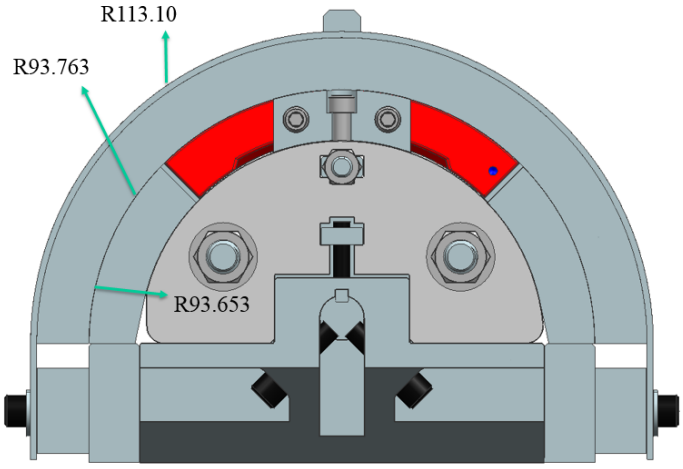

Tooling/ Shims	R or t (mm)	+ tol. (mm)	- tol. (mm)	Max. (mm)	Min. (mm)
Mandrel	74.873	0.01	0.01		
Kapton	0.127	0.01	0.01		
	75	0.02	0.02	0.1	-0.02
L1 Sector pusher	75	0.08	0		
Coil OD	93.653	0	0.05		
Mylar	0.1	0.01	0.01		
	93.753	0.01	0.06		
Curing spacer	93.763	0.08	0	0.15	0
	113.10	0	0.08	0.13	0
Curing retainer	113.10	0.05	0		
90mil stock	2.286	0.014	0.127		
	115.386	0.014	0.127	0.151	0
Curing mold	115.4	0.01	0		

Figure 5.12: Inner Layer Packaging for Curing.

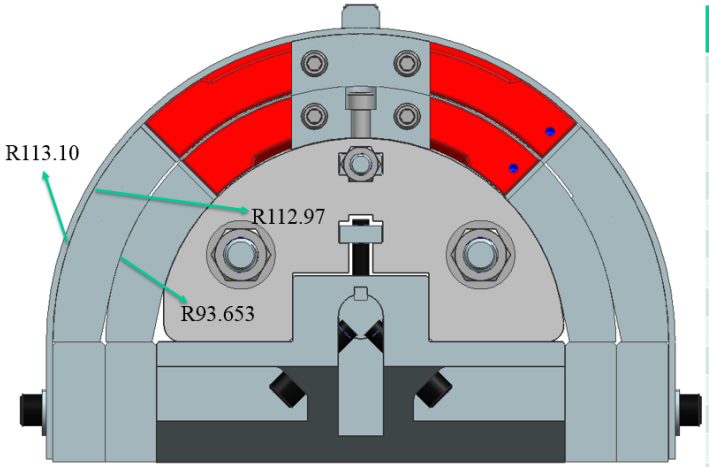

Tooling/ Shims	R or t (mm)	+ tol. (mm)	- tol. (mm)	Max. (mm)	Min. (mm)
Mandrel	74.873	0.01	0.01		
Kapton	0.127	0.01	0.01		
	75	0.02	0.02	0.1	-0.02
L1 pusher	75	0.08	0		
	93.653	0	0.08		
Interlayer	0.660	0.019	0.048		
	94.313	0.019	0.128		
L2 pusher	93.653	0.08	0	0.16	0
Cutout	94.653	0.08	0	0.321	0.548
Coil OD	112.97	0	0.05		
Mylar	0.1	0.01	0.01		
	113.07	0.01	0.06		
Curing retainer	113.10	0.05	0	0.14	0.02
90 mil stock	2.286	0.014	0.127		
	115.386	0.014	0.127	0.151	0
Curing mold	115.4	0.01	0		

Figure 5.13: Outer Layer Packaging for Curing.

The 8.8 m long curing press is shown in Figure 5.14, and the press load to cure a QXFA coil is shown in Table 5.3. The results of the stress analysis are shown in Figure 5.15. The maximum stress under normal operation is less than 100 MPa, lower than 1/3 of steel 1050's yield strength (580 MPa).

Figure 5.14: Curing Press

Table 5.3: Curing Press Load for Curing QXFA Coil.

	Capacity (pump psi)	Max. force/cylinder kN (ton)	Spacing cm(inch)	Unit Force kN/m/psi (lb/in/psi)
Main Cylinders	10000	1780 (200)	30 (12)	0.6 (3.34)
Mandrel Cylinders	10000	134 (15)	15 (6)	0.09 (0.5)

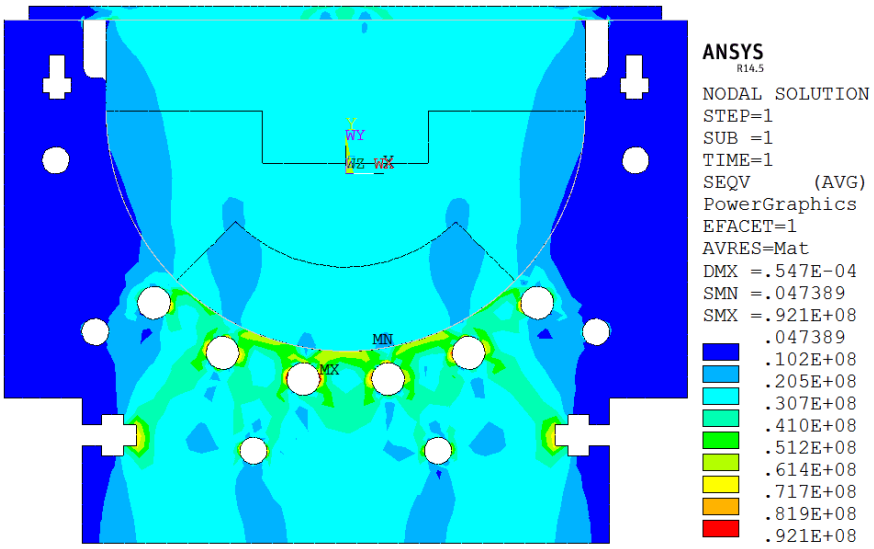

Figure 5.15: QXFA coil curing mold analysis.

A detailed version of the procedures can be found online at [1].

To reduce the production risk, the rotation table is prepared as the backup winder for coil winding, as shown in Figure 5.16.

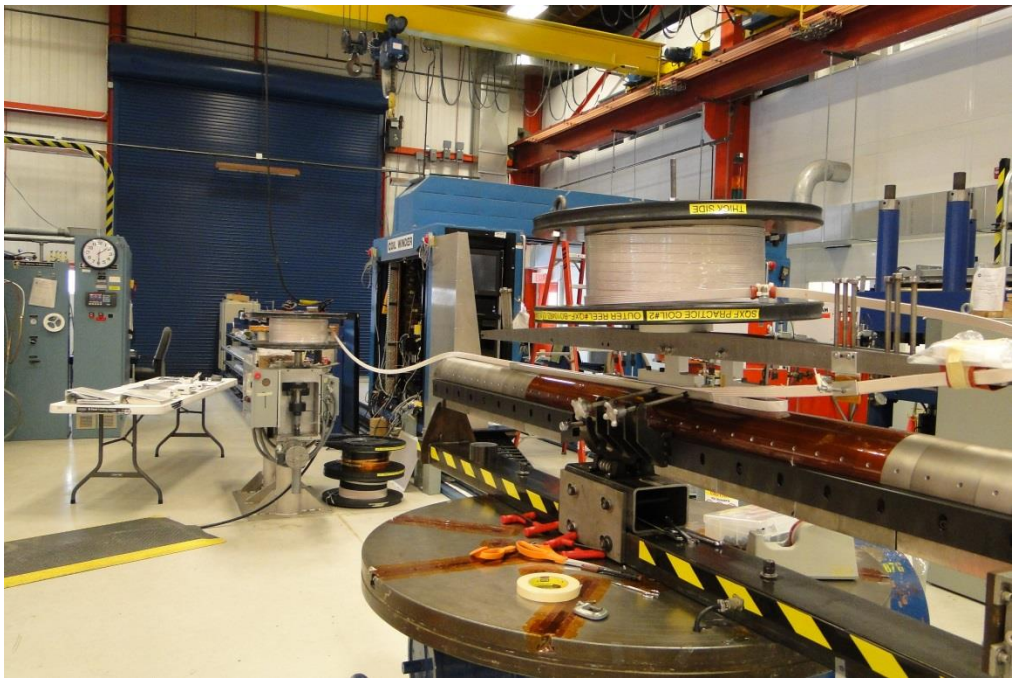

Figure 5.16: Rotation Table.

5.2.2 Reaction

The QXFA coil reaction/impregnation tooling design is based on the designs used for QXFS, HQ and LHQ coils. A cross section of the reaction fixture is shown in Figure 5.17. The closed cavity mold defines the coil size precisely and alignment pins are used to position the pole pieces during reaction and impregnation. The nominal fixture dimensions are shown in Table 5.4. Slender links connect the end saddles to the coil pole to keep the saddles in contact with the cable turns during reaction. A 0.6 mm radial filler is included to allow for the possibility of a small adjustment to the coil outer diameter. The fixture temperature during reaction is monitored continuously by thermocouples bolted to the outside of the reaction fixture.

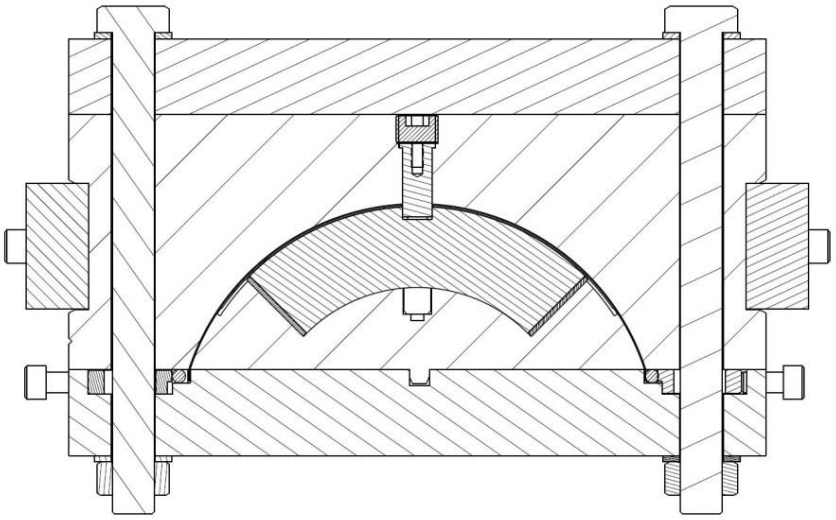

Figure 5.17: Reaction fixture cross section

Table 5.4: QXF Reaction/Impregnation Fixture Dimensions.

Description	Dimension
Inner radius	74.750 mm
Outer radius	113.630 mm
Midplane offset	0 mm

Note:

Dimensions are with liner, radial filler and midplane shims installed.

Reaction takes place in a gas tight oven using an automatic program. The target cycle for the reaction fixture is shown in Table 5.5. The durations and ramp rates for the oven control may be varied in order to achieve the target temperature for the reaction fixture. The reaction fixture is sealed and a continuously flowing argon atmosphere is used to carry away any contaminates that are released during the reaction cycle. Argon flow is supplied independently to the oven at 50 SCFH and to the reaction fixture within the oven at 25 SCFH. Flow rates are sufficient to maintain the oven at a small positive pressure relative to the external atmosphere and the reaction fixture at a positive pressure relative to the internal oven atmosphere. Argon flow is maintained throughout the entire cycle, until the fixture has cooled to a temperature below 100°C. Temperature uniformity within the furnace volume can be maintained to within ±3°C at all three temperature plateaus.

Table 5.5: QXF Coil Reaction Fixture Target Cycle.

	Step	**Description**	**Average Rate**	**Time**
Step 1	Ramp	from 20°C to 210°C	25 C/hour	
Step 2	Soak	210°C		48 hours
Step 3	Ramp	from 210°C to 400°C	50 C/hour	
Step 4	Soak	400°C		48 hours
Step 5	Ramp	from 400°C to 665°C	50 C/hour	
Step 6	Soak	665°C		50 hours
Step 7	Ramp	from 665°C to 20°C		~ 80 hours

Notes:

- Average fixture ramp rate shall not exceed rates listed above.
- Before step 3 the temperature of the reaction fixture shall NOT exceed 215°C.
- Target cycle to be confirmed by the conductor group before each coil reaction.

Mica sheets are set around the coil in preparation for the reaction in order to reduce friction between materials with different thermal expansions. A sketch of the layers of material installed for reaction is shown in Figure 5.18.

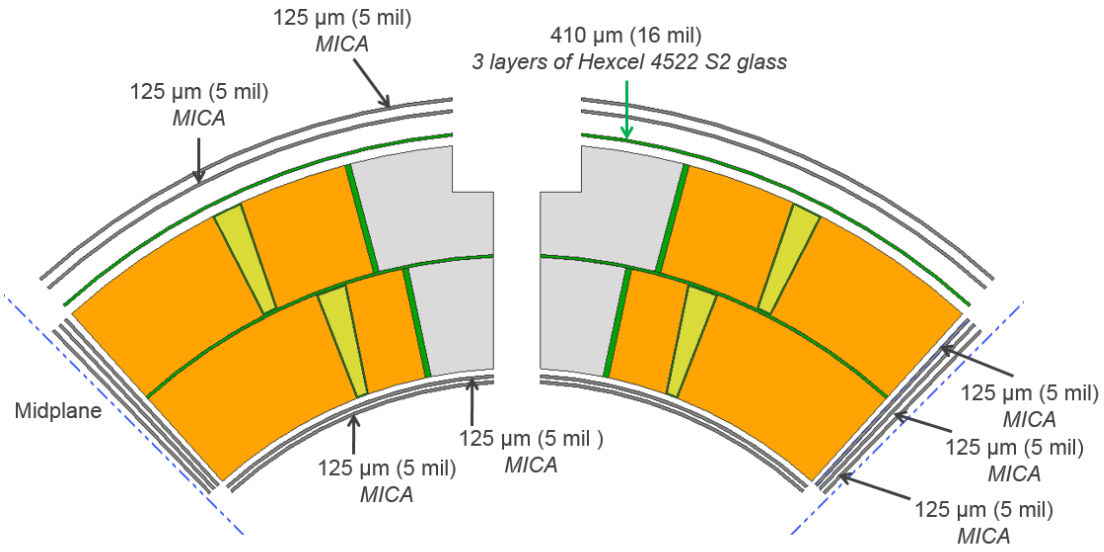

Figure 5.18: Coil cross section during Reaction.

Materials:

- Mica – Cogebi Cogemica Hi-Temp 710-1.
- Fiberglass – Hexcel 4522.

5.2.3 Impregnation

After reaction, coil lead splices are made and the instrumentation trace circuits are installed. The trace circuits consist of copper plated stainless steel foil, for the protection heaters and the voltage tap wiring, glued to a layer of polyimide film. The magnet is rotated Counterclockwise facing the leads. A sketch of the layers of material installed for impregnation is shown in Figure 5.19. The coil is vacuum impregnated with CTD-101k epoxy using a fixture similar to the one used for reaction. The nominal impregnated coil dimensions are shown in Table 5.6.

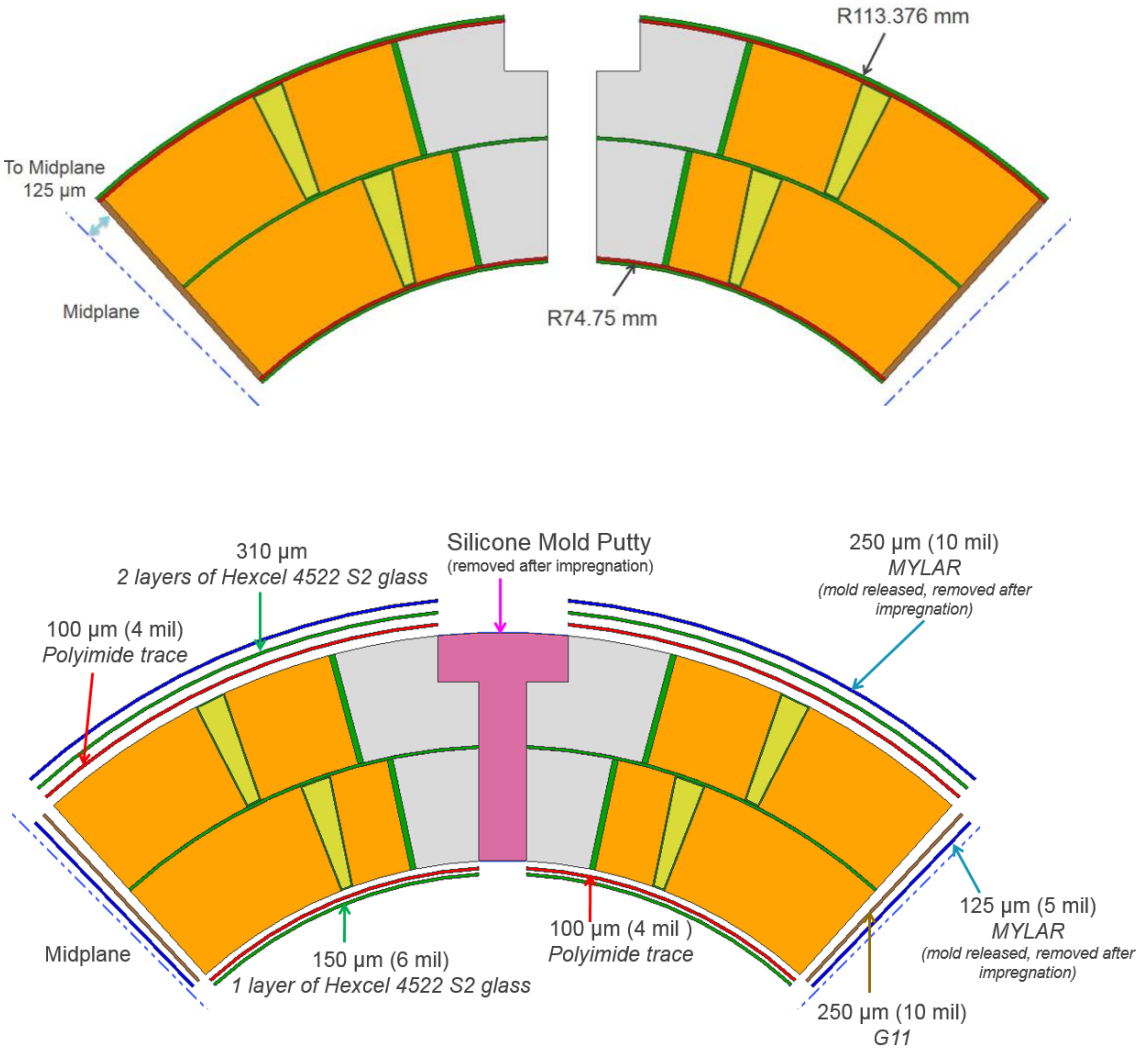

Figure 5.19: Coil cross section during Impregnation.

Materials:

- Trace – Polyimide + copper plated stainless steel.
- Fiberglass – Hexcel 4522.
- G11 – .250 mm thick.
- Mylar, midplanes – .125 mm thick (mold release applied).
- Mylar, coil OD – .250 mm thick (mold release applied).

Table 5.6: QXF Nominal Impregnation Coil Dimensions.

Description	Dimension
Coil inner radius	74.750 mm
Coil outer radius	113.376 mm
Coil midplane offset	0.125 mm

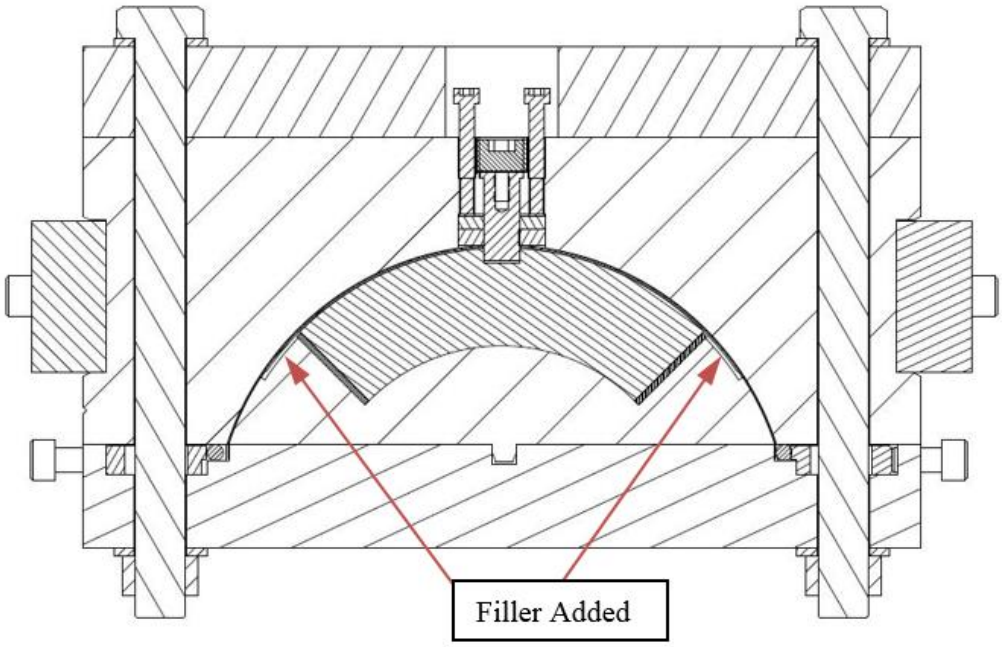

Figure 5.20: Impregnation fixture cross section.

The impregnation tooling is used to epoxy impregnate the coil in a vacuum oven. Fillers are installed to fill the gaps on each side of the mandrel blocks, as shown in Figure 5.20. This is done to help force the epoxy to flow through the coil instead of through the gaps. The coil is positioned at an incline within the vacuum furnace with the lead end of the coil elevated above the return end. The temperature and vacuum pressure is 55°C and 25 um Hg respectively and is maintained for 45 hours before the epoxy is introduced. Epoxy mixing, heating and out gassing occurs about 2 hours prior to the start of epoxy flow to the coil. Once the epoxy flows out into the overflow reservoir from the lead end of the coil, the epoxy input hose is clamped off at the return end and a 17 hour dwell period at atmospheric pressure begins. During the dwell period, small amounts of epoxy back-fills into the coil from the overflow reservoir. After the dwell, the cure

cycle of 5 hours at 110 °C followed by 16 hours at 125 °C is achieved using external heaters attached to the tooling.

Table 5.7: QXF Coil Impregnation Cure Cycle.

Step	Description	Time / Rate
Ramp	from 55°C to 110°C	10 C/hour
Soak	110°C	5 hours
Ramp	from 110°C to 125°C	10 C/hour
Soak	125°C	16 hours

5.3 Coil Fabrication at BNL

5.3.1 Winding and Curing

Coil winding will be done on the existing 10m shuttle winder using an automated winding program. All coil parts will be procured by FNAL and supplied to BNL.

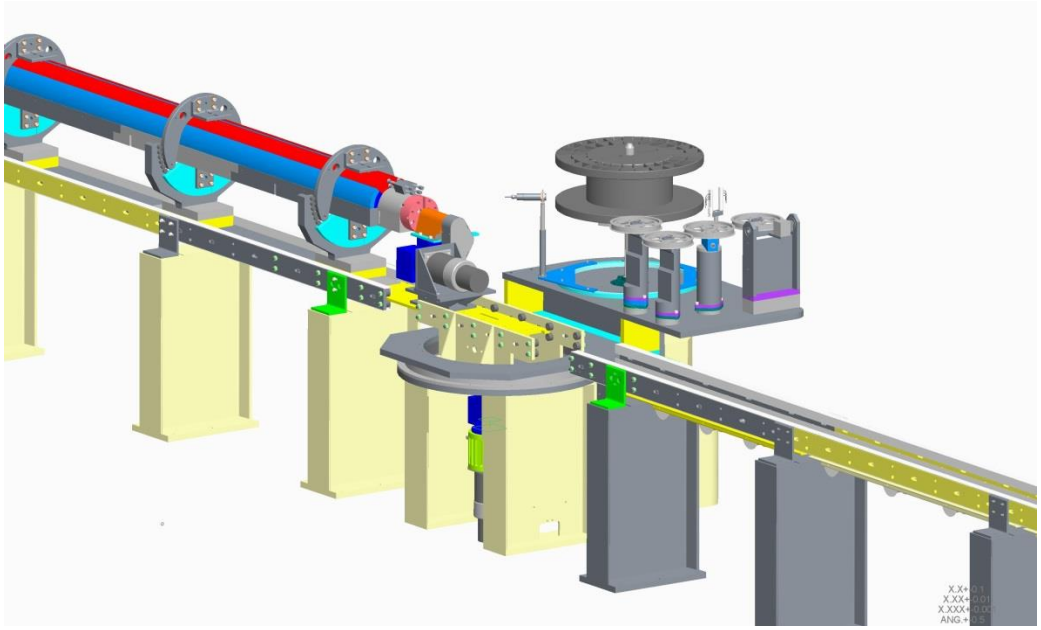

Figure 5.21: Winding Machine.

Coils will be cured utilizing an existing 10m long curing press. The coil mandrel assembly will be bolted down into the curing press to set the radial cavity. Azimuthal pressure will be applied to the coil using hydraulic cylinders, until the mold is closed to the nominal coil size. The coil tooling is heated with electric cartridge heaters installed in the mandrel and formblock.

Figure 5.22: Winding Machine.

5.3.2 Reaction

The QXF coil reaction/impregnation tooling design is based on the designs used for HQ and LHQ coils. A cross section of the reaction fixture is shown in Figure 5.23. The closed cavity mold defines the coil size precisely and alignment pins are used to position the pole pieces during reaction and impregnation. The nominal fixture dimensions are shown in Table 5.8. Slender links connect the end saddles to the coil pole to keep the saddles in contact with the cable turns during reaction. The fixture temperature during reaction is monitored continuously by thermocouples bolted to the outside of the reaction fixture.

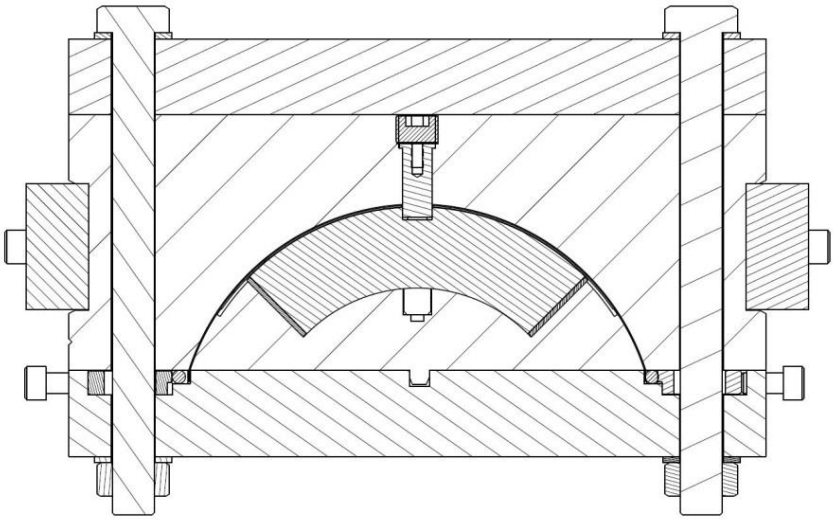

Figure 5.23: Reaction fixture cross section.

Table 5.8: QXF Reaction/Impregnation Fixture Dimensions.

Description	Dimension
Inner radius	74.750 mm
Outer radius	113.630 mm
Midplane offset	0 mm

Note:

Dimensions are with liner, radial filler and midplane shims installed.

Reaction takes place in an existing gas tight 5 meter long oven using an automatic program. The target cycle for the reaction fixture is shown in Table 5.9. The durations and ramp rates for the oven control may be varied in order to achieve the target temperature for the reaction fixture. The reaction fixture is sealed and a continuously flowing argon atmosphere is used to carry away any contaminates that are released during the reaction cycle. Argon flow is supplied independently to the oven at 50 SCFH and to the reaction fixture within the oven at 25 SCFH. Flow rates are sufficient to maintain the oven at a small positive pressure relative to the external atmosphere and the reaction fixture at a positive pressure relative to the internal oven atmosphere. Argon flow is maintained throughout the entire cycle, until the fixture has cooled to a temperature below 100°C. Temperature uniformity within the furnace volume can be maintained to within ±3° C at all three temperature plateaus.

Table 5.9: QXF Coil Reaction Fixture Target Cycle.

	Step	Description	Average Rate	Time
Step 1	Ramp	from 20°C to 210°C	25 C/hour	
Step 2	Soak	210°C		48 hours
Step 3	Ramp	from 210°C to 400°C	50 C/hour	
Step 4	Soak	400°C		48 hours
Step 5	Ramp	from 400°C to 665°C	50 C/hour	
Step 6	Soak	665°C		48 hours
Step 7	Ramp	from 665°C to 20°C		~ 80 hours

Notes:

- Average fixture ramp rate shall not exceed rates listed above.
- Before step 3 the temperature of the reaction fixture shall NOT exceed 215°C.
- Target cycle to be confirmed by the conductor group before each coil reaction.

Mica sheets are set around the coil in preparation for the reaction in order to reduce friction between materials with different thermal expansions. A sketch of the layers of material installed for reaction is shown in Figure 5.24.

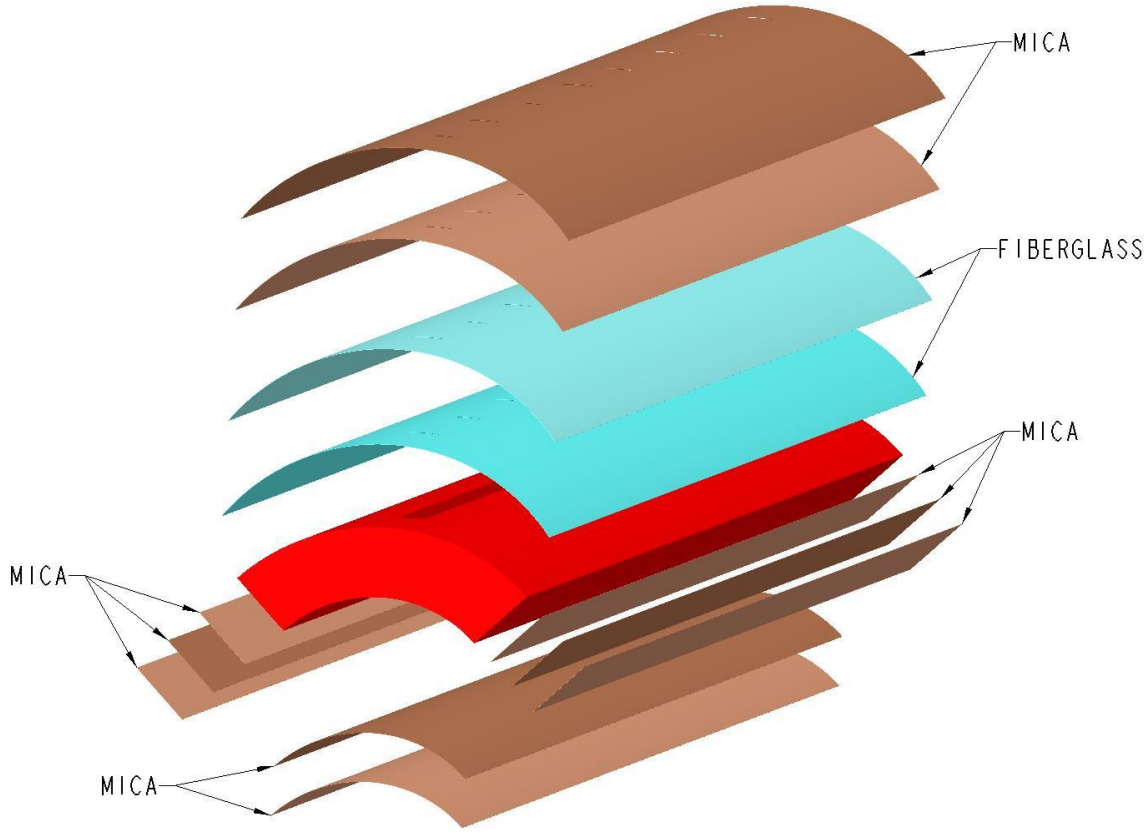

Figure 5.24: Materials installed for reaction.

Materials:

- Mica – Cogebi Cogemica Hi-Temp 710-1.
- Fiberglass – Hexcel 4522.

5.3.3 Impregnation

After reaction, coil lead splices are made. The Nb_3Sn coil leads are soldered to a pair of NbTi cables, using MOB39 flux and 96/4 tin/silver solder. Next the instrumentation / heater trace circuits are installed. The trace circuits consist of copper plated stainless steel foil, for the protection heaters and the voltage tap wiring, glued to a layer of polyimide film. Fiberglass cloth and G11 shims are then added to the coil. A sketch of the layers of material installed for impregnation is shown in Figure 5.25. The coil is flipped end-over-end to access the coil ID and OD. The coil is vacuum impregnated with CTD-101k epoxy using a fixture similar to the one used for reaction. The nominal impregnated coil dimensions are shown in Table 5.10.

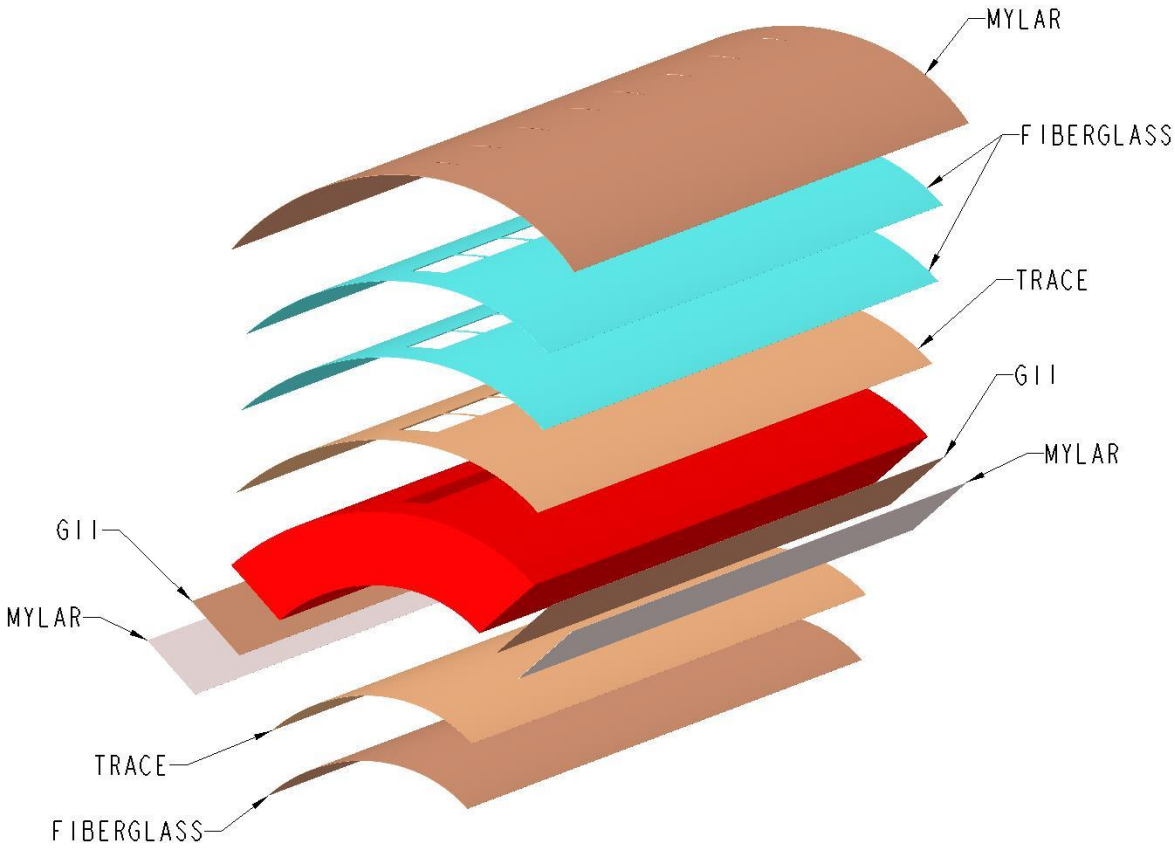

Figure 5.25: Materials installed for impregnation.

Materials:

- Trace – Polyimide + copper plated stainless steel.
- Fiberglass – Hexcel 4522.
- G11 – .250 mm thick.
- Mylar, midplanes – .125 mm thick (mold release applied).
- Mylar, coil OD – .250 mm thick (mold release applied).

Table 5.10: QXF Nominal Impregnation Coil Dimensions.

Description	**Dimension**
Coil inner radius	74.750 mm
Coil outer radius	113.376 mm
Coil midplane offset	0.125 mm

The impregnation fixture is closed and sealed. The fixture is hung vertically, lead end up, in a vacuum tank. Strip heaters mounted to the outside of the fixture are used for heating. The fixture and the vacuum tank are evacuated to a vacuum level of 500 mTorr or less. While under vacuum, the coil is baked at 110ºC for 8 hours then cooled back down to 55ºC before the impregnation is started. The epoxy is mixed, warmed to 55ºC, and degassed to the same vacuum level as the coil. Once degassed, the vacuum level in the fixture and in the vacuum tank is brought up to 800 mTorr. The epoxy pot is let up to atmospheric pressure and the pressure differential forces epoxy into the coil. The epoxy is introduced into the bottom of the impregnation fixture. The fill rate is controlled by a peristaltic pump, with pump speed set to result in a fill time of about 4 hours. An exit line from the top of the impregnation fixture is connected to a resin trap outside the vacuum tank. When epoxy reaches the resin trap, the exit line is closed. The supply line remains open, with atmospheric pressure continuing to force resin into the coil. The coil is held overnight, for approximately 16 hours, at 55ºC while allowing epoxy to continuously draw into the coil. After the overnight soak, the cure cycle is initiated. The epoxy is cured using an automatic cycle as shown in Table 5.11. Vacuum is maintained in the vacuum tank until the cure is complete.

Table 5.11: QXF Coil Impregnation Cure Cycle.

Step	Description	Time / Rate
Ramp	from 55°C to 110°C	10 C/hour
Soak	110°C	5 hours
Ramp	from 110°C to 125°C	10 C/hour
Soak	125°C	16 hours

5.4 Coil Handling & Shipment

MQXFA coils are made of brittle Nb_3Sn conductor. In order to prevent conductor degradation, all handling and shipment operations shall meet the following requirement:

Coil H&S Requirement #1: The conductor strain shall never exceed 500 microstrain in any part of the coils during any handling or shipping operation.

A coil shipping fixture is used to support the coils for shipment between labs. The fixture consists of an aluminum support tube mounted in an aluminum channel using rubber shock mounts. Side rails support the full length of the coil midplane. A series of clamps are applied over the coil OD. Longitudinal restraint is provided by bolts contacting the ends of the coil saddles. The fixture is shown in Figure 5.26.

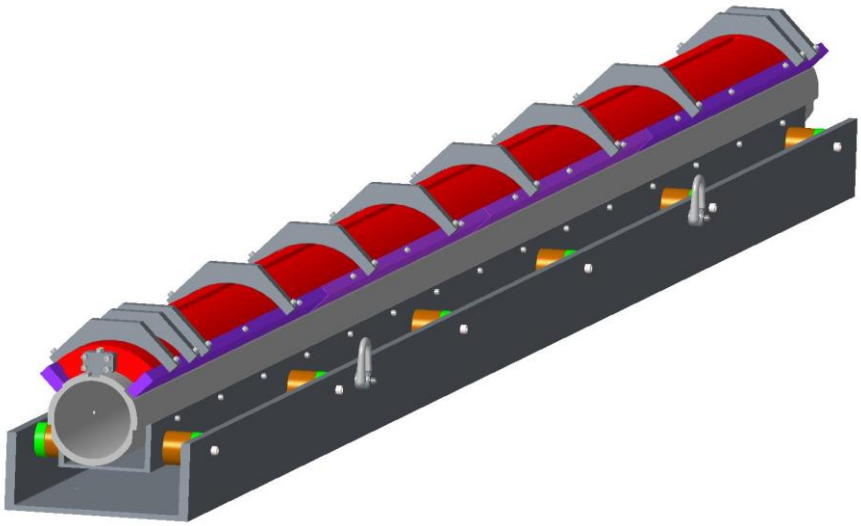

Figure 5.26: Coil shipping fixture.

The shipping fixture is installed inside a wooden crate. Shipment is made using a dedicated truck such that the once the crate is loaded onto the truck at the origin lab, it remains on the truck until it arrives at the destination lab. There is no loading and unloading permitted while on route.

References

[1] https://vector-offsite.fnal.gov/Tools/TravelerWriter/TravelerWriterPreviewDocument.asp?qsSpecificationID=1653&qsRevisionID=3

6 MQXFA Structure and Magnet Assembly

6.1 Structural Assembly Features

As described in the section 4.3, the main features of the support structure design as shown in Figure 6.1 are:

- Shell-based support structure replying on the "bladder and key" technology to perform azimuthal pre-loads, which allows a reversible assembly process and tunable preload;
- The aluminum shell is segmented into sections to minimize axial tension in the shell and to ensure a uniform azimuthal load on the coil;
- The use of master key packages between the yokes and the pads allow for assembly clearances prior to preload operations.
- G11 alignment keys inserted into the pole pieces provide the coil alignment and to also intercept some of the forces from the shell during pre-load and cool-down conditions;
- Axial pre-load is applied by four stretched axial stainless steel rods that react against endplates on each end that transfer the forces to the coil.

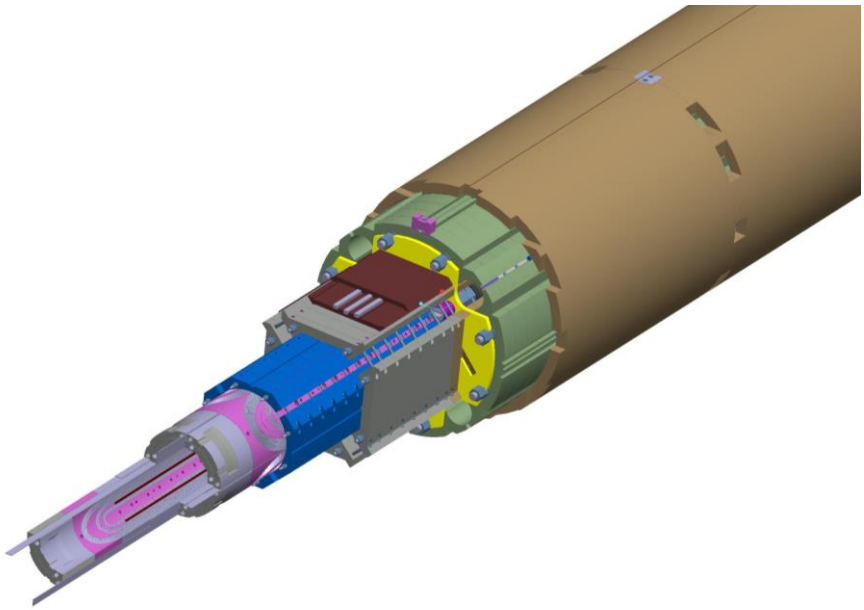

Figure 6.1: 3D exploded view of the end of an MQXF magnet (axial end loading and splice connection components not shown).

6.2 Magnet Assembly Breakdown Structure

Figure 6.2 shows the magnet assembly breakdown structure (ABS) flowchart of the long magnet assembly. This assembly structure and processes are described below.

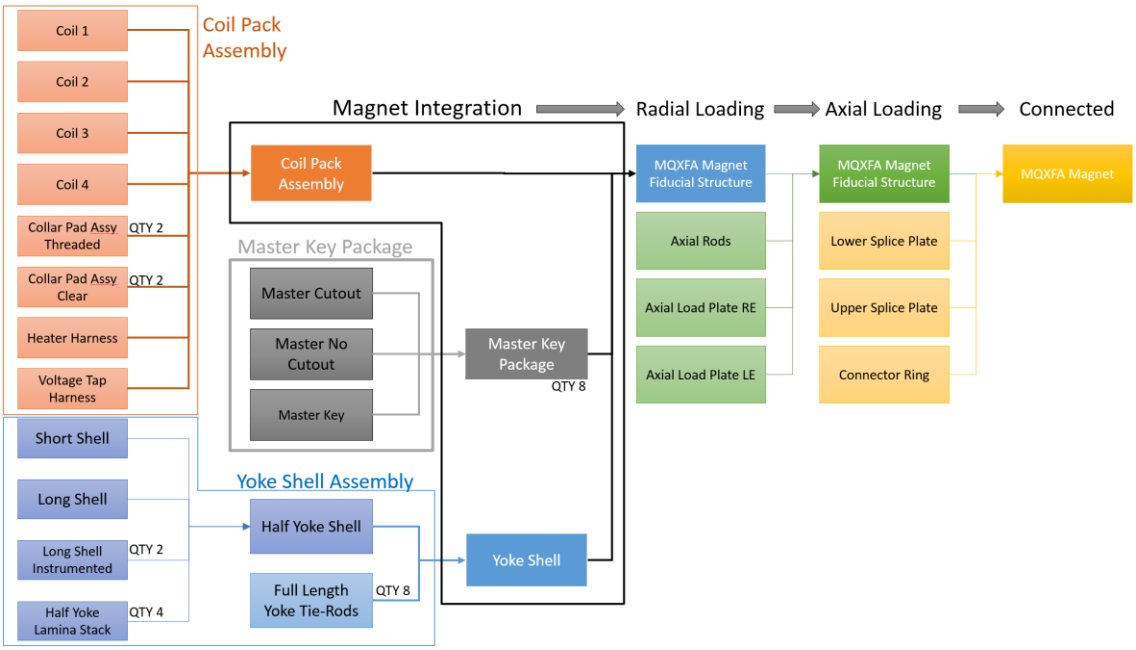

Figure 6.2: MQXFA magnet assembly breakdown structure flowchart.

6.2.1 Shell-Yoke Subassembly

- **Shells**

The MQXF magnet adopts segmented shells to minimize the axial tension in the shell segments and to ensure a uniform azimuthal load on the coils. There are two lengths of shell segments used in the assembly: a 325.65 mm long segment (two ea.) used at each extremity; and six 651.29 mm long segments stacked in between the short ones.

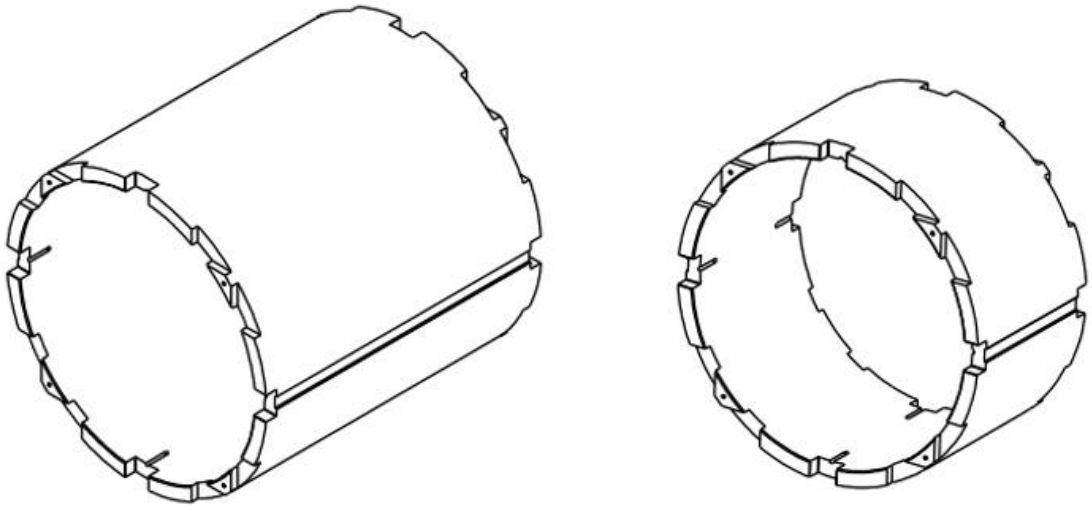

Figure 6.3: The long and short shell segments.

As shown in the Figure 6.3 each shell segment has various cutouts on each end, for alignment, tooling, and supports. There are pin slots machined into each quadrant of the ID on each end of the shells, though pins will be used only in one quadrant during magnet assembly operations.

The shells will be fabricated and inspected by the vendor, but upon receipt, each individual shell will then be measured again. The cylindricity and average radii will also be measured at five axial locations along the length of each shell segment: approximately 25 mm from each end, and three equally spaced mid-length locations. These measurements are used to determine an optimum arrangement and order that will be used when assembling these shells in the magnet structure.

Once the order of shells is determined, three of the six long shells will be instrumented with strain gauges so that preload operations can be measured against the analytical targets.

- **Yokes**

The iron yoke laminations are typically 50 mm (1.96 in) thick and made of ARMCO Pure Iron (Grade 4). Each quadrant of the yoke stacks are joined using two 19.05 mm (¾") stainless steel tie rods, and aligned by close-fitting aluminum bronze bushing sleeves. Each tie rod is pre-tensioned to 40,000 N (9000 lbs).

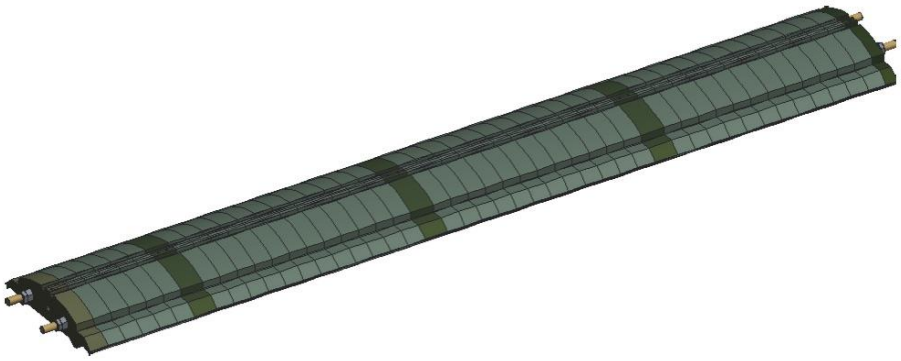

Figure 6.4: 3D model of a half-length yoke stack.

The yoke laminations are initially stacked into "sub-stacks" corresponding to the lengths of the shell segments. These sub-stacks are then assembled into eight 2281.5 mm (89.82") long sub-assemblies, which is half the length of the magnet. See Figure 6.4. Four of these subassemblies will be assembled into half-length shell-yoke subassemblies prior to the final integration of the full-length structure.

While all the yoke laminations all have the same geometry, the laminations located at the junction between two shell segments have tapped holes, which are provisions for the welding block that will be attached when the SST LHe cryostat shell is welded after over the cold mass. The fact that these laminations bridge between shell segments increases the longitudinal stiffness of the shell assembly. However, when joined together the half-length shell-yoke subassemblies are not bridged: only the yoke bushings and the coil pack assembly components bridge the full-length structure.

- **Shell-Yoke Assembly operations**

When assembling the shell-yoke subassembly, four shells (three long, one short) are initially stacked vertically on the assembly stand. Pins are inserted only in the "Top" quadrant slots initially aligns the shells prior to the insertion of the half-length yoke stacks.

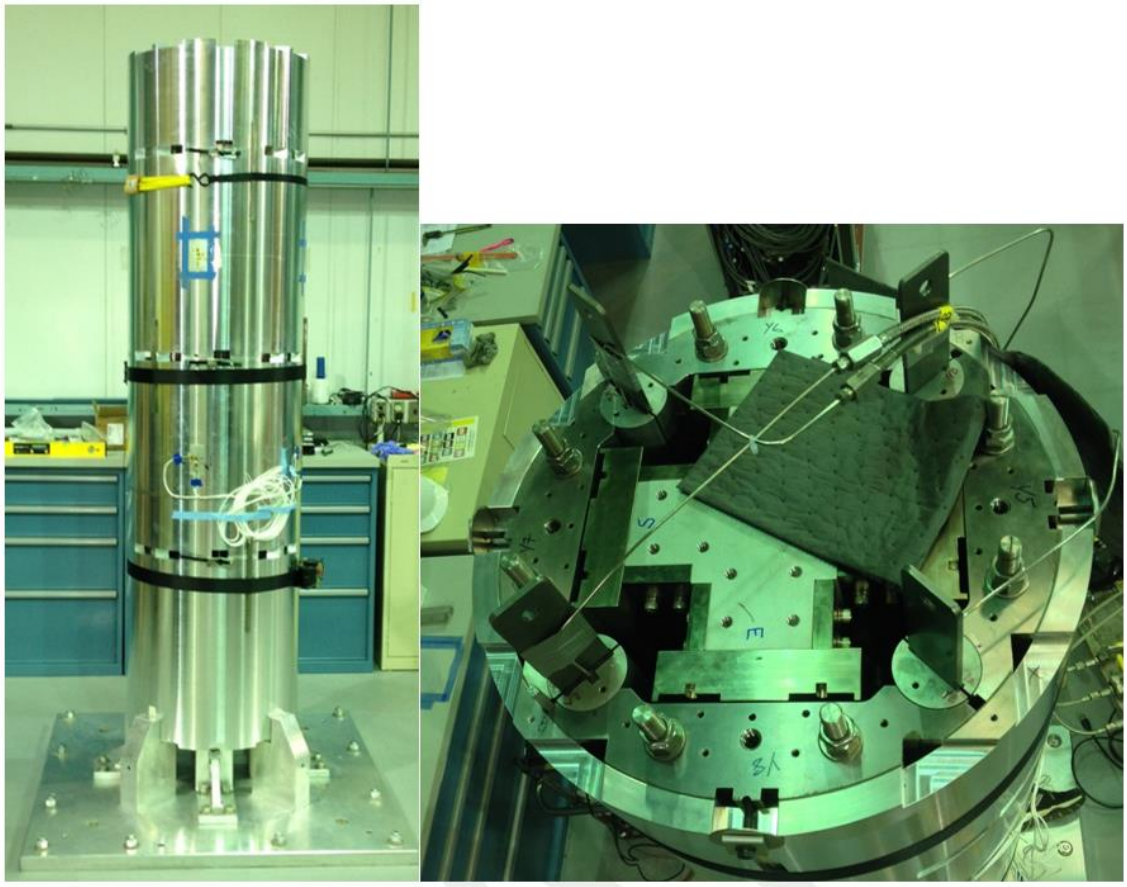

Figure 6.5: (L) Half-length shell stack on the assembly stand. (R) View from the top, with the yoke quadrants ready to be preloaded.

The four yoke stacks are then inserted vertically inside the stack of shells (Figure 6.5). A bladder operation is performed to insert the gap keys and constrain the yokes against the shells. The cooling holes in the yokes are utilized as the bladder locations to open up the gaps, which is more efficient than the operating the bladders at internal cross support geometry. The nominal yoke gap is 12 mm, but the gap keys are shimmed to a shell strain of approximately 200 μm/m.

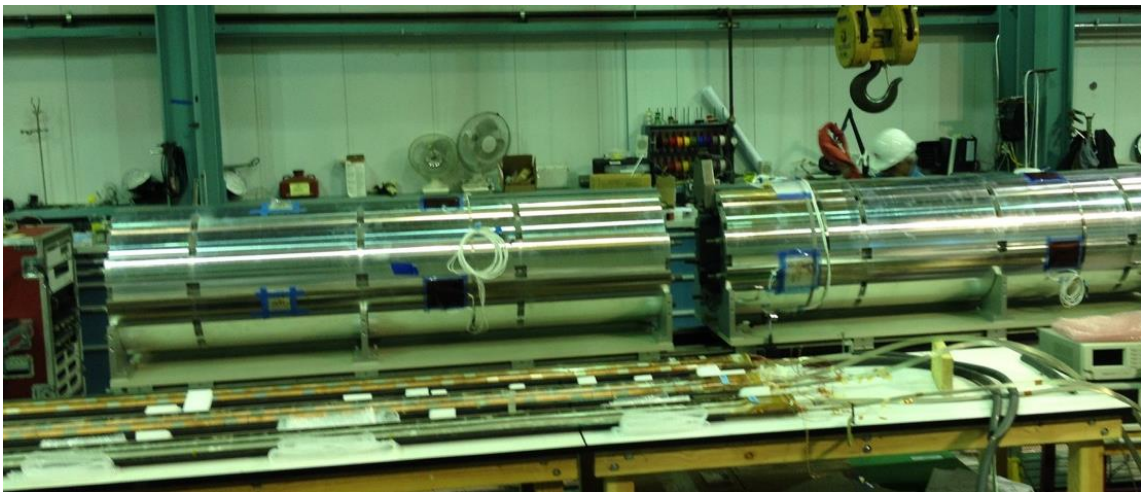

Figure 6.6: Two half-length yoke-shell subassemblies, ready to be joined.

Once the tooling is removed and the assembly has been moved, the process is repeated for the second half-length subassembly, after which they are both placed on the magnet integration table; see Figure 6.6. The dimensional size of the yoke opening is measured, and these values are used to calculate the master key initial shim package. When both half-length assemblies are joined together the centermost bronze bushing sleeves are replaced, as well as the short yoke tension rods with full-length ones. A hydraulic rig is used to pre-tension these full-length yoke tension rods to carry 9000 lbs. each. See Figure 6.7. This completes the shell-yoke subassembly.

Figure 6.7: Hydraulic rig for pre-tensioning the yoke tie rods.

6.2.2 Coil Pack Sub assembly

- **Dressed Coils**

When received, each impregnated coil undergoes a series of electrical and mechanical CMM measurements. A polyimide + B-stage ground plane insulation (GPI) layer is attached to each coil around the OD and midplanes. The CMM measurements may define whether additional shim layer at the midplane are required in later assembly operations.

Currently, coils are instrumented with strain gauges on the pole islands that allow for measuring strain in the azimuthal and axial directions. It is still to be decided whether these gauges will continue to be used for the series production.

- **Load Pad-Collar Stacks**

The aluminum collar laminations and the load pad laminations will be assembled together in four full-length stacks, one for each quadrant. Both lamination types are typically 50 mm (1.969 in) thick. While the collars are all 6061 aluminum, the load pads must be stainless steel on the ends (to reduce peak field), instead of ARMCO Pure Iron (Grade 4) in the center.

The load pad is assembled first using short "sub-stacks" that correspond to the length between particular collar laminations. These sub-stacks are assembled into a full-length load pad assembly stack, aligned by aluminum bronze bushing sleeves, and joined using two 11.11 mm (7/16") pre-tensioned stainless steel tie rods.

Collar laminations are then stacked upon each assembled load pad. The collars are aligned by aluminum bronze bushing sleeves, as well as the key feature of the load pad geometry. Two 6.35 mm (¼") stainless steel tie rods are tensioned to 1000 lbs. each. The collars assembly is held to the load pads via bolts through certain load pad and collar laminations. These bolts are removed prior to the final assembly. See Figure 6.8.

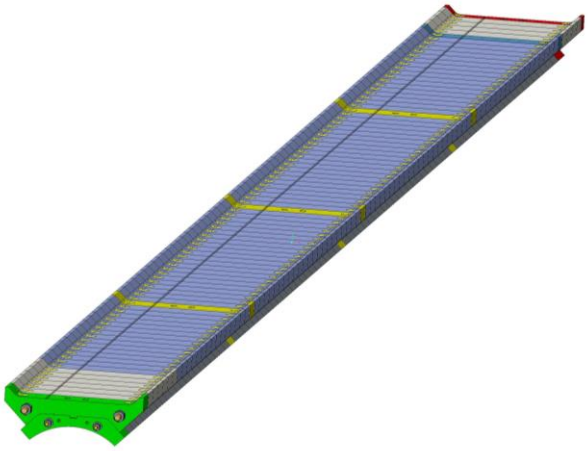

Figure 6.8: Full-length load pad-collar assembly. The lighter colored ends of the load pads are SST instead of ARMCO Pure Iron.

- **Coil Pack Assembly Operations**

The bottom pad-collar assembly is placed on the coil pack assembly table, and the two side pad-collar assemblies are assembled on the two pivot tables beside the primary assembly table. Based on the earlier CMM measurements performed on the coils, the inner curved surface of the collar stacks are lined with layers of G11 and/or polyimide as radial shims. The first build also incorporates the use of pressure sensitive film as part of the radial stack up. These layers are eventually replaced by either polyimide or G11 in the final build.

The bottom pair of dressed coils is then moved onto the bottom pad-collar assembly. The upper pair of coils follows this operation, being secured on the assembly before the side pad-collar assemblies are rotated into place. See Figure 6.9. Finally, the upper pad-collar assembly is placed on top, and all the pads are bolted together. At this stage, with unshimmed alignment keys inserted into the coils the gaps between these keys and the collars are measured.

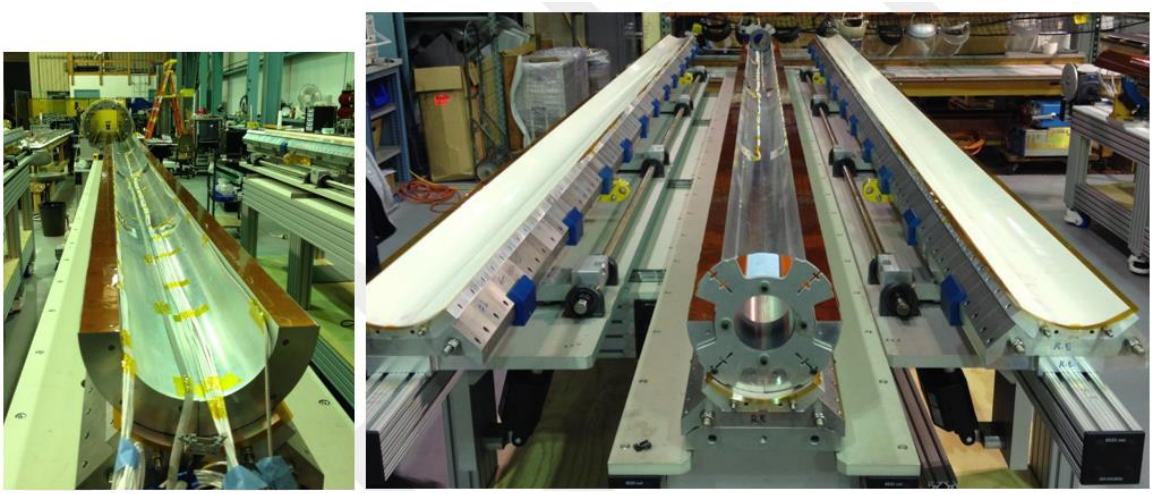

Figure 6.9: The bottom pair of (dummy) coils placed on the bottom pad-collar assembly. (R) The side pivot tables shown.

This first assembly with pressure-sensitive paper is disassembled so that the layers can be replaced with the appropriate radial shims, and the alignment keys can be shimmed correctly to ensure collar-key contact. This will ensure both alignment and some force interception from the shell. This final coil pack is measured; these measurements are used to calculate the initial shim package of the master keys described in the next section.

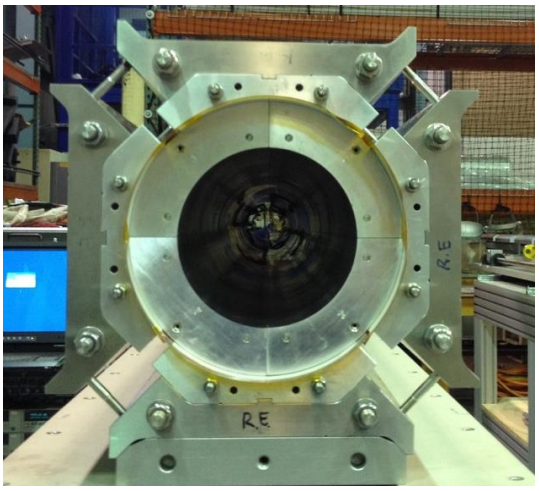

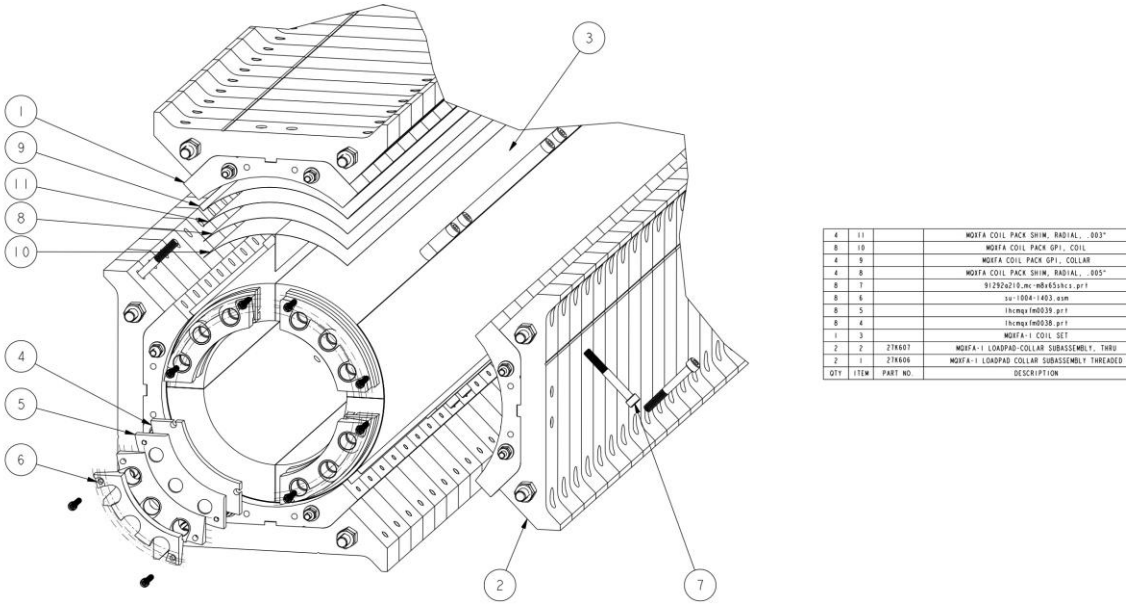

QTY	ITEM	PART NO.	DESCRIPTION
4	11		MQXFA COIL PACK SHIM, RADIAL, .003"
8	10		MQXFA COIL PACK GP1, COIL
4	9		MQXFA COIL PACK GP1, COLLAR
4	8		MQXFA COIL PACK SHIM, RADIAL, .005"
8	7		91292a210,mc-m8x65shcs.prt
8	6		su-1004-1403.asm
8	5		lhcmqxfm0039.prt
8	4		lhcmqxfm0038.prt
1	3		MQXFA-1 COIL SET
2	2	27K607	MQXFA-1 LOADPAD-COLLAR SUBASSEMBLY, THRU
2	1	27K606	MQXFA-1 LOADPAD COLLAR SUBASSEMBLY THREADED

Figure 6.10: The coil pack assembly (dummy coils shown above).

6.2.3 Magnet Integration

- **Master key packages**

The mechanical measurements of the yoke opening and the coil pack are used to calculate the initial master key package shims. The master assembly consists of two master key plates, each with slots for bladders, load keys, and an alignment key. The master assemblies will be assembled ("kitted") with a uniform amount of shims in all the quadrants initially. See Figure 6.11.

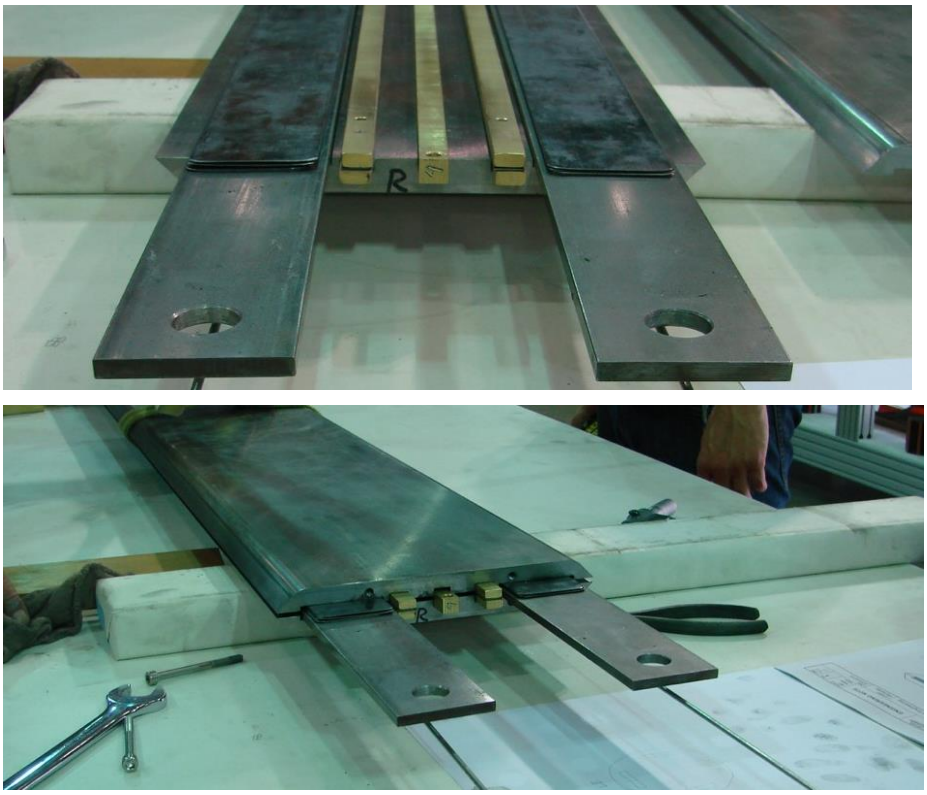

Figure 6.11: (Top) Kitting the master key packages; (bot) assembled master key package.

The coil pack is inserted into the yoke opening using a set of rollers in the yoke cooling hole slots. Only the bottom quadrant master keys are present in this stage (Figure 6.12). Once the coil pack inserted, however, the rest of the master keys can be inserted into each quadrant.

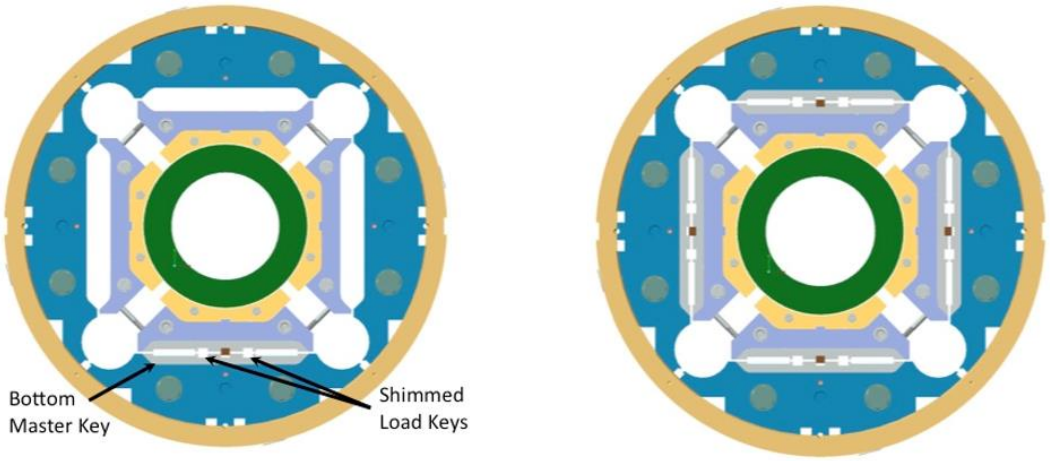

Figure 6.12: (L) The coil pack slides into the yoke opening with a single master key set inserted on the bottom. (R) The rest of the master keys are inserted into all the quadrants.

- **Magnet Preload Operations**

The high-pressure pump is attached to the bladders on both ends of the magnet (keys and bladders are half-length). The load keys will be shimmed to obtain the target strain on the shells and coils, as measured by the strain gauges. A magnet fiducial survey is being planned at this stage, since the subsequent axial load components will cover up any fiducial features at the ends of the coils.

When the azimuthal preload is completed, the axial loading rig is attached to the axial rods to perform the axial preload operations (Figure 6.13). This completes the magnet preload operations. Electrical QC measurements are taken at this stage to ensure that none of these operations have damage coils, or insulation layers.

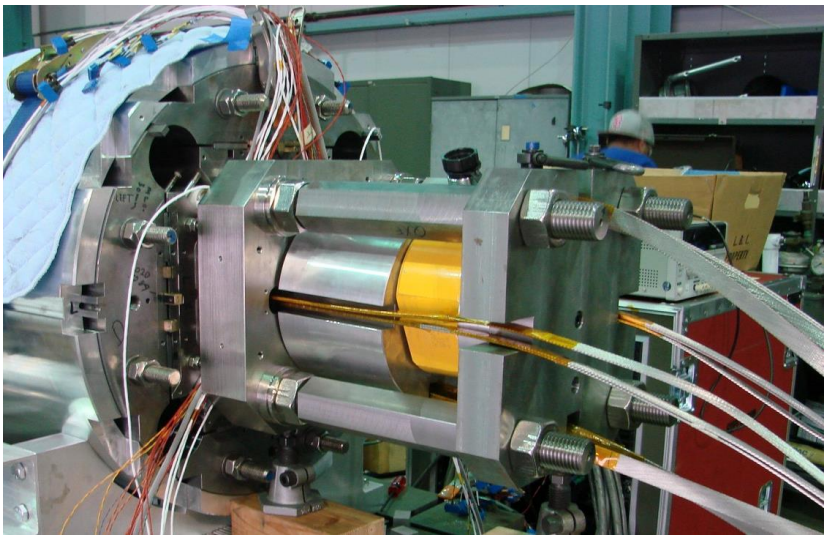

Figure 6.13: Axial preloading operation with the axial loading rig.

6.2.4 Magnet Finishing Operations

- **Splice connections**

The magnet splice connections are made after the magnet preload operations are complete. Figure 6.14 shows the physical layout of the magnet splice connections box, which is made up of two layers due to space constraints and the bend radius of the cables.

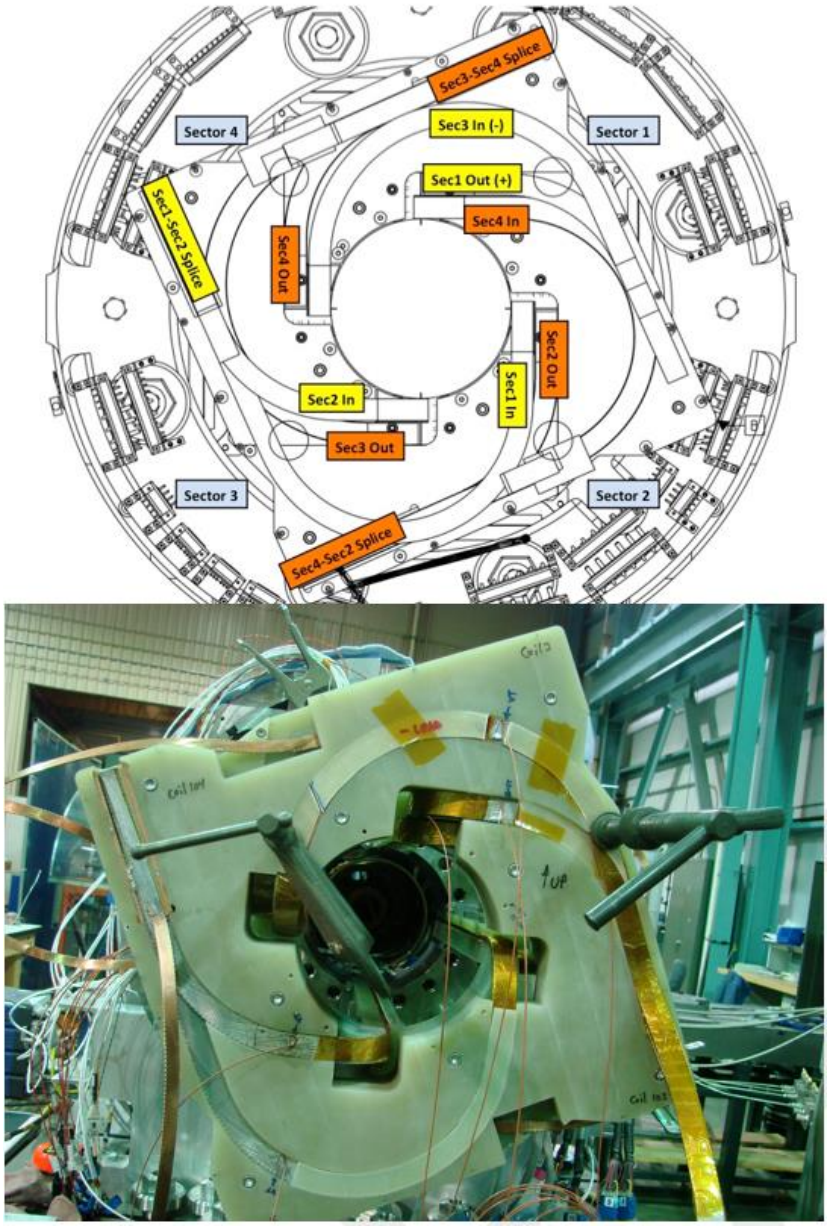

Figure 6.14: Splice connections for the MQXFA.

- **Connector skirts**

After the splice connections are completed, the final operation is to mount all the instrumentation connectors. This includes protection heaters, voltage taps, strain gauges, etc. for the entire magnet. See Figure 6.15. After a final QC check of all these connections the magnet will be ready to be packaged for shipment.

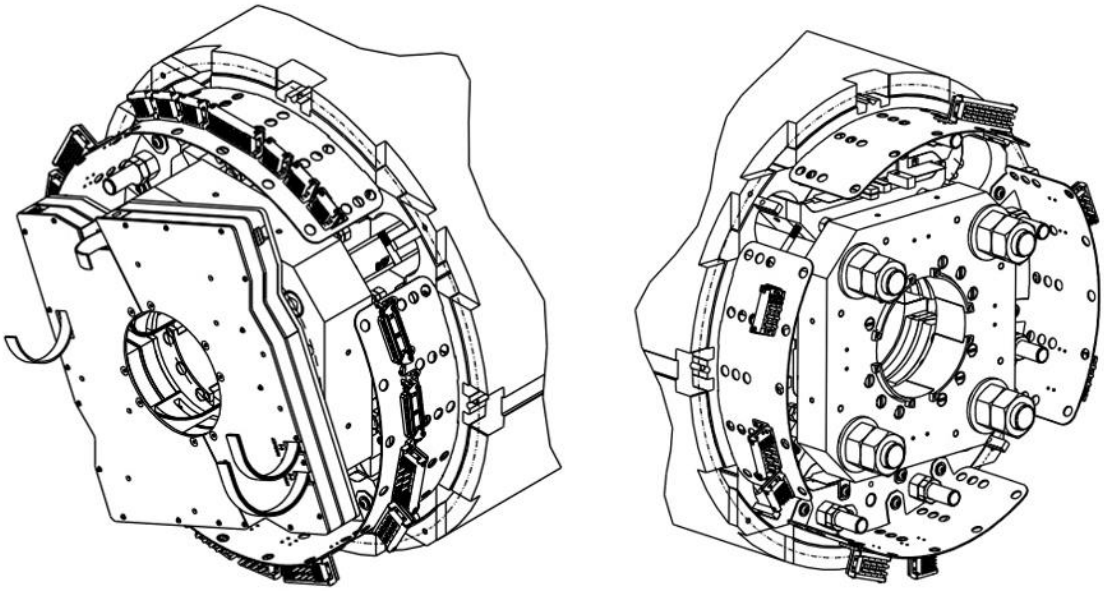

Figure 6.15: Detail of the connector skirts for the LE (L), and RE (R).

6.3 MQXFA Handling, Shipping and Uprighting

The iron lamination making the MQXFA pads and yoke are pre-compressed by stainless-steel tie rods, which give longitudinal rigidity to the MQXFA structure. The following requirements prevent conductor degradation, and preserve MQXFA structure integrity:

MQXFA H&S Requirement #1: The conductor strain shall never exceed 500 microstrain in any part of the coils during any MQXFA handling or shipping operation.

MQXFA H&S Requirement #2: Every point of the contact surface between iron laminations shall always remain in compression during any MQXFA handling operation (for instance lifting, lowering, rotation and up-righting).

A support fixture is used to ship the completed magnet between labs. The fixture consists of two heavy steel channels and a series of aluminum cradles and clamps. The fixture is shown in Figure 6.16. The fixture is installed inside a wooden crate. Shipment is made using a dedicated truck, such that the once the crate is loaded onto the truck at the origin lab, it remains on the truck until it arrives at the destination lab. There is no loading and unloading permitted while on route. Truck is required to have an air ride suspension.

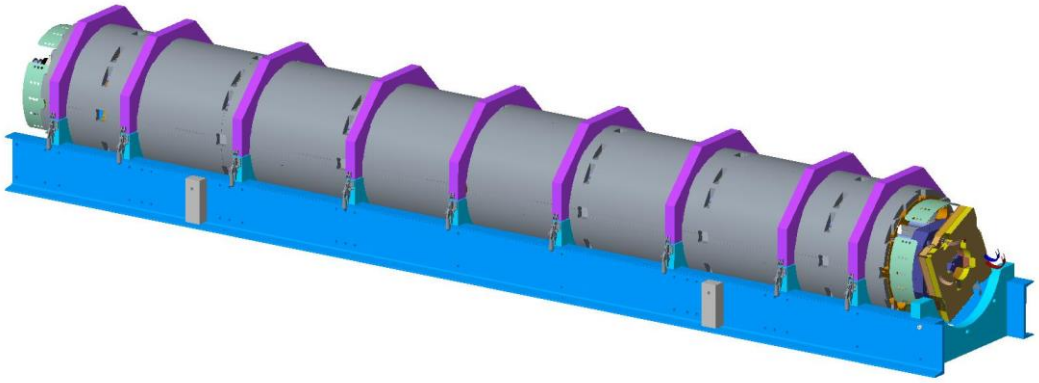

Figure 6.16: Magnet shipping fixture.

The magnet is uprighted in preparation for vertical cold testing. The magnet remains clamped in the support fixture during uprighting. The support fixture is connected to a pivot base assembly at the non-lead end. Hanging rods are installed in two of the magnet yoke holes and an endplate is installed at the lead end. The lead end of the magnet is then lifted with the overhead crane and the magnet is brought to vertical. Figure 6.17 shows the magnet during uprighting.

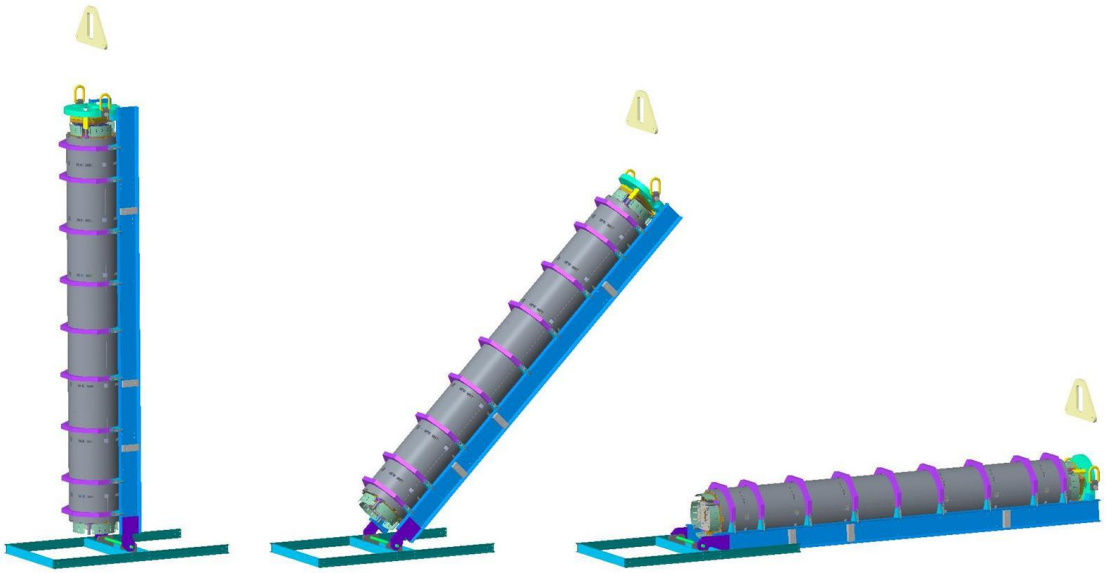

Figure 6.17: Magnet uprighting.

The magnet always remains supported by the overhead crane. Once the magnet is vertical, it is released from the support fixture and is moved to a wiring stand to be prepped for vertical cold testing.

7 MQXFA Vertical Test

All prototype and production MQXFA magnets will be fully trained and tested in the vertical test facility (Figure 7.1) at Brookhaven National Laboratory (BNL), and on acceptance will be shipped to FNAL for assembly into LQXFA cold masses to be tested there. Comprehensive magnetic field measurements will also be performed at BNL. There will be 2 prototype and 22 production models of MQXFA, so there will be a total of 24 tests at the BNL vertical test facility. The cold masses at FNAL will be assembled into the cryo-assemblies that will become the Q1 and Q3 elements of the HL-LHC inner triplets.

Vertical test stand 3 (Figure 7.2), to be used for the MQXF testing, is one of the vertical test cryostats previously used for over 30 years to test a wide variety of superconducting magnets, including RHIC and SSC arc dipole and quadrupole short prototypes, all the RHIC corrector magnets, and many others. This particular test stand has been upgraded to accommodate the size of the MQXFA magnets and also to provide testing at 1.9 K, and less, and at a pressure of 1 bar, or more, and to also provide powering up to 24 kA with fast switching capabilities for quench protection. In parallel with this, the cryogenics facility has also seen extensive upgrades in 2016, most of which have been funded by BNL. In the fall of 2016, the new facility was successfully commissioned, and in late 2016 and Jan of 2017, the first ever long coil of MQXF design was tested in a mirror configuration (MQXFPM1) and it reached the LHC ultimate operating point of 17.890 kA in 11 quenches, and after 19 quenches, reached 8% above ultimate (Figure 7.3). Along with this, quench protection heater tests and other R&D type measurements were done.

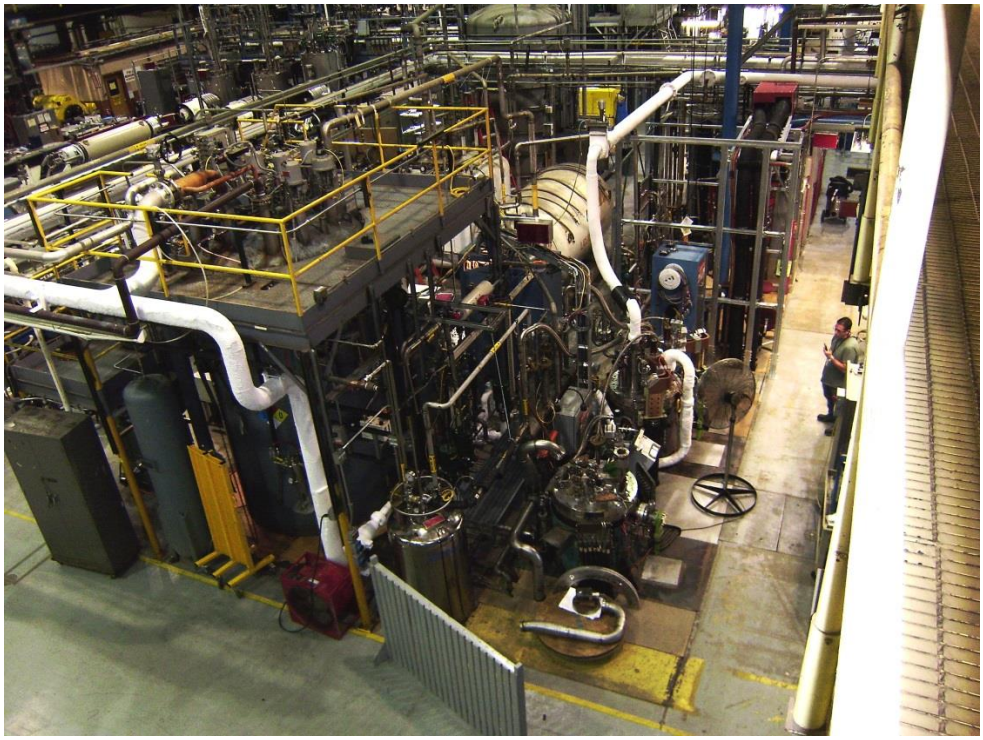

Figure 7.1: Vertical Test Facility at BNL, showing two of the five test cryostats and the backup refrigerator.

Figure 7.2: Vertical Test Stand 3, upgraded to provide 1.9 K at 1 bar (nom) and 24 kA, for testing of the 4.2 m-long MQXFA quadrupoles. The picture shows the test stand with the mirror MQXFPM1 under test.

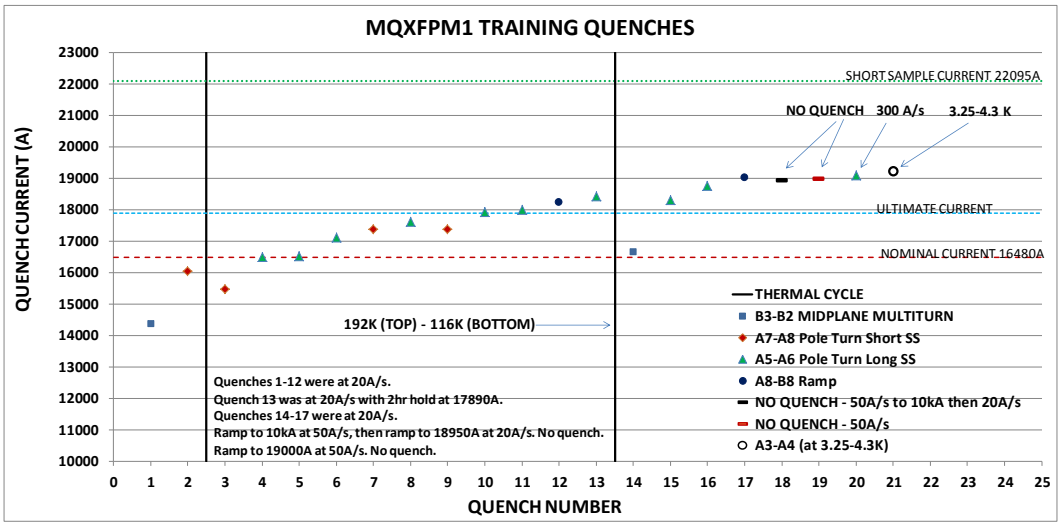

Figure 7.3: Plot of training quenches for the MQXFPM1 mirror at the BNL Vertical Test Facility.

7.1 Vertical Test Scope and Objectives - Prototypes

There will be two MQXFA prototype models, and the primary objective of the prototype testing is to provide information to magnet designers to validate design choices, verify performance, and reduce risk of MQXFA production. Another objective is acceptance before delivery to FNAL for possible assembly into a cold mass and a spare LQXFA cryo-assembly. The scope of these tests includes quench performance and training of magnets, room temperature (warm) and 1.9 K (cold) magnetic field quality and integral field measurements, and tests designed to determine the characteristics and parameters of the quench protection systems, among others.

MQXFA prototype magnets will be quench-tested to train to the maximum required test current of 19.8 kA, to verify stable mechanical and electrical operation. Magnet protection during training will make use of energy extraction to an external dump resistor as well as copper clad stainless steel quench protection heater strips. In addition, quench protection studies with protection heaters and CLIQ units, but without external energy extraction, will be performed. As already mentioned training and other spontaneous quench tests will be done with the external energy extraction system included, in order to save liquid helium and reduce the quench recovery time during training.

NbTi-NbTi splices between the magnet leads and the power bus-bars will be inspected at room temperature and monitored after cool down and during testing.

Major checkouts and measurements to be conducted for the two prototypes at the vertical test stand include:

At room temperature before cool down

- Electrical checkouts and tests ensuring the integrity of the insulation (high voltage, or hipot)
- Magnetic measurements: integral field strength and field harmonics (rotating probe)

Measurements during cooldown and warmup

- Temperature sensor (RTD) measurements
- Strain Gauge measurements
- Residual Resistivity Ratio (RRR) Measurements

After cool down to 1.9 K

- Hipot Measurement
- Magnetic Measurements
  - **Rotating probe measurements**
- Quench Training up to 19.8 kA
- Quench Characterization
  - **Voltage taps measurements**
  - **Quench Antenna measurements**

- Strain Gauge measurements
- Ramp Rate Dependence Measurements
- Holding ultimate operation current (2-8 hours)
- Quench Protection Studies with heaters and/or CLIQ
- Measurement of the magnet inductance versus current
- Quench Propagation Studies
- Voltage Spikes Measurements
- Energy Loss Measurements
- Splice Measurements (at 1.9 or 4.5 K)

Measurements at 4.5 K

- Assess short sample limit percentage at 4.5 K after 1.9 K training
- Ramp Rate Dependence at 4.5 K in case of issues at 1.9 K

At room temperature after warm-up

- Electrical checkouts and tests ensuring the integrity of the insulation (high voltage, or hipot)
- Magnetic measurements: integral field strength and field harmonics (rotating probe)

A thermal cycle will be included to verify that the magnet retains its training.

For planning purpose, we may assume 50 training quenches.

A magnet re-test after pre-stress adjustment or coil exchange may be needed and should be planned for all prototypes. The test plan for prototype re-tests should be shorter than the plan for a new magnet, aiming at assessing quench performance improvements/changes and completing the test plan. For planning purpose, we may assume 30 training quenches and ½ effort for protection and other studies. A thermal cycle should be planned also for MQXFA re-tests.

7.2 Vertical Test Scope and Objectives – Production Magnets

The primary objective of the production testing is quench training, magnet qualification and quality assurance. Each magnet will be tested and trained prior to cold mass (LMQXFA) assembly, in order to check its quality and verify that it meets all requirements. Production magnets will not be tested above 17.890 kA (ultimate operating current).

The test cycle of production magnets is expected to be shorter: production magnets will not have prototype instrumentation (for instance only voltage taps for splice measurement and quench detection and not for quench localization), and a thermal cycle may not be part of the test plan if the prototype testing demonstrates sufficient training memory, or if the production model training starts above operating current during production tests. Presently, the following numbers of quenches are suggested for planning purpose: 20 quenches at 1.9 K, 2 quenches at 4.5 K, and 2 quenches at 1.9 K after the thermal cycle (if needed).

NbTi-NbTi splices between the magnet leads and the power bus-bars will be inspected at room temperature and monitored after cool down and during testing.

Major checkouts and measurements to be conducted for the 22 production models at the vertical test stand include:

At room temperature before cool down

- Electrical checkouts and tests ensuring the integrity of the insulation (high voltage)
- Magnetic measurements: integral field strength and field harmonics

After cool down to 1.9 K

- Electrical checkouts(including high voltage)
- Quench test training – to 17.890 kA (ultimate operating current)
- Magnetic measurements: integral field strength and field harmonics
- Holding the ultimate current for an extended period of time
- Quench Protection Heater tests to verify nominal operation
- Splice measurements

At room temperature after warm-up

- Magnetic measurements: integral field strength and field harmonics
- Electrical checkouts before shipping to FNAL

7.3 Field Quality Measurements

Magnetic field measurements are performed at room temperature before and after the cool down, and at 1.9 K. The field harmonics are measured with a rotating probe based on the multi-layer printed circuit board design [1]. Integral field strength is determined with z-scans using the rotating probe.

At room temperature, field harmonics will be measured at low currents.

Field measurements will be done after cool down to 1.9 K. Integral field strength and field harmonics will be measured at a series of currents including injection (960 A) and collision (16480 A) currents.

A standard list of magnetic measurements with rotating probe for prototype magnets developed jointly with CERN include and already being performed on short models are:

- Z-scan
- Integral field measurements (as much as possible within test facility constraints)
- Loops (14, 20 and 40 A/s)
- Stair steps (with large steps)
- Accelerator cycle

For the production magnets, the list of measurements has not yet been decided, but will at least include room temperature and cold harmonics and integral field measurements (stair steps and z-scan).

A more detailed discussion of the test procedures and measurements can be found in the Functional Test Requirements document for MQXFA magnets [2].

7.4 Acceptance Tests

Requirements for qualification (acceptance) of the MQXFA magnets must be met before shipment to FNAL and assembly into LQXFA cold masses. The magnets will be accepted for shipment if all requirements, including quench performance at 1.9 K and specified tolerances for field quality for the integral magnetic field and the field harmonics before and after and during testing at 1.9 K.

7.5 High-Voltage Withstand Levels (Hipot Tests)

Requirements for testing electrical integrity of magnets were developed together with a working group at CERN [3]. The values of withstand voltages for the acceptance of MQXFA quadrupoles were finalized during the 1st International Workshop on Superconducting Magnet Test Stands [4] at CERN:

Table 7.1: Hipot values.

Circuit Element	**V hi-pot**	**I hi-pot [µA]**	**Minimum time duration [s]**
Coil to Ground at room temperature (RT)	3.7 kV	10	30
Coil to Quench Heater at RT	3 kV	10	30
Coil to Ground at cold (1.9 K)	1.8 kV	10	30
Coil to Quench Heater at cold (1.9 K)	2.3 kV	10	30

References

[1] J. DiMarco et al., "Application of PCB and FDM Technologies to Magnetic Measurement Probe System Development", IEEE Trans. Appl. Supercond., vol. 23, no. 3, 9000505, 2013

[2] MQXFA Magnets Functional Test Requirements, US-HiLumi-doc-137

[3] Follow the link: **HL-LHC HVWL Working Group**

[4] See the workshop materials here: https://indico.cern.ch/event/507584/

8 LMQXFA Cold Mass

8.1 Overview

The Inner Triplet (IT) quadrupoles are the magnetic system used that allow reaching low beta functions around the Interaction Point (IP). The triplet is made of three optical elements: Q1, Q2, and Q3. The upgrade of the Inner Triplets in the high luminosity insertions is the cornerstone of the LHC upgrade. The decision for HL-LHC heavily relies on the success of the advanced Nb_3Sn technology that provides access to magnetic fields well beyond 9 T, allowing the maximization of the aperture of the IT quadrupoles. A 15-year-long study led by the DOE in the US under the auspices of the U.S. LARP program, and lately by other EU programs, has shown the feasibility of Nb_3Sn accelerator magnets. The HL-LHC is expected to be the first application of accelerator-quality Nb_3Sn magnet technology in an operating particle accelerator.

For HL-LHC, 20 IT Nb_3Sn quadrupoles (16 plus spares) are needed: they all feature 150 mm aperture and operating gradient of 132.6 T/m, which entails 11.5 T peak field on the coils. In addition, HL-LHC will use the same Nb_3Sn technology to provide collimation in the Dispersion Suppression (DS) region, which will be achieved by replacing a number of selected main dipoles with two shorter 11 T Nb_3Sn dipoles (MBH).

Figure 8.1 shows a conceptual layout of the HL-LHC interaction region, and Figure 8.2 shows the CERN nomenclature of the IT system.

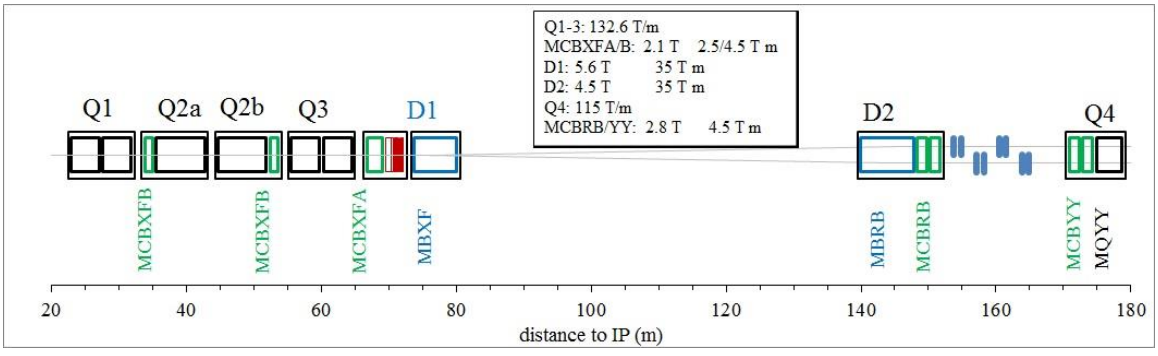

Figure 8.1: Conceptual layout of the IR region of HL-LHC– thick boxes are magnets, thin boxes are cryostats.

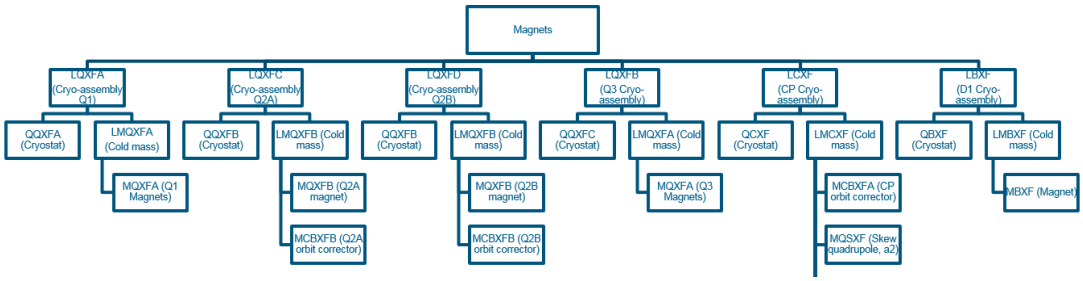

Figure 8.2: CERN Naming Conventions for HL-LHC Inner Triplets.

The MQXFA magnet is the quadrupole magnetic element of Q1 and Q3, including the coils and mechanical support pieces to a perimeter defined by the outer shell of the magnets and the end plates of each magnet. Figure 8.3 shows the LMQXFA cold mass cross section (without the LHe SS vessel one obtains the MQXFA magnet cross section). A pair of ~ 5m MQXFA magnet structures is installed in a stainless steel helium vessel, including the end domes, to make the Q1 and Q3 Cold Mass (LMQXFA). Q2a and Q2b each consist of a single unit MQXFB ~ 7m long. The LMQXFA, when surrounded by the QQXFA or QQXFC cryostat shields, piping, and vacuum vessel, is then the LQXFA cryo-assembly for Q1 and the LQXFB cryo-assembly for Q3, as installed in the tunnel of LHC. The US provides the Q1 and Q3 assemblies for two interaction regions.

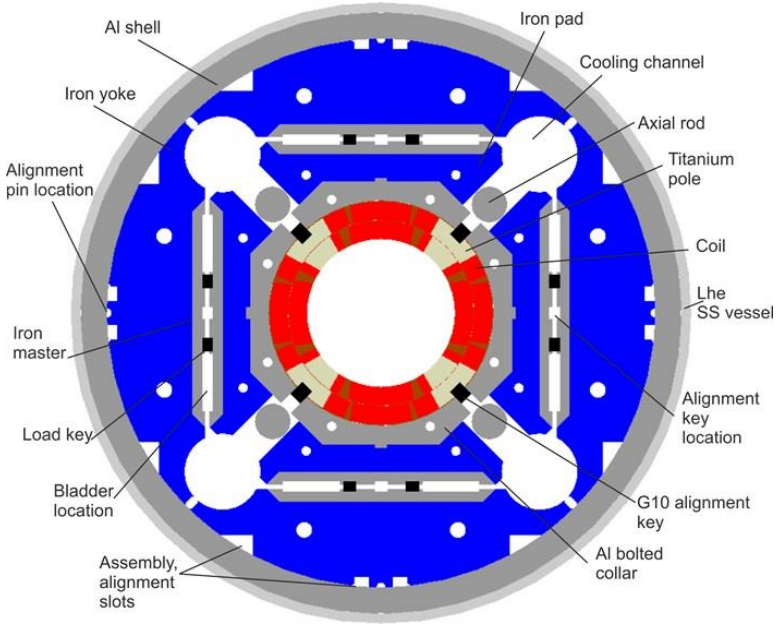

Figure 8.3: LMQXFA Cross Section. The difference between the cold mass LMQXFA and magnet MQXFA is the LHe SS vessel.

8.2 Scope

The main objective for this L3 subproject is to fabricate 1 LMQXFA cold mass assembly prototype and 10 LMQXFA production cold mass assemblies. Each cold mass has two MQXFA magnets inside a stainless steel helium containment vessel. Scope includes:

- Design the Prototype and Production Cold Mass
- Parts procurement for 11 cold mass assemblies
- Receive and inspect cold mass assembly parts from CERN
- Assemble 12 cold mass assemblies (1 prototype, 10 production, and 1 re-assembly). Activities include pressure vessel fabrication, wiring and bus work, safety compliance and all the relevant tests that is necessary for the assembly process (like alignment) and for QC/QA
- The tooling design, procurement of tooling parts, assembly the tooling at the Cold Mass fabrication facility and testing that the tools are safe to use

Scope Assumptions/Exclusions:

- Several cold mass parts are assumed to be provided by CERN (shell, end cover, beam tube, bus-work, instrumentation, wiring, heat exchangers)
- 10% of the cold mass assembles (1 out of 10) are assumed to need to be re-worked before they can pass horizontal acceptance test

Deliverables to CERN: A minimum of 10 accepted LMQXFA cold mass assemblies with their corresponding QC and safety reports. Deliverables for the "Cryo-assembly fabrication and shipment" L3 subproject also includes the prototype LMQXFA cold mass.

The deliverables will be designed and fabricated to satisfy the Functional Requirement Specifications [1].

8.3 Conceptual Design

The cold mass is defined as the helium pressure boundary containing two MQXFA magnets. The Q1 and Q3 cold masses of the interaction region triplet will require 10 cold masses identified as LMQXFA. With the understanding that the Q1 and Q3 assemblies are identical, the term cold mass will refer to both, Q1 and Q3 cold masses.

The MQXFA magnet pair will be aligned axially with return ends facing each other. The distance between the two magnet ends inside the cold mass is critical for the accelerator layout and performance, and for the magnet to magnet splice design. The two (2) magnets will be aligned to maintain critical tolerances for pitch, yaw and roll angle as well as overall length and distance between magnetic centers.

The cold mass pressure vessel must be designed for a working pressure differential of 20 bar at 1.9K He and must be designed to withstand asymmetrical axial forces due to quench on other magnets and other events.

The cold mass major components consist of:

- Stainless Steel Half Shells
- Stainless Steel End Covers
- Heat Exchangers (designed & supplied by CERN)
- Stainless Steel Beam pipe (Supplied by CERN)
- Bus
- Instrumentation.

8.3.1 Shell

The shell will be fabricated from 5/16 inch (8mm) thick 316/316L stainless steel plate that will be cut and formed into two (2) 180° half shells with tangents and extra length to allow for pre-weld machining as well as any required weld shrinkage. Material for the shells will be supplied by CERN to meet low Cobalt content requirements.

The 5/16 inch (8mm) thick shell is required for a maximum internal design pressure of 20 bar and also meet the maximum physical outer diameter requirements of 630 mm. This OD specification limit does not include attachments for interfacing with or mounting to the cryostat.

The shell will be attached to the MQXFA magnets physically at each of the two longitudinal seams, 180 degrees apart. Each MQXFA magnet has 9 openings per side (18 total/magnet or 36 total/cold mass) through the aluminum outer shell that will allow for stainless steel blocks to be fastened with bolts to the inner iron yoke and sit flush with the aluminum shell. A matching slot through the stainless blocks and aluminum shell will allow for fitting a stainless steel backing bar that will be attached to each of the blocks by welding. This backing bar will serve a dual purpose. First, a barrier between the aluminum shell and stainless steel weld seam. Second, a root penetration weld that will lock or fix the shell and magnet together. See Figure 8.4.

Figure 8.4: Left: Tack Block Assembly; Right: Tack Block

a. Stress Requirements on the Shell

There is no minimum pre-stress requirement for the stainless steel shell. A zero pre-stress is acceptable although there is somewhat of a preference that the stainless steel skin is snug with no gaps between the shells but also completely welded and attached to the magnet via the longitudinal weld seam backing strip.

On the other hand, an excessive pre-stress of the stainless steel shell can cause misalignment issues for the cold mass but also affect the magnet performance. As analyzed by LBNL, a maximum coil stress at 4.2K will exceed 200 MPa when the pre-tension in the stainless steel shell is over 130 MPa. Thus, a maximum of 100 MPa pre-stress in the stainless steel shell must be maintained and controlled during welding of the shell.

b. Shell Tolerance Calculations Based on Weld Test results

Using a RT modulus of 198 GPa for Stainless Steel, a +/- 2.3 mm circumferential tolerance will equal a +/-37 MPa variation in the shell pre-stress (Heng Pan – LBNL). The shrinkage experienced by Fermilab welders during a mock up sample was 0.100” (2.5 mm) on a 24” long weld seam. For 2 longitudinal seams, we add 0.11” (2.8 mm) to the shell circumference. A shell total shrinkage of 0.200” (5.1mm) will result in a 0.09” (2.3mm) interference for a 37MPa shell pre-stress. An additional 0.09” (2.3 mm) shrinkage in the circumference will result in an additional 37MPa for a maximum pre-stress of 74 MPa. A 0.09” (2.3 mm) less than expected shrinkage of the shell will result in the shell to be snug on the aluminum shell of the magnet for a minimum (0) pre-stress.

c. Design Drawings of the shell

The shell is designed to allow for one half shell to be fit in place and tacked in place to backing bar prior to rotating (rolling) the cold mass assembly, installing the instrumentation, Bus, Beam Pipe, Heat Exchangers and fit/tack the second half shell. The half shell overall length and weld preps are machined per print with tangents to allow for any weld shrinkage in the stainless-steel shell. Tolerances shall be included to maintain shell straightness and geometry during forming as well as any tangent lengths and weld preps during machining.

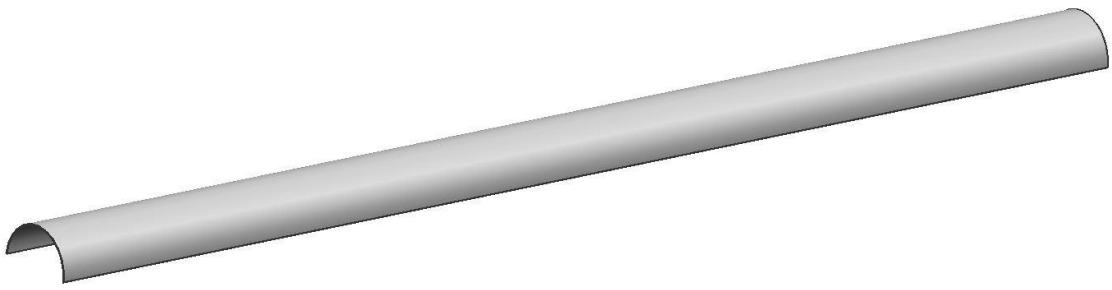

Figure 8.5: Half Shell.

8.3.2 End Cover

Cold mass end cover (Figure 8.6) has several openings that serves several functions:

- Instrumentation port – used for the main bus bars, CLIQ leads and the instrumentation wires
- Heat Exchanger opening – used for inserting the Heat Exchanger into the cooling hole of MQXFA
- Beam Tube – used for inserting the Beam Absorber
- LHe inlet – for the liquid Helium to enter to the Cold Mass volume.

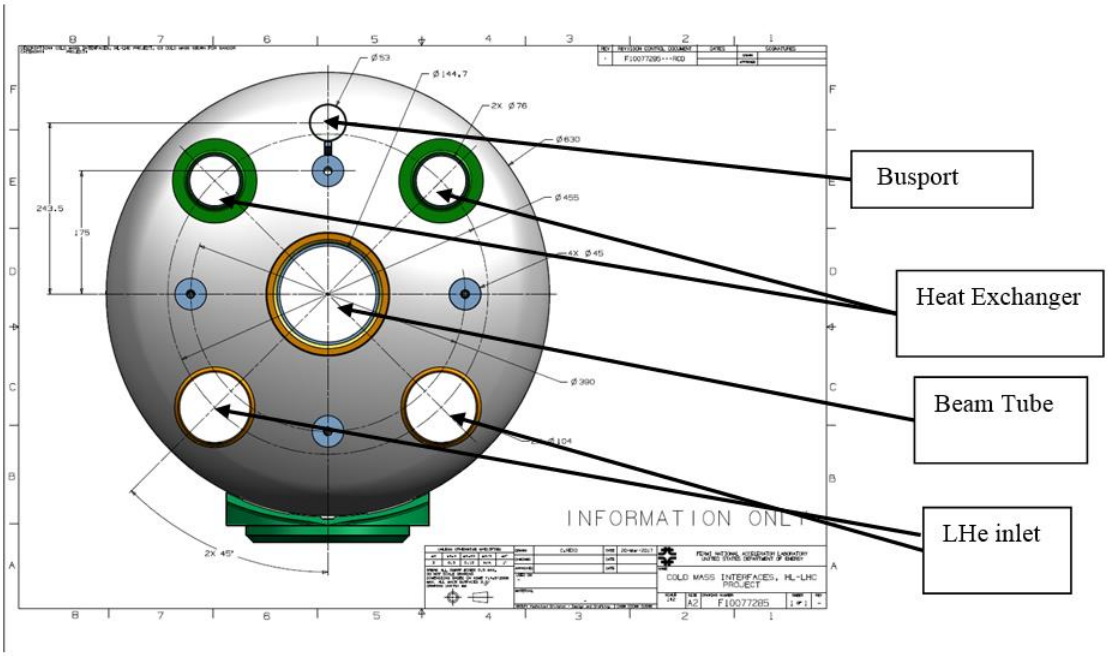

Figure 8.6: End Cover containing several openings.

The 316/316L plate material for the End Covers will be supplied by CERN and comply with low Cobalt content requirements. The End Cover can be formed or spun to a 2:1 elliptical or ASME Flanged & Dished Head profile if only the raw material is supplied by CERN.

In addition to above defined nozzles, the End Covers will also require (3) machined pads to define a reference plane on both ends of the cold mass.

8.3.3 Heat Exchanger

Two (2) Heat Exchangers for each cold mass will be supplied by CERN. The Heat Exchangers will be installed in the two upper 77 mm diameter quadrant cooling channels of the MQXFA yoke and run the length of the cold mass. The 74 mm OD Heat Exchangers will be

installed with supports to provide sufficient annular space and allow adequate flow for maximum heat extraction.

8.3.4 Beam Pipe

One (1) Beam Pipe for each cold mass will be supplied by CERN. The Beam Pipe material must be seamless low cobalt content 316LN stainless steel. The Beam pipe is installed and centered in the MQXFA magnets by contact between insulation on the outside of the Beam Tube and the ground insulation that covers the pole of the collars in the magnet assembly. The Beam Pipe is terminated with a flange at either end of the cold mass at the End Domes.

8.3.5 Bus work

a. Bus design

The LHC bus that has been successfully used for the IR triplet is a suitable bus design for the HiLumi project. Another option is to use the pair of NbTi cables used for coil and magnet leads.

b. Bus Expansion Loops

The bus and expansion loops for the LMQXF cold mass will be similar to the design implemented on the previously built MQXB cold masses. Each Q1 and Q3 include a power lead (lead A), a local bus (lead B), a through bus and 4 CLIQ leads. The bus port through the magnet iron will contain all these leads as shown in Figures 3.5.1 and 3.5.2. Each cable will have a “loop” on each end. The current plan is based on the assumption that the bus is fixed to shell of the cold mass at the center, between the return ends of the two magnets.

The configuration of the Q1 will be identical to that of the Q3. The QB is “flipped” vertically with respect to the Qa to provide the appropriate field rotation necessary between the Q1a and the Q1b. Since the Qb is “flipped” vertically with respect to the Qa the bus work on the face of the Qb will be slightly different in shape to that of the Qa.

Figure 8.7 shows an entire string with the cold masses connected. Figure 8.8 shows the configuration of a single Q1/Q3 cold mass. Figure 8.8 is identical to the area inside the dotted box in Figure 8.7, except that the positions of the voltage taps are added.

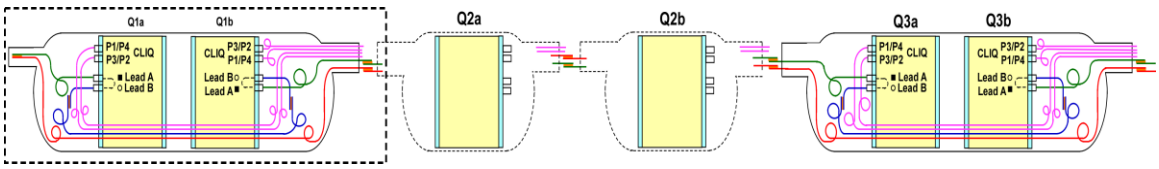

Figure 8.7: Bus work (entire string shown). Green lines represent lead A, blue lines represent lead B, red lines represent the through bus, and purple lines represent the CLIQ leads.

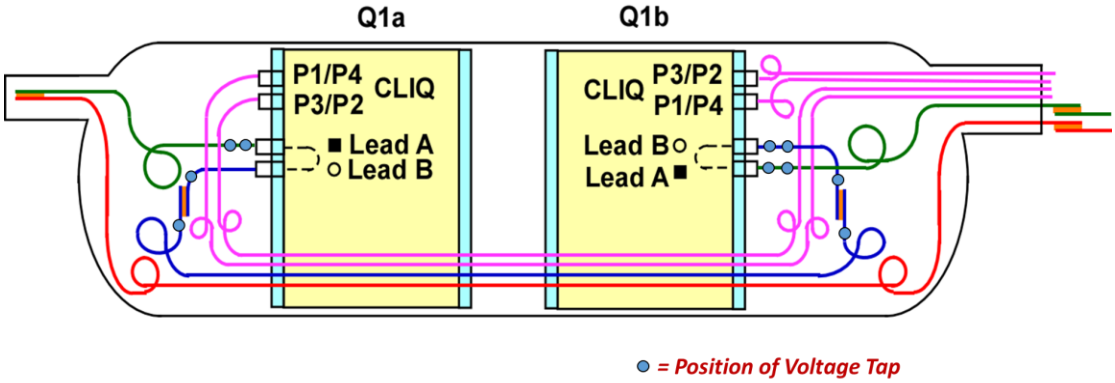

Figure 8.8: Bus work of a single cold mass. In addition to the leads, positions of the voltage taps are shown by the light blue dots.

End views of the Q1 cold mass are shown in Figure 8.9, showing the general shapes of the leads as they traverse the outside surface of the magnet. The various types are represented by colored lines, using the same convention as in Figure 8.7 and in Figure 8.8.

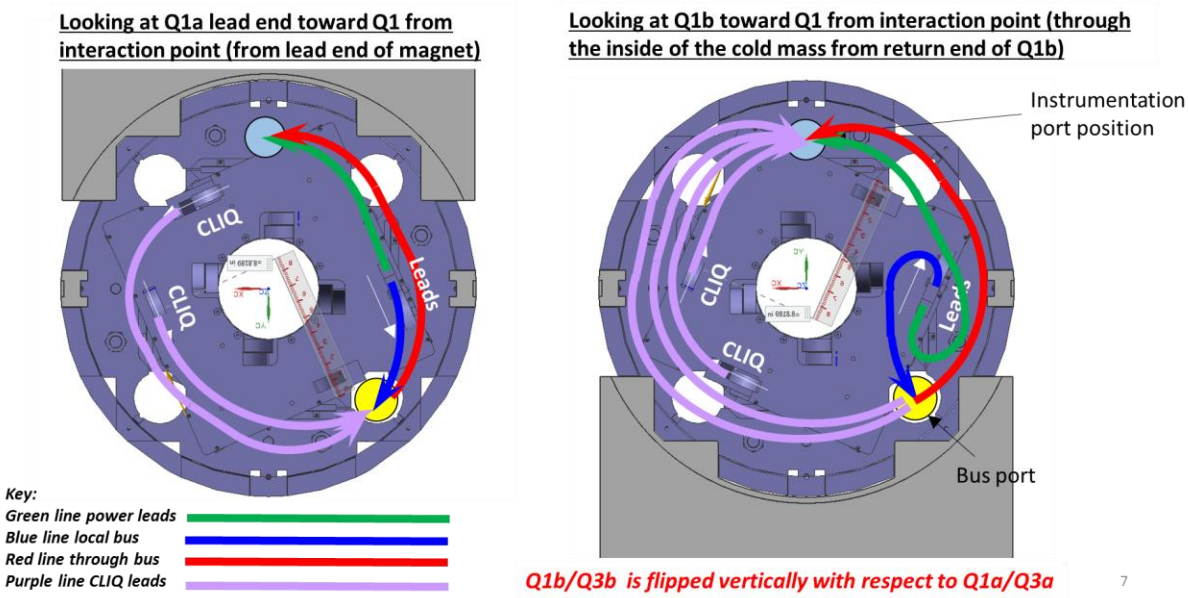

Figure 8.9: End views of a single cold mass. Note that both views are from the same direction, The Q1a is viewed from the lead end looking toward the return end, while the Q1b is viewed from the return end looking through the magnet toward the lead end. The magnet is "flipped" vertically, providing the appropriate field rotation necessary between the Q1a and the Q1b.

The general configuration of the LQMXF expansion loops will be similar to those used on the MQXB Q2 cold masses. Figure 8.10 shows a picture and illustration of these loops. A mockup will be built to determine the exact shape and position of the loops.

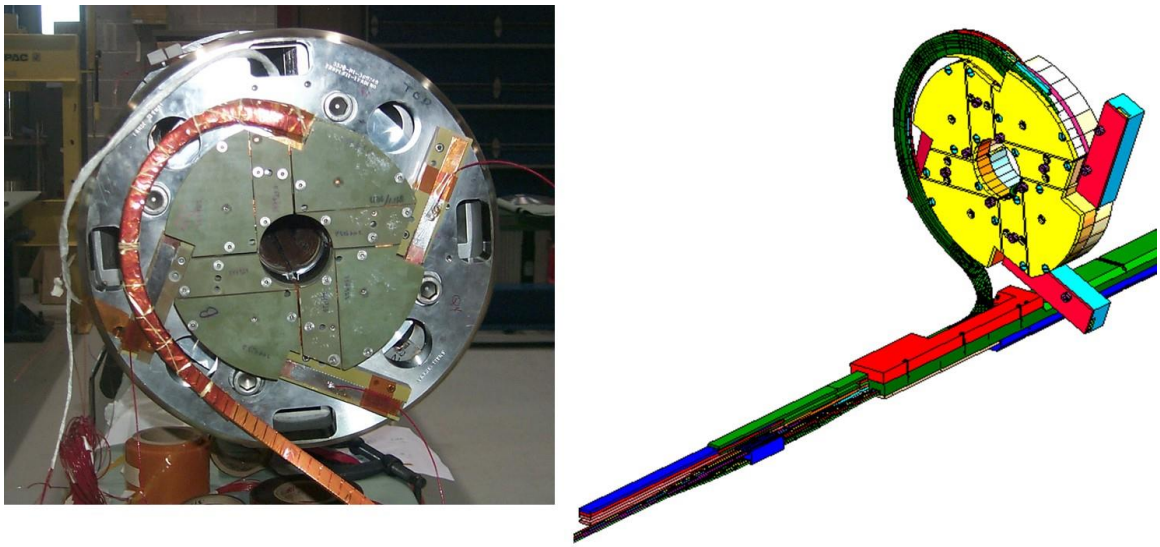

Figure 8.10: Picture and illustration of the MQXB Q2 expansion loops.

The maximum axial travel for any loop is expected to be no more than 50 mm. Figure 8.11 shows the approximate amount of space within the LMQXF end dome, from the "pizza box" to the inside of the dome surface. There should be sufficient space to allow for all loops to be formed.

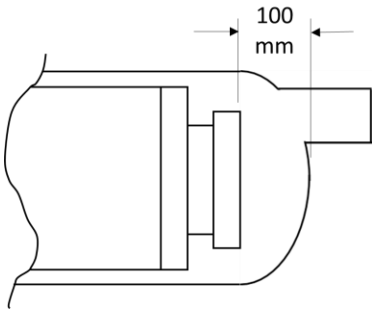

Figure 8.11:Space inside LQMXF cold mass end dome.

c. Bus support

A single bus housing, made of G-11, will be placed within the designated bus port at the position shown in Figure 8.9. A cross section of the bus housing is shown in Figure 8.12. This is similar in design to the bus housing used for the MQXB Q2 cold masses. The housing will be supported by "spiders" (not shown in the figure) at a fixed position within the bus port.

An illustration of the previous MQXB Q2 bus housing is shown in Figure 8.13.

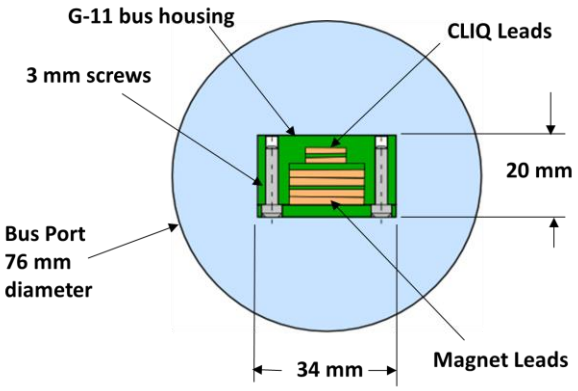

Figure 8.12: Cross section of bus housing.

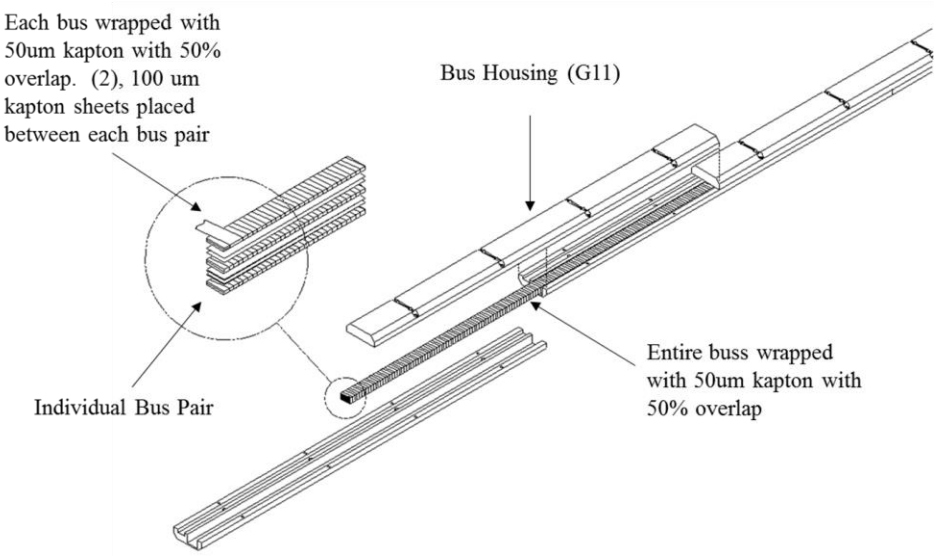

Figure 8.13: Illustration of bus housing used in the MQXB Q2 cold mass.

8.3.6 Instrumentation

The Cold mass is instrumented with temperature sensors, warm up heater and Voltage taps. Additional to this there are several other V-taps that are mounted onto the MQXFA magnets. These V-taps also had to be routed out through the instrumentation port.

a. Temperature sensors

Two (2) temperature sensors will be installed at least one meter from the end-plate, on the rim of the yoke. These sensors are the short type thermometer assembly (36 mm x 12 mm x 10 mm) typically used and specified by CERN.

b. Warm up heater

A 50 W warm up heater should be attached to each of the four MQXFA end plates. These heaters are independently powered. CERN will supply the warmup heaters at no cost to US HL-LHC AUP.

c. Voltage Taps

The LMQXFA cold mass assembly include a total of 16 voltage taps to verify the splice resistance between each MQXFA magnet and the main current bus and to protect the magnet and the bus.

8.3.7 Tooling

The cold mass fabrication process will consist of multiple stations. The first station with tooling will require a table levelled and anchored to support the length of the cold mass. Support fixtures mounted on the table to support each magnet horizontally for leveling and aligning the pair prior to assembling components and fit/tack welding one half shell on the same station.

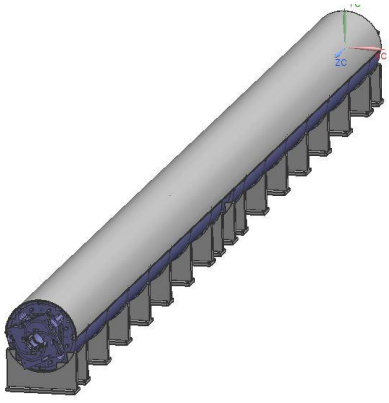

Figure 8.14: Alignment Tooling.

A spreader beam or lifting fixture will be used to support the weight and full length of the cold mass to move the assembly from one station to the next. A Cold Mass & Cryostat weight estimate summary is included in Figure 8.15.

Item	Description	Weight (per unit, lbs.)	Units (per assy)	New Weight 4/15/16 (Subtotal)	Tons
Magnet	LBNL QXF Magnets - model weight	21,100	2	29800	*14.9*
Shell	316L SS He Pressure Shell	2550	1	2350	*1.175*
Heads	316L SS He Pressure Heads	75	2	150	*0.075*
CERN Beam	Est. 316LN Tube	110	1	120	*0.06*
CERN Ht –X	Est. Cu Corrugated Tube w/ Flgs	100	2	200	*0.1*
Bus/Misc	Est. Electrical & G10 supports	500	1	500	*0.25*
CERN Cryostat kit	from Delio370kg/m: VV,Shield,piping & supports		1	7782	*3.891*
	Cryostat TOTAL			***40902***	***20.451***
	Est. Spreader Bar		1	7000	*3.5*
	BTH weight total			***47902***	***23.951***

Figure 8.15: Cryostat Weight Summary.

A second station will be utilized for rotating the cold mass 180 degrees using weld rollers.

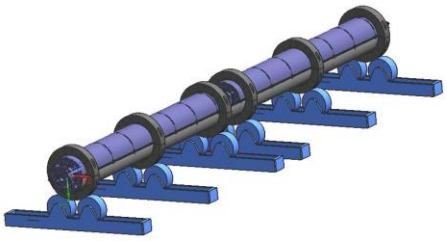

Figure 8.16: Rolling Station.

A third station will be another table levelled and anchored with saddle supports to fit the length of the cold mass. The saddle fixtures will support the cold mass with the bottom half shell fit and tacked in place. This station will be used to install the bus, instrumentation, Heat Exchangers and Beam Pipe prior to fitting and tack welding the top half shell. This same station will also host the longitudinal welding sequence. A semi- automatic modular drive system on rails used to simultaneously weld on both sides using a gas metal arc welding (GMAW) process. Additional supports and mounting brackets will be designed/fabricated to support welding equipment as well as fixtures for aligning and fixturing the End Covers for tack welding in place.

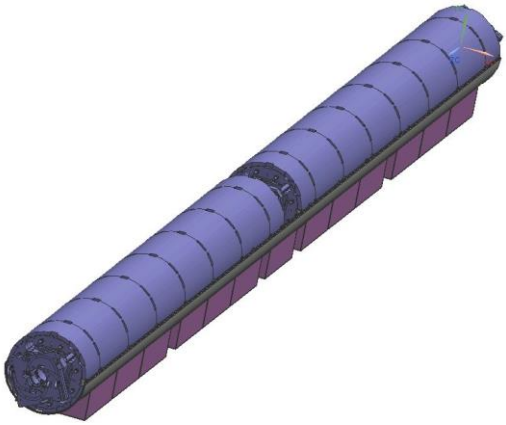

Figure 8.17: Saddle Station.

A preliminary floor layout of the workstations is below.

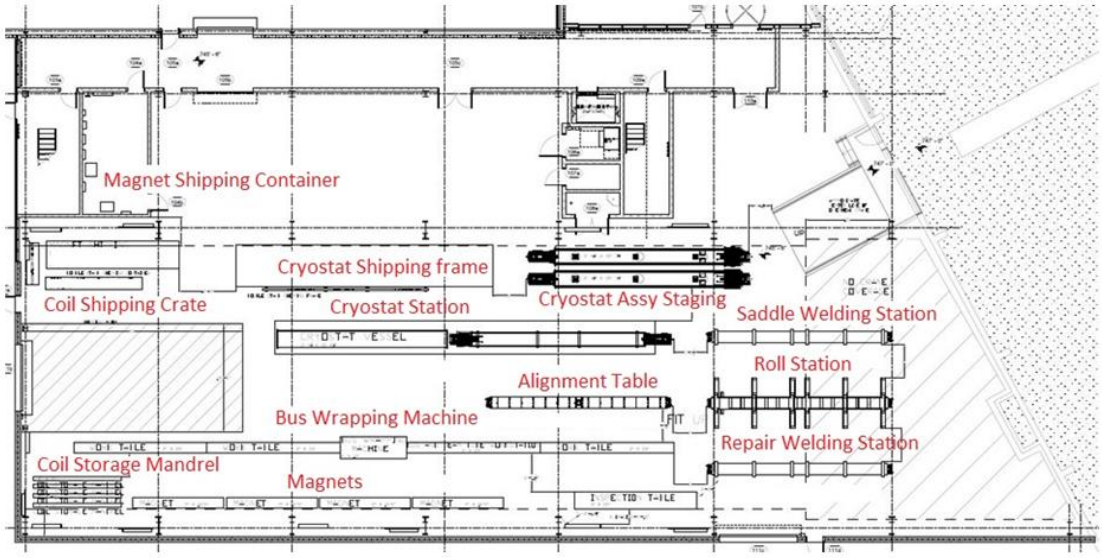

Figure 8.18: Fabrication Floor Plan 1.

8.4 Fabrication

The cold mass assembly will require a few formed or machined components to be procured prior to assembly. Some, if not most of the fabrication may be done by outside vendors. The list of the major components to be procured is included in the following section.

8.4.1 Component Procurement

A list of major components that will need to be procured through outside vendors:

- Shell… forming & machining
- Heads… forming & machining
- Flat Bar for weld backing … material
- Tack Blocks… material & machining
- Pipe/Tube Nozzles & Flanges for End Covers…material
- Fasteners for Tack Blocks…material

8.4.2 Assembly Procedures

Assembly of each cold mass begins with delivery of the first MQXFA magnet and continues until the cold mass is tested and ready for installation into a cryostat. Below is a sequence of the assembly steps.

1. Magnets reception (visual inspection, mechanical and electrical measurement)
2. Magnets alignment on the dedicated bench
    a. Individual geometrical measurements of straightness in horizontal and vertical planes, twist over full length.
    b. Pitch, yaw and roll angle between magnets.
3. Install tack blocks & Backing bar.
4. Fit & tack SS Half Shell (Bottom shell located in the top position at this point)
5. Mount lifting fixtures and prepare for lifting - transport to rolling station.
6. Roll assembly 180 degrees and transport to assembly/welding station.
7. Confirm alignment – Straightness, twist, roll and pitch.
8. Install instrumentation, bus work, warm bore/beam pipe and heat exchangers.
9. Electrical Checkout
10. Fit & tack SS Half Shell (Top shell located in the top position at this point).
11. Set up semi-automatic welding and simultaneously weld both longitudinal seams.
12. Confirm alignment – Straightness, twist, roll and pitch.
13. Visually inspect welds and spot radiograph test (RT) welds – 6 inch spot between MQXFA magnets on both welds by NDE vendor (reduce foot traffic through work area – evening/weekends).
14. Fit/Weld mounting pads for Cryostat interface.
15. Weld End Dome & nozzles
16. Utilize End dome centering fixtures to Fit/align/tack End Domes in place and beam tubes.
17. Fit Blanks to port flanges for pressure test.
18. Pneumatically pressure test cold mass.
19. He mass spectrometer leak test cold mass after pressure test.

8.4.3 Tests

During assembly of the cold mass, various test are performed to confirm quality of the welds and to verify performance tolerances. Test included are:

- Mechanical tests
    - In process dimensional inspection on machined/formed components.
    - Visual weld inspection.

- Spot Radiography testing (RT) of longitudinal weld seams. A 6 inch spot is required for every 300 Ft. of weld.
- Pneumatic Pressure test.
- He mass spectrometer leak test.
- Charpy impact notch toughness testing (samples)?

– Electrical Tests
- Dielectric voltage standoff test of the Cold Mass
- V-tap continuity measurements

– Warm magnetic measurements for alignment purposes
- Magnetic length measurement using small rotating coil probe
- Stretched wire axis measurements for each magnet upon insertion
- Subsequent measurements as necessary during fine adjustment of magnet position

8.4.4 Alignment

Survey will be done several times during the assembly process to assure proper alignment of the magnets relative to the cold mass vessel (and each other) and relative to the cold mass end cover piping:

– Survey effort will be combined with warm magnetic measurements to find the magnet axis and the centers of the magnets relative to each other and relative to the shell. The survey activity will be performed before and after the welding of the shell.
– Survey effort will be combined with warm magnetic measurements to find the field angle of the cold mass before and after welding the end cover to the shell.

8.4.5 QC &QA

To maintain a consistent quality throughout the production and prototype units, fabricated parts shall be dimensionally inspected and assemblies shall be verified for form, fit and function per the requirements of the LMQXFA Cold Mass Functional Requirement Specifications (FRS).

The FRS specifies the functional requirement for the High Luminosity LHC (HL-LHC, or HiLumi LHC) LMQXFA Cold Masses. Ten (10) of these cold masses are expected to be fabricated and delivered to CERN by the U.S. HL-LHC Accelerator Upgrade Project (US HL-LHC AUP) as part to the U.S. contributions to the LHC High Luminosity Upgrade.

If all the threshold functional requirements specified in the document are verified, then US HL-LHC AUP LMQXFA cold mass deliverables should be fit for the intended use and satisfy CERN's needs for the HL-LHC upgrade. The quality of the US HL-LHC AUP LMQXFA deliverables will be measured by the degree to which its characteristics fulfill the requirements specified in the FRS document.

To satisfy pressure vessel safety, the Fermilab Environment, Safety and Health Manual chapter 5031 for pressure vessels and ASME B&PV Code Section VIII div.1 rules shall apply to all cold mass design and fabrication.

Pending outcome from discussions with CERN, various sections of the European Pressure Vessel Directive (PED) may also apply for design and fabrication of the cold mass (See Section 6, ES&H).

8.5 Interfaces

The responsibility for the cryostat interfaces are described in the "Cold Mass Interface Control" document. The interface specifications should address the following areas:

- Magnet
  - Bus work
  - Instrumentation wiring
  - CLIQ leads
  - Lifting and Handling
- Cryostat
  - Piping dimension – Instrumentation port, helium inlets, beam line
  - Heat exchanger
  - Beam screen
  - Instrumentation – bus wiring, temperature sensor wiring, Voltage tap wiring
  - Cold Mass Position Monitoring
  - Cryostat feet
  - Thermal shield
- Interconnect
  - Piping dimensions – helium lines, thermal shield lines
  - Vacuum vessel flange

8.6 ES&H

ES&H is integrated into all phases of the Project: Design, Construction, Installation. ES&H requirements are clearly defined within the Project. It will follow Fermilab Environment, Safety and Health Manual as well as each HL-LHC work package will be subject to safety requirements specified in a CERN "Launch Safety Agreement (LSA)" document [2]. This LSA will specify the CERN safety rules and host state regulations applicable to the systems/processes and the minimal contents of the Work Package safety file needed to meet the Safety Requirements. The LQXFA/LQXFB cryostat assembly must comply with CERN's Launch Safety Agreement (LSA) for IR Magnets**.**

Design & installation review process includes an ESH component Utilize Fermilab's and CERN's work planning requirements & processes.

References

[1] LMQXFA Functional Requirements, US-HiLumi-doc-64

[2] CERN Launch Safety Agreement for IR Magnets (WP3), CERN EDMS 1550065

9 LQXFA Cryostat Assembly

9.1 Overview

The MQXFA magnet is the quadrupole magnetic element of Q1 and Q3, including the coils and mechanical support pieces to a perimeter defined by the outer shell of the magnets and the end plates of each magnet. A pair of ~ 5m MQXFA magnet structures is installed in a stainless steel helium vessel, including the end domes, to make the Q1 and Q3 Cold Mass (LMQXFA). Q2a and Q2b each consist of a single unit MQXFB ~ 7m long. The LMQXFA, when surrounded by the QQXFA or QQXFC cryostat shields, piping, and vacuum vessel, is then the LQXFA cryo-assembly for Q1 and the LQXFB cryo-assembly for Q3, as installed in the tunnel of LHC. The US provides the Q1 and Q3 assemblies for two interaction regions.

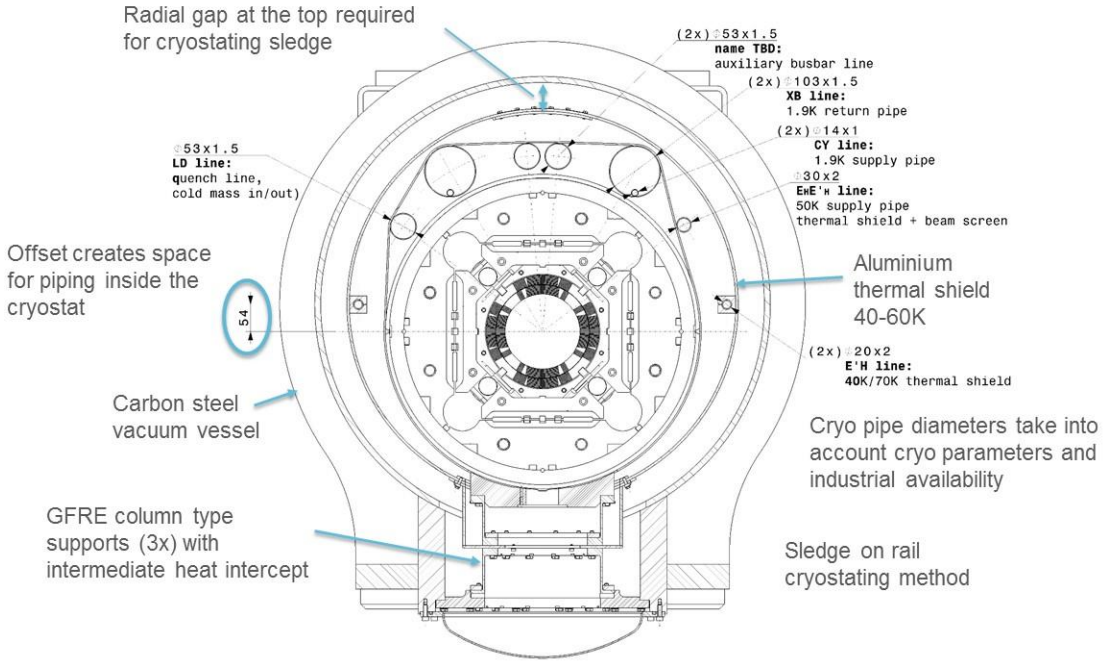

Figure 9.1: LQXFA/LQXFC Cross Section.

9.2 Scope

The scope is the assembly of 12 Q1/Q3 cryo-assemblies (1 prototype, 10 production, and 1 re-work). Each cryo-assembly has one LMQXFA cold mass assembly inside the CERN-supplied QQXFA cryostat kit. Activities include receiving QQXFA cryostat parts from CERN, procuring necessary additional parts, assembling the CERN QQXFA cryostat, inserting the LMQXFA cold mass assembly into the cryostat, and delivering the cryostat to the Horizontal Test Facility for

testing. After a successful horizontal test, the cryo-assembly is prepared for shipment and ship to CERN.

Scope assumptions/exclusions are as follows:

- CERN is solely responsible for the QQXFA cryostat design. Fermilab responsibility is limited to performing essential checks of the design making sure the design is sound and it can be operated safely in Fermilab's test facility.
- Parts for the entire cryostat are assumed to be provided by CERN
- 10% of the cryo-assemblies (1 out of 10) are assumed to need to be re-worked before they can pass horizontal acceptance test.

The deliverables to CERN are a minimum of 5 Q1 and 5 Q3 accepted cryo-assemblies.

The deliverables will be designed and fabricated to satisfy the Functional Requirement Specifications [1].

9.3 Conceptual Design

Cryostat design is the full responsibility of the CERN HL-LHC partner. The cryostat design concept currently developed by CERN has a lot of similarity with the design that has been produced for the LHC magnets. The main difference is the cold mass size, which has increased from the previous cold masses. For the present design, the calculated heat loads for the Q1 and Q3 magnets are summarized in Table 9.1.

Table 9.1: Calculated Heat Load.

Component	**Q1**	**Q3**
Length [mm]	10100	10100
Cold Mass		
Temperature [K]	1.9	1.9
Total heat Load [W]	134.5	138.2
Static [W/m]	0.85	0.84
Thermal Shield		
Temperature [K]	40-60	40-60
Total Heat Load [W]	66.6	54.3

Designers must continually be cognizant of the heat load to the helium system and of the structural loads imposed on the cryostat systems from static weight, shipping and handling, quench loads,

and ambient ground motion. These two considerations are generally at odds with one another. Low heat load implies a minimum of structural material conducting heat from the environment. Sound structural design implies material with sufficient strength to resist both static and dynamic forces. The structural requirements of the Q1 and Q3 are summarized in Table 9.2.

Table 9.2: Structural Requirements.

Component	**Q1**	**Q3**
Weight [kg]	22000	22000
Vacuum Vessel		
Temperature [K]	295.0-1.9	295-1.9
Pressure differential [bar]	±1	±1
Cold Mass		
Temperature [K]	295.0-1.9	295-1.9
Pressure [bar]	20	20
Maximum End Loads		
Vacuum force [kN]	80	
Pressure force [kN]	60	

This section summarizes the results of the design effort to date on the HL-LHC interaction region quadrupole cryostats. Thermal and structural aspects of the design will be described in detail. It will be addressed in turn; vacuum vessel, thermal radiation shield, multi-layer insulation (MLI), cryogenic piping, support system, and magnet interconnect.

9.3.1 Vacuum Vessel

The vacuum vessel is the outermost cryostat component and, as such, serves to contain the insulating vacuum. In addition, it functions as the major structural element to which all other systems are ultimately attached to the accelerator tunnel floor. Furthermore, it serves as a pressure containment vessel in the event of a failure in an internal cryogen line.

The solid model for the Vacuum vessel concept is shown in Figure 9.2. The Material choice for the vacuum vessel is low carbon steel certified resilience down to -50 C for pressure applications. The vessel is designed for 1/0.5 bar pressure differential (outside/inside). The end flanges (made from 304L forged rings) have to meet the interface specifications with the interconnect sleeve. The reinforcement rings have to clear up the space for the interconnect sleeve for interconnect opening and closing activities. Several openings are planned on the Vacuum Vessel shell:

- 3 ports for the support system
- 1 port for the relief valve
- 1 port for the feedthrough of instrumentation wiring
- 3 ports for cold mass position monitoring

There are several attachments to the Vacuum vessel:

- Survey monuments
- Support system reinforcement rings
- Lifting lugs

The expected weight of the vacuum vessel and its accessories is 3500 kg.

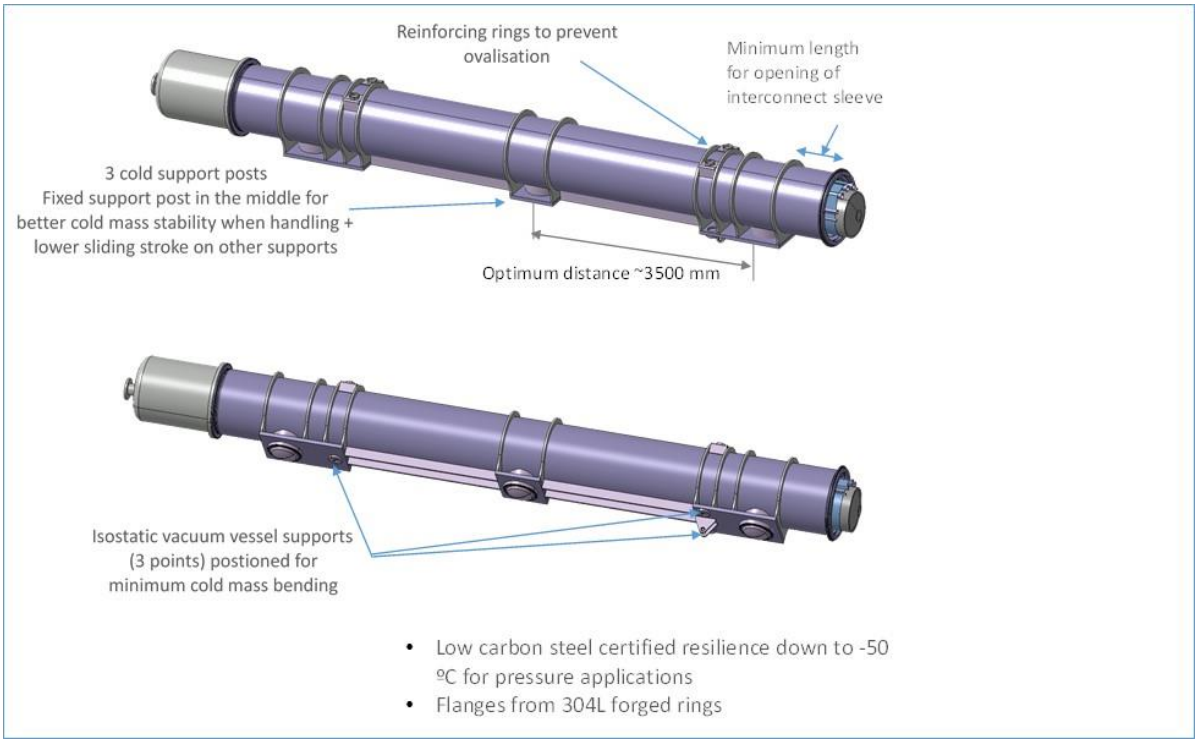

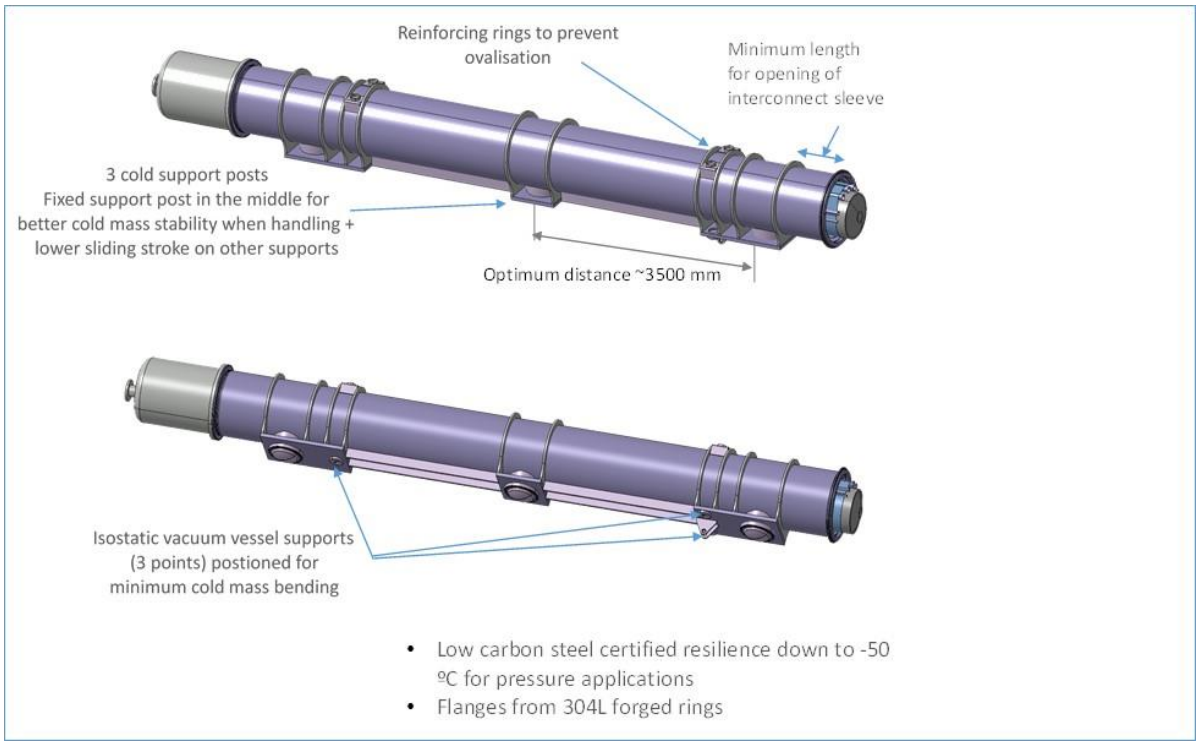

Figure 9.2: Vacuum vessel.

9.3.2 Thermal Shield

The QQXFA and QQXFC cryostats each have a single shield cooled by helium gas at between 40K and 60K. The shields intercept heat radiated from the 300K surface of the vacuum vessel and conducted through the support system. The thermal shield is comprised of two aluminum extrusions, each with a shield cooling flow line. The shield itself is a formed shell attached to the cryostat at the support structure. The nature of the shield function requires that the shell have high thermal conductivity to minimize thermal gradients around its circumference. Aluminum was chosen for this application. The shields most likely will be segmented along their length to minimize the effect of thermally induced distortions during cooldown caused by the possible asymmetric cooling of the two shield flow lines.

9.3.3 Multi-Layer Insulation

The multi-layer insulation system planned to be the same as it is used in the current LHC: 10 layers around the cold mass and 30 layers around the thermal shield.

9.3.4 Cryogenic Piping

In addition to providing the necessary structural support and thermal insulation for the cold mass assembly, the cryostat serves to contain the piping for all of the cryogenic services required for magnet and magnet system operation. The shield extrusions are anchored at one of the magnet supports and are free to slide axially at the other to allow for thermal contraction. All of the 1.9 K pipes are attached to supports that are in turn attached to the cold mass. This scheme minimizes the heat load to the structural supports. These pipes are also axially anchored at only one point. Table 9.3 summarizes the size of all the cryostat pipes. Table 9.4 lists the flow required design pressures, temperatures and flows.

Table 9.3: Cryostat pipe sizes.

	OD (mm)	**Tkns (mm)**	**Notes**
Vacuum vessel	1055	12.0	Carbon steel
Quench line	53	1.5	
Auxiliary busbar line	53	1.5	
1.9 K supply line	14	1	
1.9 K return line	103	1.5	
40-60K shield shell	TBD	TBD	Aluminum shell
50 K shield supply	30	2	Aluminum extrusion
40/70 K shield return	20	2	Aluminum extrusion
LMQXFA	630	8	

Table 9.4: Cryostat piping flow parameters.

	Fluid	**P oper (atm)**	**P max (atm)**	**T (approx)**	**Flow (g/s)**
Quench line	Lhe	TBD	TBD	TBD	TBD
Auxiliary busbar line	Lhe	TBD	TBD	TBD	TBD
1.9 K supply line	Lhe	TBD	TBD	TBD	TBD
1.9 K return line	Lhe	TBD	TBD	TBD	TBD
50 K shield supply	Ghe	TBD	TBD	TBD	TBD
40/70 K shield return	Ghe	TBD	TBD	TBD	TBD

9.3.5 Cold Mass and Cryostat Support System

The support system in any superconducting magnet serves as the structural attachment for all cryostat systems to the vacuum vessel that in turn anchors them to the accelerator tunnel floor. The emphasis was on meeting the allowed suspension system conduction heat load from Table 9.1, satisfying the structural requirements in Table 9.2, and maximizing the suspension stiffness. This last constraint is not explicitly defined in the design criteria, but comes from experience testing similar magnets. Assemblies that are more rigid tend to be more structurally stable during shipping and handling. The design concept has a lot of similarity with the LHC support system (Figure 9.3) that has:

- Two-part GFRE column
- Aluminium heat intercept plate (perfect heat intercept)
- Fixed support in the centre of cold mass rigidly connecting the cold mass to vacuum vessel
- Sliding support bolted to the cold mass and sliding on vacuum vessel
- Bolted assembly using invar washers and lock tab washers to ensure preload maintained at cold
- Thermal shield supported by the heat intercept plates, thus without additional heat load
- Thermalization straps on sliding support for independent movement between cold mass and thermal shield

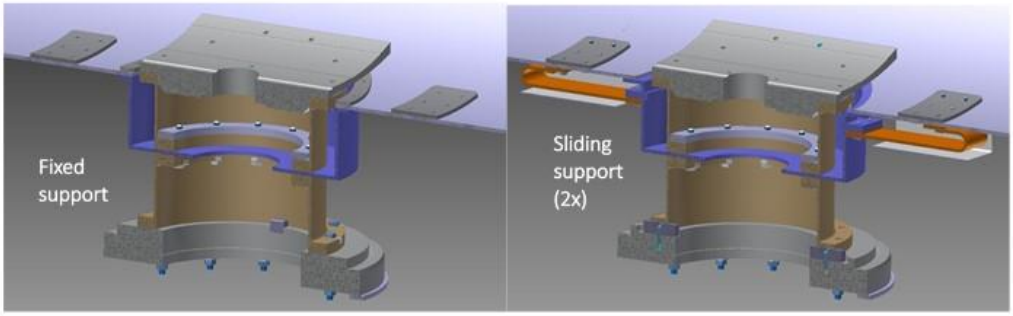

Figure 9.3: LHC support posts.

9.3.6 Interconnect

Interconnect design specifications are not part of the scope of this L3 document. However, they are an essential part of the interface specifications. It is also important to complete analysis of the interconnect forces that are additional constraints on the interconnect bellows design and the cryostat support system.

9.3.7 Tooling

The concept of the tooling is seen in Figure 9.4. The main tooling to be designed and procured are the:

- Cold mass and shield lifting jacks
- Sledge
- Rails

This method of inserting and securing the cold mass into the cryostat has been used successfully during the production of the LHC magnets.

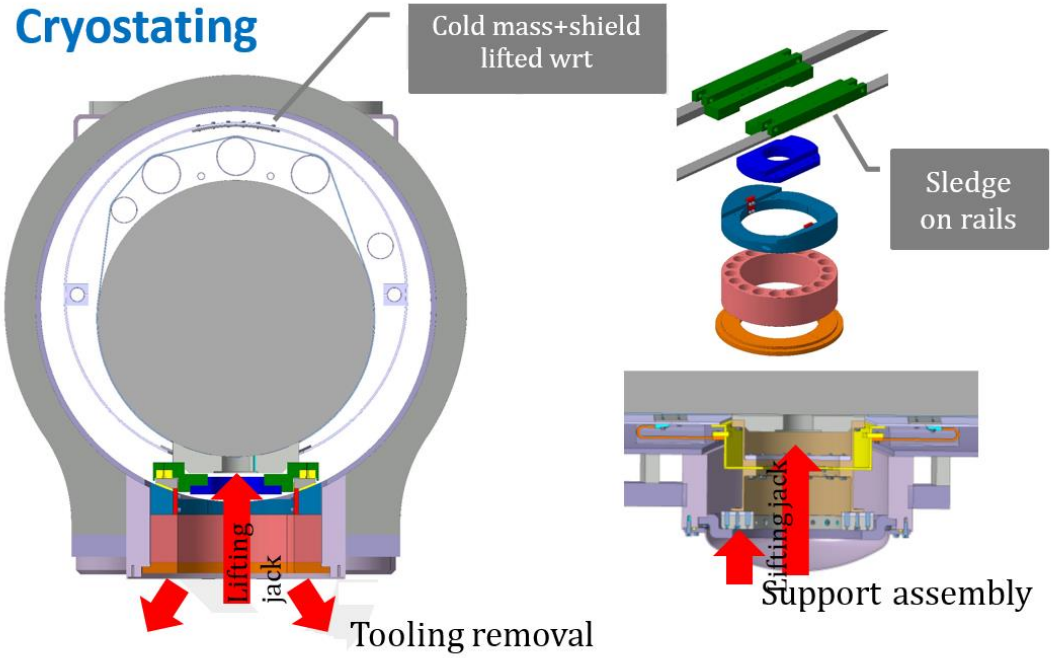

Figure 9.4: Cryostat assembly tooling.

9.4 Fabrication

9.4.1 Component Procurement

All the cryostat components including the tooling is the responsibility of CERN. The components will be shipped to FNAL in two batches:

- Prototype Cryostat Assembly parts and tooling
- Production Cryostat Assembly parts

After the parts have been cleared by Customs, they will go through incoming inspection. The incoming inspection will verify that the cryostat parts have met the design specification and are ready for assembly.

9.4.2 Assembly Procedures

The first cryostat assembly work will be done for the prototype cryostat assembly. This assembly will contain the stand and the tooling preparation for the cryostat assembly work. The current layout for the Cold mass and Cryostat work is shown in Figure 9.5.

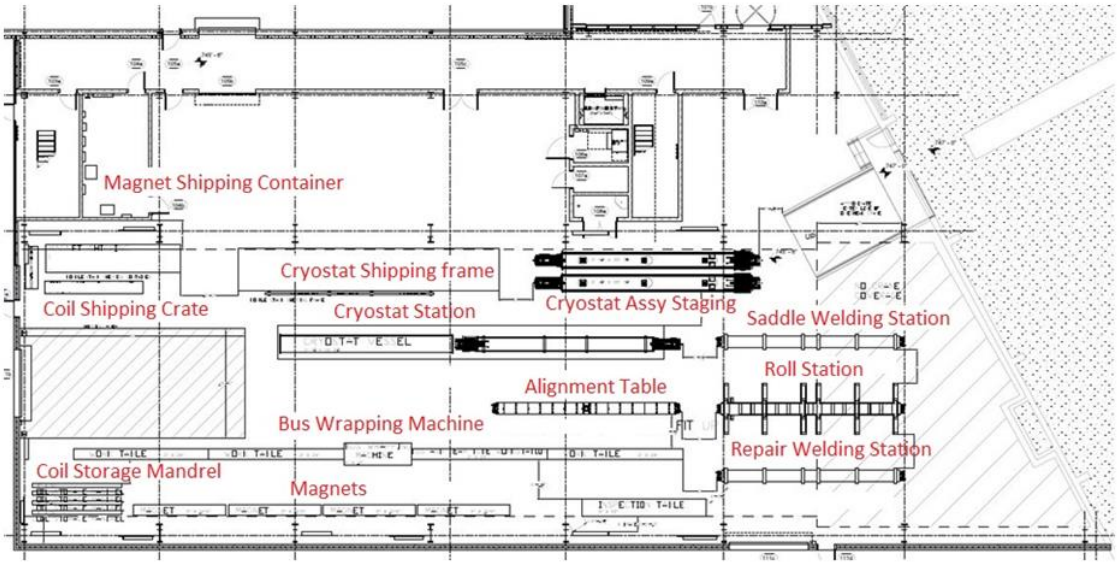

Figure 9.5: IB2 floor layout for the Cold mass and Cryostat work.

a. Prototype

The following four major steps need to be worked out in great detail:

1. Preparation of the cryostat assembly stands and the assembly tooling
2. Cold mass, heat shield, and piping assembly preparation
3. Vacuum vessel preparation
4. Cold mass, heat shield, and piping assembly insertion into the Vacuum vessel
5. Mechanical and electrical tests to verify that the Cryostat assembly is acceptable for the horizontal test

b. Production

The following three major steps need to be worked out in great detail:

1. Cold mass, heat shield, and piping preparation
2. Vacuum vessel preparation
3. Cold mass, heat shield, and piping assembly insertion into the Vacuum vessel
4. Mechanical and electrical tests to verify that the Cryostat assembly is acceptable for the horizontal test

9.4.3 Tests

During the Cryostat assembly process, several tests will be performed to verify that the Cold mass meets the electrical and mechanical specifications at each step of the assembly process. The tests will include:

- Mechanical tests
  - Dimensions and location of cryostat components
  - Leak check for the cold mass and vacuum vessel
  - Pressure tests of the cold mass and vacuum vessel
- Electrical tests
  - Dielectric voltage standoff test of the cold Mass
  - Temperature sensor four wire measurements
  - V-tap continuity measurements
- Warm magnetic measurements for alignment purposes
  - Stretched wire axis measurements for each element upon insertion
  - Subsequent measurements as necessary during fine adjustment of magnet position
  - Survey transfer of measurements to cryostat fiducials in final position

9.4.4 Alignment

Survey will be done several times during the assembly process to assure proper alignment of the Cold mass relative to the vacuum vessel and external (relative to the cold mass) piping:

- Cold mass support components (that will be attached to the support system) will be surveyed before and after installation of the feet
- Cryostat piping installation onto the cold mass including the heat and radiation shield will be surveyed before and after installation.
- Cold mass survey before and after insertion of the cold mass into the vacuum vessel (mechanical centering determination and transfer for 4.3 above)

9.4.5 QC &QA

The cryostat assembly work QA plan follows from the US HiLumi Project Quality Assurance Program (HiLumi-doc-xxx). Consistent with the project QA plan, the Cryostat Assembly QA process uses a graded approach to in the implementation of the plan. The scope of the QA program includes 1.) Design of systems and components 2.) Procurement of commercial items 3.) Fabrication of components 4.) Calibration of instruments and 5.) Design Documentation.

The cryostat team includes staff from FNAL as well as the collaborating institutions CERN. The internal QA plans and procedures of the partnering institutions are used when applicable such as when items are procured through the partnering institution.

9.5 Interfaces

The responsibility for the cryostat interfaces are described in the “Cryostat Assembly Interface Control” document. The interface specifications need to address the following areas:

- Cold mass
  - Piping dimension – Instrumentation port, helium inlets, beam line
  - Heat exchanger
  - Beam screen
  - Instrumentation – bus wiring, temperature sensor wiring, Voltage tap wiring
  - Cold Mass Position Monitoring
- Interconnect
  - Piping dimensions – helium lines, thermal shield lines
  - Thermal shield
  - Vacuum vessel flange

9.6 ES&H

ES&H is integrated into all phases of the Project: Design, Construction, Installation. ES&H requirements are clearly defined within the Project. It will follow Fermilab Environment, Safety and Health Manual as well as each HL-LHC work package will be subject to safety requirements specified in a CERN "Launch Safety Agreement (LSA)" document [2]. This LSA will specify the CERN safety rules and host state regulations applicable to the systems/processes and the minimal contents of the Work Package safety file needed to meet the Safety Requirements. The LQXFA/LQXFB cryostat assembly must comply with CERN's Launch Safety Agreement (LSA) for IR Magnets**.**

Design & installation review process includes an ESH component Utilize Fermilab's and CERN's work planning requirements & processes.

References

[1] LQXFA/LQXFB Functional Requirements, US-HiLumi-doc-246

[2] CERN Launch Safety Agreement for IR Magnets (WP3), CERN EDMS 1550065

10 LQXFA Horizontal Test

Cryo-assemblies with the Q1 and Q3 quadrupole elements of the HL-LHC inner triplet will be tested at the Fermilab's horizontal test stand. Currently we do not differentiate Q1 and Q3 elements, therefore further in the text both cryo-assemblies will be referred as LQXFA.

One prototype and 11 production cryo-assemblies will be tested at Fermilab. One cryo-assembly could be re-tested in case of failure during the initial testing. Therefore, total of 13 cryo-assembly tests are foreseen within the HL-LHC project.

All prototype, production and spare MQXFA magnets will be fully trained and tested in the vertical test stand at Brookhaven National Laboratory (BNL). Therefore, no or minimum amount of training quenches are expected at the horizontal test stand. Comprehensive magnetic measurements also will be performed at BNL.

Horizontal test stand at Fermilab previously was used for testing the existing LHC inner triplet quadrupoles (LQXB).

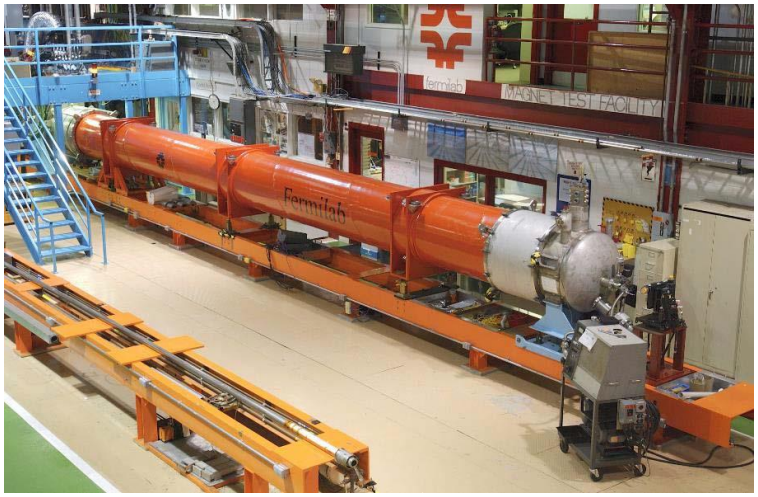

Figure 10.1: Horizontal Test Stand at Fermilab previously used for testing the LHC inner triplet quadrupoles (LQXB) in 2002-2006.

10.1 Horizontal Test Scope and Objectives

The primary objective of the horizontal test is full qualification and acceptance of the project deliverable – LQXFA cryo-assembly. The scope of these tests includes quench performance checkout of magnets in the cryo-assembly, room temperature (warm) and 1.9 K (cold) alignment measurements, translation of the cold mass magnetic axis to the external fiducials, field quality measurements.

MQXFA magnets will be powered up to the nominal (16.5 kA) and ultimate (17.9 kA) currents to verify stable operation and quench training memory of magnets. Magnet protection with protection

heaters and CLIQ units but without external energy extraction will be confirmed for the prototype and the first production cryo-assemblies only. Further testing will be done with the external energy extraction system to save liquid helium and reduce the quench recovery time in case of induced or spontaneous quenches.

NbTi-NbTi splices between the magnet leads and the power bus-bars will be inspected at room temperature and monitored after cool down.

Major checkouts and measurements to be conducted at the horizontal test stand include:

At room temperature before cool down
- Mechanical checkouts
- Electrical checkouts and tests ensuring the integrity of the insulation
- Magnetic measurements

After cool down at 1.9 K
- Electrical checkouts
- Ramp up to the nominal and ultimate currents
- Magnetic measurements: alignment, integral field strength, field harmonics
- Holding the nominal current for an extended period of time
- Thermal cycle for the prototype and first two production magnets
- Protection tests
- Splice measurements

At room temperature after warm-up
- Magnetic measurements
- Electrical checkouts

10.2 Alignment and Field Quality Measurements

Alignment and field quality measurements are performed at room temperature before and after the cool down, and at 1.9 K. Alignment and integral strength measurements are performed with a Single Stretched Wire (SSW) system [1]. The field harmonics are measured with a rotating probe based on the multi-layer printed circuit board (PCB) [2].

Alignment measurements are critical for positioning the quadrupoles in the LHC beamlines. Relative positioning of the cold mass within the cryostat and the actual cold mass positions must be measured and transferred to the external fiducials which are used for magnet installation in the LHC tunnel. There will be extensive alignment measurements to determine waviness of the magnetic axis in the cryo-assembly. The magnetic axis in each individual Q1/Q3 element will be compared to the average (common) magnetic axis in the cryo-assembly.

A laser tracker is used to transfer fiducial positions of the SSW stage to the external fiducials of the cryo-assembly.

At room temperature, we will measure integral field strength and field harmonics at low currents.

All these measurements will be repeated after cool down at 1.9 K. Integral field strength and field harmonics will be measured at the injection (960 A) and collision (16480 A) currents.

Alignment stability should be verified over thermal cycles, as well as after transportation from the assembly building to the test facility.

10.3 Acceptance Tests

Requirements for qualification (acceptance) of the cryo-assembly are still under discussion with CERN colleagues. The cryo-assembly will be accepted if all requirements, including quench performance, field quality and alignment, are met.

Comprehensive field quality measurements will be performed at BNL (vertical test stand). The integral field strength and field harmonics will be measured at Fermilab's horizontal test stand at the injection (960 A) and collision (16480 A) currents. The magnetic measurements at Fermilab will serve as an acceptance test for the magnet field quality.

Most of the magnet alignment will be done during the cold mass assembly. Alignment adjustments are possible only during the cold mass assembly.

For magnet acceptance, the alignment measurements will be repeated at the horizontal test facility before and after the magnet cool down. Specified tolerances must be met for the relative positioning of the cold masses within the cryostat.

10.4 High-Voltage Withstand Levels

Requirements for testing electrical integrity of magnets were developed together with a working group at CERN [4]. The values of withstand voltages for the acceptance of LMQXFA cold mass were finalized during the 1st International Workshop on Superconducting Magnet Test Stands [5] at CERN:

Table 10.1: Values of withstand voltages for the acceptance of LMQXFA cold mass.

Circuit Element	V hi-pot	I hi-pot [µA]	Minimum time duration [s]
Coil to Ground at room temperature (RT)	3.7 kV	10	30
Coil to Quench Heater at RT	3 kV	10	30
Coil to Ground at cold (1.9 K)	1.8 kV	10	30
Coil to Quench Heater at cold (1.9 K)	2.3 kV	10	30

No impulse voltage tests will be performed with magnets in the cryostat.

10.5 Helium and Nitrogen consumption

Helium and Nitrogen consumption at the horizontal test stand were estimated from the previous experience of testing the old LHC IR quadrupoles and based on the proposed test plan of LQXFA cryo-assemblies. Dedicated model was developed for cryogen cost estimate utilizing experience of running cold magnet and cavity tests at Fermilab's magnet test facility over the last 8 years.

Based on short term contracts with the Helium and Nitrogen suppliers about 3.5% increase of Helium price and 3-6% increase of Nitrogen price is expected every year. Two largest helium delivery companies have merged recently into one company and this may create a less competitive environment when it comes to pricing.

References

[1] J. DiMarco et al., .Field alignment of quadrupole magnets for the LHC interaction regions., IEEE Trans. Appl. Supercond., Vol. 10, No. 1, March 2000.

[2] J. DiMarco *et al.*, "Application of PCB and FDM Technologies to Magnetic Measurement Probe System Development", *IEEE Trans. Appl. Supercond.*, vol. 23, no. 3, 9000505, 2013

[3] G. Velev et al., "Magnetic Field Measurements of LHC Inner Triplet Quadrupoles Fabricated at Fermilab", *IEEE TRANSACTIONS ON APPLIED SUPERCONDUCTIVITY*, vol. 17, no. 2, June 2007

[4] Follow the link: HL-LHC HVWL Working Group

[5] See the workshop materials here: https://indico.cern.ch/event/507584/

11 Production Plan

The purpose of this document is to provide a description of the production plan for the Q1/Q3 Cryo-assemblies scope for the US HL-LHC Accelerator Upgrade project. This plan is used as input for the project Resource Loaded Schedule and Basis of Estimates (BOEs)

11.1 Reference Documents

All reference documents below can be found in http://us-hilumi-docdb.fnal.gov/

Project Execution Plan: US-HiLumi-doc-93

Key Assumptions: US-HiLumi-doc-78

WBS Chart: US-HiLumi-doc-104

WBS Dictionary: US-HiLumi-doc-39

MQXFA Functional Requirements Specification: US-HiLumi-doc-36

LMQXFA Functional Requirements Specification: US-HiLumi-doc-64

MQXFA Magnets Functional Test Requirements: US-HiLumi-doc-137

Q1/Q3 Cryo-assemblies Conceptual Design Report: US-HiLumi-doc-140

Basis of Estimates (BOEs) for WBS 302.2 Q1/Q3 Cryo-assemblies:

BOE 302.2.01 Final Design and Integration: US-HiLumi-doc-122

BOE 302.2.02 Strand Procurement and Testing: US-HiLumi-doc-118

BOE 302.2.03 Cable Fabrication: US-HiLumi-doc-121

BOE 302.2.04 Coil Pars, Materials, and Tooling Procurement: US-HiLumi-doc-125

BOE 302.2.05 Coil Fabrication at FNAL: US-HiLumi-doc-115

BOE 302.2.05 Coil Fabrication at BNL: US-HiLumi-doc-117

BOE 302.2.06 Coil Fabrication at FNAL: US-HiLumi-doc-115

BOE 302.2.07 Structure Fabrication and Magnets Assembly: US-HiLumi-doc-127

BOE 302.2.08 Magnets Vertical Test: US-HiLumi-doc-126

BOE 302.2.09 Cold Mass Assemblies Fabrication: US-HiLumi-doc-128

BOE 302.2.10 Cryo-assemblies Fabrication: US-HiLumi-doc-129

BOE 302.2.11 Cryo-assemblies Horizontal Test: US-HiLumi-doc-139

11.2 Deliverables

The Q1/Q3 Cryo-assemblies deliverables that this production plan must support are:

- 5 Q1 Cryo-assemblies (LQXFA)
- 5 Q3 Cryo-assemblies (LQXFB)

The Q1/Q3 Cold Mass Assemblies and Cryo-assemblies will be designed to be interchangeable to the extent possible, and for simplicity there will be no distinction made between a Q1 and a Q3 in this production plan.

A critical schedule milestone is delivery of Cryo-assembly #8 by December 2023. This is the last Cryo-assembly for HL-LHC tunnel installation, so it must arrive at CERN on schedule to support installation during CERN's Long Shutdown 3. The rest of the deliverables are for CERN spares.

11.3 Manufacturing Flow

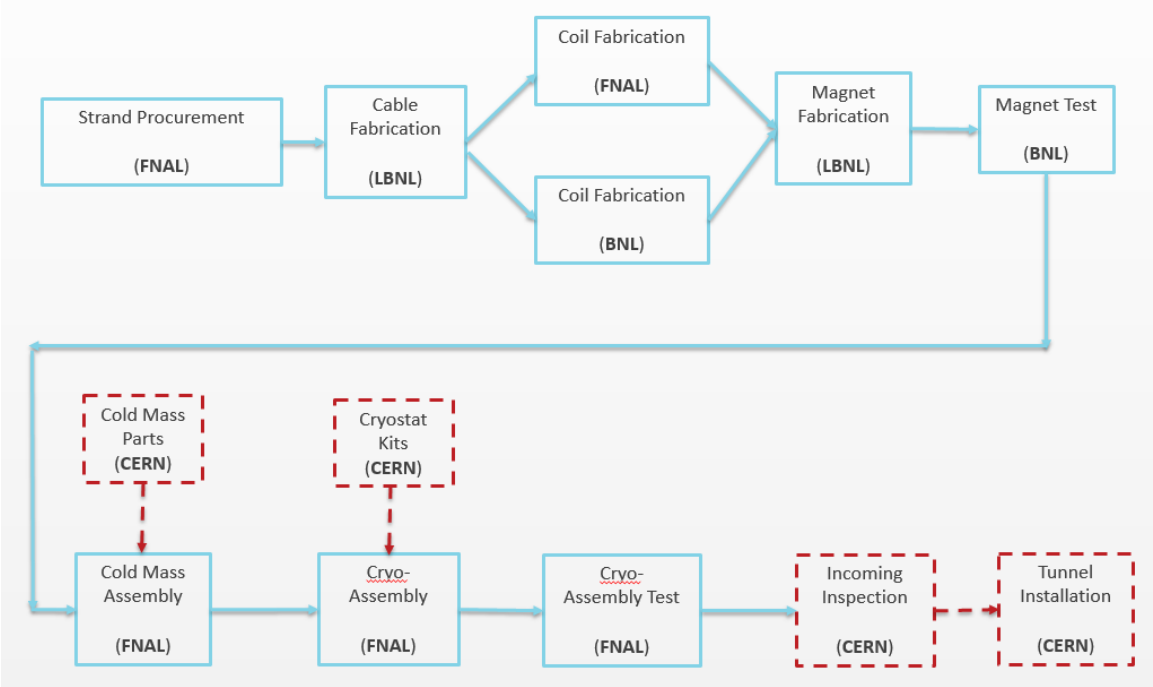

11.4 WBS 302.2.01: Final Design and Integration

This WBS is for Level of Effort (LOE) associated with the analysis of test results, preparation of final design reports and other documents for integration. This LOE is distributed across BNL, FNAL, and LBNL, and goes on for the duration of the project.

In addition, this WBS contains all the L3 management LOE.

11.5 WBS 302.2.02: Strand Procurement and Testing

Each unit of cable requires 40 Nb_3Sn strands. The Strand Unit Length (UL) is 500 m, which is the length to be re-spooled onto the cabling machine and accommodate cable pitch and samples (c.f. Cable Unit Length in WBS 302.2.03). A supplier will receive credit for delivering strand ULs. The total length of strand per cable is 40 × 0.5 km = 20 km, and at 5 kg/m this is 100 kg of strand for each unit of cable. The project baseline considers 102 cables (see next section), therefore the total amount of strand needed is 102 x 20 km = 2,040 km or 10,200 kg.

A total of 12 cable ULs of strand (240 km) with their corresponding QC is assumed to be available from an off-project source (LARP), so the project needs to procure an additional 90 Cable ULs of strand (1,800 km)

Strand is shipped by the vendor in “pieces” of continuous length wrapped in a spool. On average, each piece is 2.3 km long, providing enough material for 4 strands of 500 m long each, but this length varies from piece to piece. Each cable therefore requires, on average, strand to be drawn from 10 different spools.

The plan is to place one order by FNAL each year in April (this date is after the first 2 quarters of the FY to mitigate Continuing Resolution funding risks). This annual order is intended to cover the cable fabrication needs of one year with a total float of a few months to mitigate the risk of vendor delays or cable fabrication delays. The plan also assumes that the vendor delivers the first shipment of strand spools 6 months After Receipt of Order (ARO), with bi-monthly shipments continuing for an additional 12 months. The total strand order is assumed to be delivered in approximately equal bi-monthly installments. To support a peak coil production rate of ~ 2 coils per month (see Section 9), bi-monthly deliveries of roughly 80 km strand are needed to support a minimum of 2 UL of cable fabrication per month (40 km = 200 kg of strand in an average of 20 pieces or spools per month).

QC verification testing by a Lab is assumed to be done on 50% of the pieces, to keep uniformity with CERN’s plan, so each cable requires 5 QC verification tests. This QC verification testing is mainly of electromagnetic properties (critical current Ic, residual resistivity ratio RRR, and n-value). Physical properties are spot tested, but most measurements are performed under WBS

302.2.03. A 90% testing yield is assumed for electromagnetic property measurement. Therefore, a total of 5×102/0.9 = 567 pieces are expected to undergo QC verification testing.

In addition, a total of 6 witness samples are taken from each coil, and 3 samples are tested for Ic and RRR. The plan requires a total of 92 coils (see coil fabrication sections), and a 90% testing yield is assumed. Therefore, a total of 3×92/0.9 = 333 witness samples are expected to undergo QC testing.

11.6 WBS 302.2.03: Cable Fabrication

The Unit Length (UL) of Cable Fabrication is 455 m. This includes length for samples (vendor QC and LBNL verification) for braiding, coil winding leads, and buffer lengths. The minimum length required to fabricate one coil is 431 m. A cable UL is the minimum length required to fabricate one coil. The fabrication of a UL of cable requires 40 strands of 500 m long each. A 90% yield is assumed for the cable fabrication process. The total number of coils required by the project is 92 (see coil fabrication sections), therefore the plan is to fabricate a total of 92/0.9 = 102 UL of cable.

Cable fabrication will be done at LBNL. From past experience, with 2 technicians it takes ~ 7 working days per cable fabrication (including preparation, QC, shipment). LBNL plans to allocate 10 months per year to this task. The rest is for equipment maintenance and to support other projects. The peak project cable fabrication rate would require ~3 cables per month, so 3 technicians will be needed to support this peak rate.

After a 7-day cable fabrication process, LBNL ships the un-insulated cable to a vendor for cable insulation. This step takes about 4 weeks (including shipment). Meanwhile, RRR measurements are performed at LBNL on extracted cable strands as part of the cable QC. Assumes 4 samples required per cable, and the sample holders can take 4 samples each time. This measurement takes about 4 weeks, including the heat treatment which lasts about 12 days including cool down. QC on the insulated cable includes measurement of post-braiding insulation thickness by the ten-stack method.

The total duration of a UL Cable Fabrication is estimated as follows:

Most likely = 3 months

Optimistic = 2 months

Pessimistic = 6 months

The most likely cable fabrication duration of 3 months is assumed for the project schedule. The peak cable production rate is 1 cable every 7 working days.

The strand order schedule follows the cable fabrication start schedule as described in the Strand section. With these assumptions, a few months of cable inventory stock is expected to be generated during project execution. This cable inventory stock mitigates the risks of project schedule delays due to strand vendor delays and unscheduled downtime of the cable fabrication process. Coil fabrication is in the project critical path, so it is important to avoid having to stop fabricating coils because cable is not available on time.

11.7 WBS 302.2.04: Coil Parts, Materials, and Tooling

11.7.1 Coil Parts

The Coil Parts required for coil fabrication are Pole Parts, End Parts, Trace Parts, and Wedges Parts. The total number of coils required by the project is 92 (see coil fabrication sections), so a total of 92 coil parts sets are needed.

A total of 15 coil part sets are assumed to be available from an off-project source (LARP), so the project needs to procure a 77 additional sets of coil parts. From past experience, the lead time required for these parts is 12 months for End Parts and Wedges, and 8 months for Poles. This lead time is after the PO is placed, and includes Plasma Coating of End Parts, Cutting of Wedge Parts, and QC activities.

The plan is to place one order by FNAL each year in April (this date is after the first 2 quarters of the FY to mitigate Continuing Resolution funding risks). This annual order is intended to cover the coil fabrication needs of one year plus 20% of the following year to mitigate risks due to vendor delays and parts rejection. Half of the Coil Parts delivered by the vendor will be shipped by FNAL to BNL each year for the fabrication of the BNL coils.

11.7.2 Coil Materials

The Coil Materials are the consumables required for Coil Fabrication, including interlayer insulation, S2 glass tape, S2 glass sheet, NbTi leads, Epoxy, Binder, etc. The following list of materials will be procured by FNAL for both FNAL and BNL coil fabrication:

- S2 glass sheet Hexcel 4522 - 5.7 mil thick
- Interlayer insulation (2 x BGF 6781 + 1x HEXCEL 4522)
- 5 mil thick 3/4" wide HT S2 glass tape pole insulation
- 5 mil FII-272 style S2 glass insulation wedge insulation
- HT and silane sizing on wedge insulation
- 7 mil S2 glass tape end part insulation
- NbTi Lead (expected to be provided by CERN)

- Electric wires for heaters and voltage taps (procured using CERN specifications)

The R/I glass and the interlayer insulation will be laser cut to final size, ready to use on the coil.

Each lab will procure the following additional materials needed for their own coil fabrication:

- CTD-1202 Binder
- 8 mm dia. 30 mm long SS 316 dowel pins (FC0050356)
- Mica sheet - 5 mil thick
- Argon Gas
- Solder Sn96Ag4 and Flux MOB39
- Zyvax Mold release
- CTD-101 Epoxy
- G11 midplane shim
- RTV 157
- MYLAR
- Silicone o-rings
- SS tubing
- Nitrogen Gas (FNAL, for vacuum impregnation oven)
- Miscellaneous

11.7.3 Coil Tooling

One set of coil production tooling is assumed to be available at each coil fabrication site (FNAL and BNL) from the LARP program. Additional tooling needs to be procured on project in FY19 to increase the coil production rate starting in FY20 and meet the project schedule. The justification for this additional tooling can be found in US-HiLumi-doc-95.

The additional tooling includes:

2 Additional Winding and Curing Tooling (Mandrel)

4 Additional Reaction Tooling

2 Additional Impregnation Tooling

FNAL will procure the additional reaction and impregnation tooling for both FNAL and BNL, and ship the BNL tooling to BNL. BNL and FNAL will procure their additional Mandrel because it is specific to their machine.

11.8 WBS 302.2.05/06: Coil Fabrication at FNAL/BNL

The plan requires two coil production lines to meet the schedule. The project assumes that there will be a fully qualified coil production line at FNAL and another at BNL as a result of prototype coil fabrication under the LARP program. In order to avoid delays due to coil QC (CMM measurements) a small dedicated CMM system is planned to be procured at both BNL and FNAL.

Coil Fabrication Process:

The coil fabrication process is described in detail in US-HiLumi-doc-95, "Fermilab Coil Production Analysis". This note shows a detailed estimate of QXFA 4.2m single coil duration, labor, and equipment occupancy based on Fermilab experience obtained with short model QXFS coils and the first long QXFA coils. Based on this estimate, the note presents an analysis of coil production rate as a function of tooling quantity, including the technician crew required to sustain this rate. The project peak coil production rate with the additional tooling and two coil production lines is ~ 2 coils per month.

Coil Quantities:

A coil series production yield of 87.5% (7 out of 8) is assumed. Series production must provide enough accepted coils for 20 magnets (each of the 10 cold masses has 2 magnets inside). Each magnet requires 4 coils, therefore the plan is to fabricate a total number of 20*4/0.875 = 92 series coils. Rejected coils are assumed to be uniformly distributed during the entire coil fabrication duration.

The project plan is to fabricate a total 5 pre-series coils for the pre-series magnet MQXFA-3 and 92 series production coils. The following coils are planned in each coil manufacturing line to support the following magnets (each magnet requires 4 coils):

3 FNAL coils for MQXFA-3 pre-series

2 BNL coils for MQXFA-3 pre-series

46 FNAL coils for MQXFA series

46 BNL coils MQXFA series

Fabrication of prototype coils were done under the LARP program. Two prototype magnets (MQXFA-1 and MQXFA-2) are needed to obtain CD-3b for production magnets, and these two prototype magnets will be used to assemble the prototype cold mass (see Cold Mass section).

A pre-series magnet (MQXFA-3) is planned after the completion of the first two prototype magnets, and this pre-series magnet will be used to verify repeatability in the production processes and make sure all is in place before launching the series production.

Learning Curve:

For the FNAL coil manufacturing line, most of the learning curve already took place during the fabrication of coil prototypes under LARP. For the pre-series coils fabricated under project, a multiplier of 1.3 x the steady production duration and labor is assumed. No further learning curve is assumed for the series production. However, provisions for training a second FNAL crew in FY19 is included in the plan in order to increase production rate in FY20.

For the BNL coil manufacturing line, there is less coil fabrication experience during LARP, especially for Winding and Curing because the winding and curing infrastructure is planned to be completed in FY17. Therefore, higher multipliers are assumed for BNL in project. For the pre-series coils, the same 1.3x multiplier is assumed for all but the winding and curing process. For winding and curing, the multiplier is 2.0x. The following learning curve multipliers are assumed for the BNL series production:

Coil QXFA-204 - 1.8x wind and cure only

Coil QXFA-205 - 1.5x wind and cure only

Coil QXFA-206 - 1.3x wind and cure only

--- New techs

Coil QXFA-207 - 1.6x all coil fab

Coil QXFA-208 - 1.4x all coil fab

Coil QXFA-209 - 1.2x all coil fab

Production Rate:

From US-HiLumi-doc-95, the total duration for a series coil fabrication is 85 working days. The project assumes that one set of tooling and technician crew is available at each location (FNAL and BNL) from the LARP program. With this existing infrastructure and personnel, some overlap is possible and the production rate at each location is estimated to be 1 coil every 35 working days. However, this production rate is not sufficient to meet the overall project schedule therefore the plan is to procure in FY19 additional tooling and acquire additional manpower to speed up the production rate. Based on the analysis in US-HiLumi-doc-95, with the additional tooling described in the section on Coil Parts, Materials, and Tooling and with additional technicians, the peak project coil production rate is 1 coil every 20 working working days at each location.

A production rate of 1 coil every 20 working days at each production line results in a coil set for a magnet (4 coils) every 40 working days in the best case (without rejected coils). With this rate, coil fabrication is in the project critical path. A plan is in place to carefully monitor the actual labor and durations during coil fabrication in FY17-18 to validate the estimates so we can have high confidence in these numbers before freezing the project baseline for CD-2.

BNL Coil and Magnets Shipping Fixtures:

Part of the BNL Coil Fabrication scope is the fabrication of additional coil and magnets shipping fixtures for all Labs.

Coil Shipping Fixtures: assuming coils are delivered at a rate of one every 20 working days from each line at BNL and FNAL, each line needs 1 fixture per month. If total time from preparing to ship (coil or empty fixture) to receipt back and forth is 2 weeks for each of 2 trips, then 4 fixtures total should suffice. Of course, there may be delays such as the inability to immediately remove an incoming coil from the fixture, so it would be wise to have a spare at each location, for a total of 6 fixtures. We already have fixtures as part of LARP, so a total of four (4) additional coil shipping fixtures must be fabricated in project in FY18.

Magnet Shipping Fixtures: a magnet shipping fixture will leave LBNL with the Magnet, then will stay in BNL during the tests waiting for the Magnet and finally it will come (with the Magnet) to FNAL for cold mass assembly. The duration from departing LBNL to returning should be approximately 120 days. Considering the top production rate of 42 days/Magnet, 3+1 spare shipping fixtures should be enough. One shipping fixture is available from LARP, so three (3) additional shipping fixtures must be fabricated in project in FY20.

11.9 WBS 302.2.07: Structures Fabrication and Magnets Assembly

The project plan is to fabricate a pre-series magnet (MQXFA-3) and 20 series production magnets. The project plan also assumes that 3 magnets will fail and need to be re-worked (e.g., disassembly and swapping a bad coil). In this re-work, parts are assumed to be reused.

The magnet fabrication will be done by LBNL, including procurement of magnet parts. Parts for 21 magnets are needed (1 pre-series and 20 series). From past experience, procurement of magnet parts has a lead time of 6 months ARO. The plan is to place phased procurements at LBNL that are activated each year in April (this date is after the first 2 quarters of the FY to mitigate Continuing Resolution funding risks). This annual order is intended to cover the coil fabrication needs of one year plus some component spares

To increase production rate and keep up with the coil production rate, additional tooling needs to be procured in FY20. This tooling currently includes the following items:

- Assembly table
- Pivot table [2x]
- Coilpack assembly table
- Lifting beams [2x]
- Rollover table
- Rocket pad
- Winch assembly
- Roller spine
- Tension system
- Bladder hydraulic system
- Strain gage monitoring system

There will not be enough long magnet prototypes fabricated by LBNL to complete the learning curve before series production begins. Therefore, the following learning curve "multipliers" have been assumed for the project plan labor (multipliers are applied to the steady production labor and duration after-learning estimates):

MQXFA-2b:x1.25

MQXFA-3: x2.0 (pre-series and first crew training)

MQXFA-4: x1.5

MQXFA-5: x1.25

MQXFA-6: x1.2

MQXFA-7: x2.0 (train Second Crew to increase production rate)

MQXFA-8: x1.0 (first crew completes learning curve)

MQXFA-9: x1.2 (second crew learning)

MQXFA-10: x1.0 (second crew completes learning curve)

Magnet fabrication can be split into two major sub-assemblies: the Yoke/Shell assembly (which can be done in advance of receiving the coils) and the Coil Pack (which can only be done after receiving the coils). These sub-assemblies are then integrated together into a complete magnet assembly. The project plan will take advantage of this feature to level resources at LBNL consistent with the available funding.

Magnet assembly plan includes measurements for assuring that alignment and field quality requirements are met. Assembly iterations may be needed to meet these requirements.

During peak production, the structure fabrication and magnet assembly process duration for each magnet is estimated to be 60 working days, with a possible overlap of 30 working days. Therefore, the peak production rate is 1 magnet every 30 working days.

11.10 WBS 302.2.08: Magnets Vertical Test

Each magnet fabricated or re-worked by LBNL will be vertically tested at the BNL vertical test facility. Testing includes quench training and magnetic measurements. As part of the project scope, some prototypes and a pre-series magnet will be tested in FY18 and FY19. In FY18, MQXFA-2 and MQXFA-2b will be tested. MQXFA-2 will be fabricated as part of the LARP program (off-scope), and MQXFA-2b is a rework of this magnet done in project (e.g., increase the preload). In FY19 there will be two tests planned for the pre-series magnet: MQXFA-3 and MQXFA-3b (a re-test of MQXFA-3 to optimize parameters such as end pre-load before going into series production).

The total number of vertical tests planned for the project is 27 (2 prototypes, 2 pre-series, 20 series threshold scope, and 3 series re-works)

The BNL vertical test facility is assumed to be fully qualified and ready to support production testing. This facility, commissioned in FY16, would have already tested the mirror magnet and the first long prototype, MQXFA-1, as part of the LARP program. The following multipliers are assumed for the prototype and pre-series magnets because the run plan is expected to be longer for these magnets (e.g., may include a thermal cycle). For the pre-series re-test, this is assumed to be a short-duration test involving no training nor thermal cycle to optimize parameters such as preload before launching series production, therefore the multiplier is 0.5.

MQXFA-2: x1.7

MQXFA-2b: x1.2

MQXFA-3: x1.7

MQXFA-3b: x 1.2

These multipliers makes the total scope equivalent to testing an additional 1.8 production magnets, so the equivalent number of production magnets tests is 28.8

It is also assumed that at the end of every test, the magnet is shipped either to FNAL if accepted or to LBNL for re-work if rejected.

The series production test duration is estimated to be 46 working days. A second top hat and wiring stand is planned to be procured in FY20 to increase the test throughput by preparing a magnet while another one is finished testing. With this second top hat, an overlap of 9 working days is possible, bringing the peak production test rate to 1 magnet every 37 working days.

11.11 WBS 302.2.09: Cold Mass Assemblies Fabrication

Each cold mass has two magnets inside a stainless steel helium containment pressure vessel. The project plan is to fabricate one cold mass assembly prototype using the first two prototype magnets MQXFA-1 and MQXFA-2, and a total of 10 series production cold mass assemblies using the 20 series production magnets. The project assumes a re-work of one cold mass assembly, so the total number of cold mass fabrication is 12 (1 prototype, 10 series, and 1 series re-work). The re-work includes opening the helium vessel and performing internal repairs.

Although the project deliverable are for Q1 cold mass assemblies and Q3 cold mass assemblies, the project plan is to fabricate them in such a way that the Q1 and Q3 cold mass assemblies are interchangeable so spares work for both quadrupole configurations.

The cold mass assemblies will be fabricated at FNAL. Several cold mass assembly components (e.g., beam tube, heat exchanger tubes, instrumentation, etc.) are expected to be supplied by CERN (see US-HiLumi-doc-381). Fabrication includes the pressure vessel fabrication/welding, magnets installation, heat exchangers installation, bus bars installation, sensors, and wiring, alignment, pressure test, etc. Some tooling is assumed to be available from the fabrication of the present LHC IR quadrupoles, and the following tooling is planned to be procured in project:

- (12x) 34"OD x 24"IDx 5" thick forging clamps
- (2x) I-Beam Spreader Bar
- (36x) alignment fixtures
- Saddles
- 1"-8 x 6ft (Threaded Rods / hold downs)
- Square Tube - Hold downs
- splice fixture
- SSW system
- Ferret probe
- Rotating Coil Datacq station
- probe transport system
- Welding equipment
- HBM Strain Gauge readout system

The most likely Cold Mass fabrication duration is estimated to be 60 working days for the prototype and 40 working days during series production.

11.12 WBS 302.2.10: Cryo-assemblies Fabrication

Each cold mass will be inserted into a cryostat to deliver a HL-LHC tunnel-ready Q1/Q3 quadrupole (with the exception of the beam screen, which will be installed by CERN after delivery). The cryostat parts will be supplied by CERN and the cryostat will be assembled at FNAL. Assumes re-work of one cryo-assembly, so the total number of cryo-assemblies fabrication is 12 (1 prototype, 10 series, and 1 series re-work).

The most likely Cryo-assembly fabrication duration is estimated to be 65 working days for the prototype and 45 working days during series production.

Shipping and Handling of the cryo-assembly to CERN is included in this WBS. After horizontal testing and passing the acceptance procedure, the cryo-assembly is prepared for shipping and shipped to CERN in a dedicated container (one container per cryo-assembly is assumed).

The most likely shipping and handling duration is estimated to be 30 working days.

11.13 WBS 302.2.11: Cryo-assemblies Horizontal Test

Each cryo-assembly will be tested in the FNAL Horizontal Test Stand previously used to test the present LHC IR quadrupoles. There will be a total of 12 cryo-assemblies tested (1 prototype, 10 series, and 1 series re-work)

The FNAL Horizontal Test Stand, Stand #4 in Industrial Building 1, needs to be brought back into reliable operation and upgraded to meet the requirements of the HL-LHC cryo-assemblies.

The project plan assumes that bringing the test stand back to reliable operation is off-project and funded by FNAL. The necessary upgrades are part of the project scope. Upgrades include interconnect and turn around can for interfacing to the new Cryo-assemblies, and magnetic measurement system including a Stretched Wire System, a Probe/Ferret system, Shaft and transport modifications, and a DAQ station. Two CLIQ units (provided by CERN) should be integrated into the protection system. Following is a list of items to be procured in project:

- Bellows
- Helium collection port
- Large Interconnect bellows
- Return can
- Instrumentation components

- All other components
- SSW system
- Probe/ferret
- Shaft and transport modifications
- DAQ station

The test stand must be ready to support testing the cryo-assembly prototype in July 2019.

The most likely Cryo-assembly horizontal test duration is estimated to be 75 working days for the prototype and the first two production cryo-assemblies, and 45 working days for the rest of the series production.